TECHNICAL UNIVERSITY OF LIBEREC
Faculty of Textile Engineering

Thermal Protective Performance of Firefighter Protective Clothing

Dissertation Thesis

Study programme:	P3106 Textile Engineering
Study branch:	Textile Technics and Materials Engineering
Author:	**Jawad Naeem, M.Sc.**
Thesis Supervisor:	prof. Dr. Ing. Zdeněk Kůs Department of Clothing technologies

Liberec 2020

Declaration

I hereby certify, I, myself, have written my dissertation as an original and primary work using the literature listed below and consulting it with my thesis supervisor and my thesis counsellor.

I acknowledge that my bachelor dissertation is fully governed by Act No. 121/2000 Coll., the Copyright Act, in particular Article 60 – School Work.

I acknowledge that the Technical University of Liberec does not infringe my copyrights by using my dissertation for internal purposes of the Technical University of Liberec.

I am aware of my obligation to inform the Technical University of Liberec on having used or granted license to use the results of my dissertation; in such a case the Technical University of Liberec may require reimbursement of the costs incurred for creating the result up to their actual amount.

At the same time, I honestly declare that the text of the printed version of my dissertation is identical with the text of the electronic version uploaded into the IS/STAG.

I acknowledge that the Technical University of Liberec will make my dissertation public in accordance with paragraph 47b of Act No. 111/1998 Coll., on Higher Education Institutions and on Amendment to Other Acts (the Higher Education Act), as amended.

I am aware of the consequences which may under the Higher Education Act result from a breach of this declaration.

July 1, 2020 Jawad Naeem, M.Sc.

TECHNICAL UNIVERSITY OF LIBEREC
Faculty of Textile Engineering

THERMAL PROTECTIVE PERFORMANCE OF FIREFIGHTER PROTECTIVE CLOTHING

Author Jawad Naeem

DOCTORAL THESIS

Table of Contents

List of Figures

List of Tables

Abstract

This study is related to the possible improvement in thermal protective performance of firefighter protective clothing when exposed to different levels of radiant heat flux density. Firefighter protective clothing normally consists of three layers: outer shell, moisture barrier and thermal liner. When thermal protective performance of firefighter protective clothing is enhanced, the time of exposure against radiant heat flux is increased, which will provide extra amount of time to firefighter to carry on their work without suffering from severe skin burn injuries. This research deals with basic understanding of firefighter clothing i.e. material composition, standards used for evaluation of firefighter protective clothing, the type of environment in which firefighter normally perform their duties along with different type of skin burn injuries and the different type of equipment used for evaluation of thermal properties and thermal protective performance of firefighter protective clothing. In the initial phase, evaluation of thermal insulation properties and thermal protective performance of firefighter clothing specimens was performed. Four sample combinations were made. Each sample arrangement has outer shell, moisture barrier and thermal barrier. Later on, improvement in thermal insulation properties of firefighter protective clothing was made with the help of aerogel blankets. Four different multilayer combinations of firefighter protective clothing were investigated. Two samples have combinations consisting of outer shell, moisture barrier and thermal liner. In other two samples, aerogel sheet was also employed as a substitute to thermal barrier. Initially, properties like thermal resistance, thermal conductivity, and water vapor resistance of multilayer fabric assemblies were investigated. Later on these combinations were exposed to different levels of radiant heat flux density i.e. at 10 kW/m^2, 20 kW/m^2, 30 kW/m^2 and 40 kW/m^2 as per ISO 6942 standard. It was noted that those combinations in which aerogel blanket was used as substitute to thermal barrier acquire greater thermal resistance, water vapor resistance and have less transmitted heat flux density values. The lesser the value of transmitted heat flux density, the better will be thermal protective performance as more amount of time will take for rise in temperature of firefighter's body. This will allow firefighters to perform their duties efficiently and effectively without acquiring significant burn injuries. Afterwards, the exterior side of outer shell was coated with layer of silver metallic particles through magnetron sputtering technology. Coating of outer shell with silver metallic particles was performed at three level of thickness i.e.

1µm, 2µm and 3µm respectively. All the uncoated and silver coated specimens were then characterized on air permeability tester, Permetest and radiant heat transmission machine. A negligible difference was witnessed in the values of air permeability and relative water vapor permeability for uncoated and silver coated specimens. However, a significant decline was recorded for the value of transmitted heat flux density Q_c (kW/m^2) and percentage transmission factor (percentage TF Q_o) in case of silver coated specimens when subjected to 10kW/m^2, 20 kW/m^2, 30 kW/m^2 and 40 kW/m^2. This indicates considerable improvement in thermal protective performance of silver coated specimen as compared to uncoated specimens. These values of transmitted heat flux density go on further reduction with increase in thickness of coating layer of silver particles. Also the silver coated specimen has lower emissivity values as compared to uncoated specimen indicating better reflective properties. The silver coated specimens were washed as per NFPA 1851 standard for investigating durability of coating and thermal protective performance. It was inferred that there was negligible decline in thermal protective performance of silver coated specimens after different cycles of washing. After wards their reflectivity and transmissivity was measured. Those specimen which are impregnated with silver metallic particles have better reflectivity values and low transmissivity values. Furthermore, stability of silver coating was evaluated for different abrasion cycles. It was observed that after 20 cycles of abrasion, there was considerable decline in thermal protective performance of silver coated specimen. In the end, Numerical model was employed to predict distribution of temperature for both uncoated and silver coated specimen. This model utilizes appropriate radiant heat transfer equations. When results of uncoated and silver coated fabric assembly obtained from numerical solution were compared, they display similar pattern as observed in the experimental work.

Key words:

Firefighter protective clothing, Thermal protective performance, Thermal insulation and Transmitted heat flux density values

Abstrakt

Tato studie souvisí s možným zlepšením tepelné ochranné výkonnosti hasičského ochranného oděvu při vystavení různým úrovním hustoty sálavého tepelného toku. Ochranný oděv hasiče se obvykle skládá ze tří vrstev: vnější skořepiny, bariéry proti vlhkosti a tepelné vložky. Zvýší-li se tepelný ochranný výkon hasičského ochranného oděvu, zvýší se doba expozice proti sálavému tepelnému toku, což hasiči poskytne další čas, aby mohl pokračovat ve své práci, aniž by utrpěl těžká zranění způsobená popálením kůže. Tento výzkum se zabývá základním porozuměním hasičského oděvu, tj. složení materiálu, standardy používanými pro hodnocení hasičského ochranného oděvu, typem prostředí, ve kterém hasič normálně plní své povinnosti, s různými typy zranění způsobených popálením kůže a různým typem zařízení používaných pro hodnocení tepelných vlastností a tepelně ochranného výkonu hasičského ochranného oděvu. V počáteční fázi bylo provedeno vyhodnocení tepelně izolačních vlastností a tepelně ochranné výkonnosti vzorků hasičů. Byly provedeny čtyři kombinace vzorků. Každé uspořádání vzorku má vnější plášť, bariéru proti vlhkosti a tepelnou bariéru. Později bylo provedeno zlepšení tepelně izolačních vlastností hasičského ochranného oděvu pomocí vrstev obsahujících aerogel. Byly zkoumány čtyři různé vícevrstvé kombinace hasičského ochranného oděvu. Dva vzorky mají kombinace sestávající z vnější vrstvy, bariéry proti vlhkosti a tepelné vložky. V dalších dvou vzorcích byla také použita vrstva aerogelu jako náhrada tepelné bariéry. Zpočátku byly zkoumány vlastnosti, jako je tepelný odpor, tepelná vodivost a odpor vodních par vícevrstvých textilních sestav. Později byly tyto kombinace vystaveny různým úrovním hustoty sálavého tepelného toku, tj. při 10 kW / m^2, 20 kW / m^2, 30 kW / m^2 a 40 kW / m^2 podle normy ISO 6942. Bylo zjištěno, že kombinace, ve kterých byla aerogelová vrstva použita jako náhrada za tepelnou bariéru, získaly větší tepelný odpor, odolnost vůči vodní páře a mají nižší hodnoty hustoty tepelného toku. Čím menší je hodnota hustoty přenášeného tepelného toku, tím lepší bude tepelný ochranný výkon, protože na zvýšení teploty těla hasiče bude potřebovat více času. To umožní hasičům účinně a efektivně vykonávat své povinnosti, aniž by utrpěli významná zranění způsobená popálením. Poté byla vnější strana vnějšího pláště potažena vrstvou stříbrných kovových částic technologií magnetronového rozprašování. Potahování vnější vrstvy vnějšího pláště stříbrnými částicemi bylo prováděno ve třech úrovních tloušťky, tj. 1 μm, 2 μm a 3 μm, v tomto pořadí.

Všechny nepotažené a postříbřené vzorky byly poté charakterizovány na zkoušečce propustnosti vzduchu, Permetestu a stroji pro přenos tepla sáláním. U vzorků nepropustných a postříbřených vzorků byl zaznamenán zanedbatelný rozdíl v hodnotách propustnosti vzduchu a relativní propustnosti pro vodní páru. Významný pokles byl však zaznamenán u hodnoty přenášené hustoty tepelného toku Qc (kW / m^2) a procentuálního faktoru přenosu (procento TF Qo) v případě vzorků potažených stříbrem, pokud byly vystaveny 10kW / m^2, 20 kW / m^2, 30 kW / m^2 a 40 kW / m^2. To ukazuje na značné zlepšení tepelné ochranné výkonnosti vzorků potažených stříbrem ve srovnání s nepotaženými vzorky. Tyto hodnoty hustoty přenášeného tepelného toku se dále snižují se zvyšováním tloušťky povlakové vrstvy částic stříbra. Také stříbrem potažený vzorek má nižší hodnoty emisivity ve srovnání s nepotaženým vzorkem, což naznačuje lepší reflexní vlastnosti. Vzorky potažené stříbrem byly promyty podle standardu NFPA 1851 pro zkoumání trvanlivosti potahování a tepelné ochrany. Bylo zjištěno, že po různých cyklech praní došlo k zanedbatelnému snížení tepelné ochranné výkonnosti vzorků potažených stříbrem. Po odděleních byla měřena jejich odrazivost a propustnost. Vzorky, které jsou impregnovány kovovými částicemi stříbra, mají lepší hodnoty odraznosti a nízké hodnoty propustnosti. Dále byla hodnocena stabilita povlaku stříbra pro různé abrazivní cykly. Bylo pozorováno, že po 20 cyklech oděru došlo ke značnému snížení tepelné ochranné výkonnosti vzorku potaženého stříbrem. Nakonec byl použit numerický model k predikci distribuce teploty pro nepotažené a stříbrem potažené vzorky. Tento model využívá rovnice, které jsou vhodné pro přenos tepla sáláním. Porovnáním výsledků měření textilií ošetřených a neošetřených stříbrem s numerickými modely uvedenými v této práci, můžeme konstatovat, že mají shodný trend.

Klíčová slova:

Hasičský ochranný oděv, tepelný ochranný výkon, tepelná izolace, hustota přenášeného tepelného toku.

Acknowledgment

Firstly, I am thankful to Allah Almighty for providing me an opportunity work with excellent brains for implementing my ideas into reality. I would like to express sincere gratitude to my supervisor Prof. Dr. Ing. Zdeněk Kůs and consultant Ing. Adnan Ahmad Mazari, PhD for their continuous support, guidance, mentoring and valuable suggestions for completion of my research work. They motivate me to share my ideas and extended their support to make my stay very comfortable in Technical University of Liberec. I am extremely thankful to Doc. Ing. Antonín Havelka, CSc from the core of my heart for his kind help and guidance during the entire process of my experimental work and thesis.

I would also like to thank Prof. Ing. Luboš Hes, Dr Sc., Dr.h.c, Prof. Ing. Jakub Wiener Ph.D and Prof. Ing. Jiří Militký, CSc, prof. Ing. Tomáš Vít, Ph.D and Ing. Ondreg Burian for their valuable recommendations and providing me an opportunity for the refinement and improvement of my thesis in its entirety.

I also want to thank Ing. Jana Drašarová, Ph.D (Dean of faculty of Textile Engineering) and Ing. Gabriela Krupincová, Ph.D (Vice Dean for Science and Research) for their precious guidance.

I am very thankful to Ing. Michal Chotěbor (Incharge of clothing Lab), Ing. Pavel Kejzlar Ph.D, Ing. Lukáš Voleský, Ph.D, RNDr. Michal Krejčík, for helping me a lot during my experimental work in the lab and preparations of samples. Furthermore, I would like to express my gratitude to Ing. Michal Martinka and Mr. Hafiz Faisal Siddique, Dr. Salman Naeem, Dr. Usman Javed and Dr. Zuhaib Ahmed for their valuable suggestions.

Special thanks to Prof. Dr. Niaz Ahmad Akhtar (former Rector NTU), Dr. Zafar Javed and Dr. Abher Rasheed for allowing me to utilize life time opportunity provided by Technical University of Liberec.

Nomenclature

$\dot{Q}$	[W/m²]	Rate of heat flow
λ	[W/m.k]	Thermal conductivity
ΔT	[ºC or K]	Temperature difference
ε		Emissivity
σ	[W/m²K⁴]	Stefan-Boltzman constant
I_T	[m² ºC/W]	Total Thermal insulation
M	[W/m²]	Rate of metabolism (interior heat generation)
W	[W/m²]	External work load
C_{conv}	[W/m^2]	Heat lost due to convection
C_{cond}	[W/m^2]	Heat lost due to thermal conduction
E_{resp}	[W/m^2]	Evaporative heat loss due to respiration
C_{resp}	[W/m^2]	Sensible heat exclusion due respiration
R_t	[m² K/W]	Thermal resistance
R_{et}	[m² Pa/W]	Water vapor resistance
T_c	[ºC]	Contact temperature
T_1	[ºC]	Initial temperature at the back of sample
T_2	[ºC]	Final temperature at the back of sample
Q_o	[kW/m²]	Incident heat flux density
Q_c	[kW/m²]	Transmitted heat flux density
R	^{o}C/s	Rate of rise of the calorimeter temperature in the linear region
A		The absorption coefficient
A	[m²]	Area
C_p	[j/Kg.K]	Specific heat capacity
M_o	[mN.cm]	Bending moment

***** Nomenclature of other variables are further explained along with each equations

Abbreviation

ASTM	American standards for testing materials
FFPC	Firefighter protective clothing
FFC	Firefighter Clothing
ISO	International organization for standardization
TPP	Thermal protective performance
RHTI	Radiant heat transmission index
LOI	Limiting oxygen Index
NFPA	National fire protection agency
PCMs	Phase change materials

CHAPTER 1: INTRODUCTION

1 Introduction

Firefighters are always performing their duties under constant threat because of hazardous working surroundings due to which they need appropriate amount of protection. Firefighters are subjected to harmful environment like intensive thermal radiation, heated climate, contact with high temperature objects, flash fires while conducting their operational activities [1][2]. Firefighter clothing is generally multi-layer clothing ensemble which guarantee the safety of firefighters from threats like flame, spillage of chemicals, external radiant heat flux and maintain thermal equilibrium to human body by avoiding any opportunity of fatal skin burn injuries [3] [4]. Firefighter protective clothing consists of exterior or outer shell, moisture barrier and thermal barrier [5] as shown in figure 1. The exterior shell is made of those materials which on having contact with flame and heat do not burn or degenerate i.e. they prevent ignition when have contact with flame and they must also possess characteristics of water repellence and good thermal insulation. Normally, fibers like combination of Nomex and Kevlar (Nomex III A), Zylon, polybenzimidazole (PBI), kermel and some flame-retardant finishes like Pyrovatex and Proban are employed for improving thermal protective performance [4].

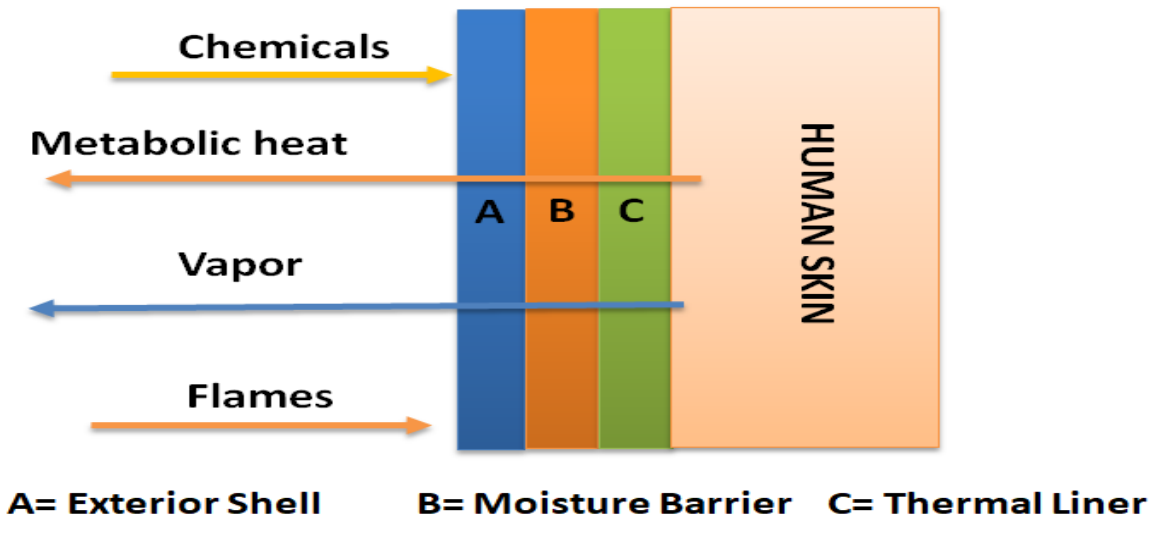

Figure 1: *Configuration of Firefighter clothing* [4][5]

The moisture barrier is a microporous membrane located between outer shell and thermal barrier. This layer permits water vapors to pass through but is impermeable to liquid water. Its primary objective is to guard the body of fire fighters from liquefied chemicals [4]. Moisture barrier is accessible in the market as Action, Proline, Goretex, Cross tech and Neo Guard. The thermal barrier shield human body by halting the environmental heat and this layer usually employs flame retardant fibers and their blends. It can be in the form of lining fabric, knitted fabric, nonwoven, quilted batting, laminated woven and spun laced [4][6][7].

The principal functionality of firefighter clothing is to make sure that the rate of escalation of human skin temperature must be declined or slowed down. In this way, adequate amount of time is provided to the firefighter for conducting their duties efficiently and effectively with minimization of hazardous injuries to human body skin [8][9]. This functionality of firefighter clothing is expressed as thermal protective performance (TPP), which is regarded as the most critical factor in the performance of firefighter clothing. TPP means how well firefighter protective clothing protects the body of firefighters before acquiring second degree burns. In terms of protective performance of firefighter clothing, time is the key factor. Enhancement in thermal protective performance of firefighter clothing extends the duration of time for firefighters to conduct their activities without embracing any significant injuries. In consequence, firefighters can consume more time in hazardous risk environment, saving precious lives and reducing damages caused by fire without enduring injuries to themselves [10][11][12][13]. Thermal protective performance test helps in determination of how well a fabric protects firefighter against second degree burns when exposed to flash fire. Thermal protective performance is evaluated by several tests like bench scale test (Heat guard plate, TPP tester)[6][7][14][15][16][17] or full scale test methodology like thermal manikin [18][19]. Moreover, properties like thermal conductivity and water vapor resistance can be evaluated by sweat guard hot plate method employing skin model as per ISO standard 11092 [19] and permeation of air of multilayer protective clothing on bench scale can be evaluated by air permeability tester. If size of sample is small or cutting of the sample is not permitted, equipment like Alambeta and Permetest can also be employed to evaluate thermal resistance, thermal conductivity and water vapor permeability respectively of specimen. The thermal protective property of clothing materials against radiant heat flux can be measured according to ISO 6942/ EN 366 [10][17].

1.2 Current State of Problem

Scientists are making lot of attempts for the enhancement of thermal protective performance of firefighter clothing. There are several approaches for incrementing thermal protective performance of firefighter protective clothing i.e.

i. By increasing thickness of firefighter protective clothing [20][21].

The thickness of fabric has significant impact on thermal behavior of textile substrate. This might be due to reason that increment in thickness of textile substrate influence the porosity of fabric due to consequent enhancement in fabric volume [22]. However, if increase in thickness can cause significant increase in corresponding weight of textile substrate, it might make thermal protective performance counterproductive [23].

ii. By increasing air gaps between different layers of protective clothing [24].

The other approach is to increase the thickness of air gap to certain degree for increasing thermal protective capability of firefighter protective clothing (FFPC) owing to good thermal insulation property of static air. However, the size limit of air gap between layers is very critical otherwise it may result into natural/forced convection reducing thermal insulation property FFPC assembly.

iii. By application of Phase change materials to thermal barrier of firefighting clothing specimens [25].

In recent years, scientists are employing Phase change materials (PCMs) on thermal barrier for increasing thermal protective performance of FFPC. PCMs provide protection from heat in passive way by absorbing heat from external heat flux [25][26]. Furthermore, the impact of phase change materials (PCM) was for very short duration of time.

iv. By Lamination of Aluminum foil on surface of firefighter protective clothing

For thermal stability and better thermal protective performance, Aluminum foil was employed on outer surface of firefighter clothing especially when they are subjected to high radiant heat flux density. However, this might cause issues in breathability of the firefighter protective clothing [26].

CHAPTER 2: SCOPE AND RESEARCH OBJECTIVES

Scientists are trying their level best to find appropriate solutions for improvement in thermal protective behavior of firefighter protective clothing by utilizing some alternate insulating materials or flame/heat resistant coating materials. For the last ten years, aerogel based insulating substrates are being used in applications like aerospace, defence and construction. Among all these aerogels, silica based aerogels have remarkable insulation and flame proof properties. Silica based aerogel is hydrophobic substrate having porosity greater than 90 percent and specific surface area of nearly 1000 m^2/g. The thermal conductivity of silica based aerogel is approximately 0.015 [W/(m.K)][27]. All of these characteristics make silica based aerogels a favorable candidate for utility in firefighter protective clothing as thermal barrier. Silica based aerogels are available on commercial basis as Nanongel particles by Cabot corporation and as aerogel blankets by Aspen aerogel [28][29].

For enhancing thermal protective performance, metallic foil of Aluminum bonded to outer shell of firefighter protective clothing are utilized because of good reflective property, inflammable nature and high melting point [30]. A significant improvement in TPP was witnessed but at the expense of breathability as exterior shell was totally covered with metallic foil. Consequently, scientists come with the idea of utilizing metallic particles for coating of textile substrate which can improve thermal protective performance without having significant difference in air permeability and water vapor permeability. Metallic particles of silver, aluminum oxide and titanium dioxide have high melting point and good reflective property. For impregnation of these particles on textile substrate, a physical vapor deposition (PVD) technique called magnetron sputtering was employed. In case of metallic particles, silver is one of the metals which have high melting of 962 ^oC along with outstanding reflective property [31][32]. In consequence, silver particles can be a good prospect for utilizing as deposition layer on exterior side of outer shell. As a result, the layer of coating is certain micrometer thick, and unlike PCM [25], the impact for enhancement might be witnessed for longer duration of time and arrangement of clothing assembly was easy as compared to that of arrangement of clothing assembly involving increment of air gap size.

2.1 Aims and objectives

1. Evaluation of thermal insulation properties of firefighter clothing specimens.

Initially, different combinations of multilayer firefighter protective clothing samples were arranged and their thermal insulation properties were measured. Later on, permeation of air and thermal protective performance was determined for each firefighter clothing specimens. This might provide useful information about different firefighter clothing assemblies in terms of thermal insulation and thermal protective behavior. Moreover, the outcomes might also be helpful in improvement of thermal protective performance for further experimental work.

2. Improvement in thermal insulation properties of firefighter protective clothing with the help of aerogel blanket.

In this scenario, comparison of thermal protective behavior of aerogel blankets was done with commonly used thermal barriers. Aerogel blanket was used as an alternate to thermal barrier for seeking improvement in thermal insulation and thermal protective behavior. As a result, more time can be acquired by firefighters without suffering acute burn injuries.

3. Effect of metallic coating on thermal protective performance of firefighter clothing specimen keeping in view the breathability and flexibility of specimens.

A suitable physical vapour deposition process was employed to coat the exterior side of outer shell with metallic particles for maintaining ergonomics of firefighter protective clothing. Thus a comparison can be made for evaluation of thermal protective performance. Moreover, breathability of these coated specimens along with their bending moment properties was also investigated.

4. Impact of metallic coating on emissivity of specimen and influence of washing on thermal protective performance of both uncoated and silver coated specimen.

The affect of metallic coating on thermal protective performance and durability of metallic coating was investigated. The influence of metallic coating on emissivity was also evaluated for uncoated and metallic coated outer shell. The purpose of the washing was to determine the durability of metallic coating and how much thermal performance is affected by the washing.

5. Implementation of Numerical model for prediction of temperature distribution for both uncoated and silver coated specimen.

Finally the Numerical model was used to predict distribution of temperature through fire fighter clothing. Numerical approach was selected considering the effect of metal coating on the outer layer. Finite difference method was employed for solution of partial differential equation and implicit method was utilized to discretize partial differential equations. The equation shows good prediction. Comparison of results for uncoated and silver coated fabric assembly obtained from numerical solution show almost similar pattern as observed in the experimental results. This work can be very useful to determine the overall heating protection property of the firefighter clothing.

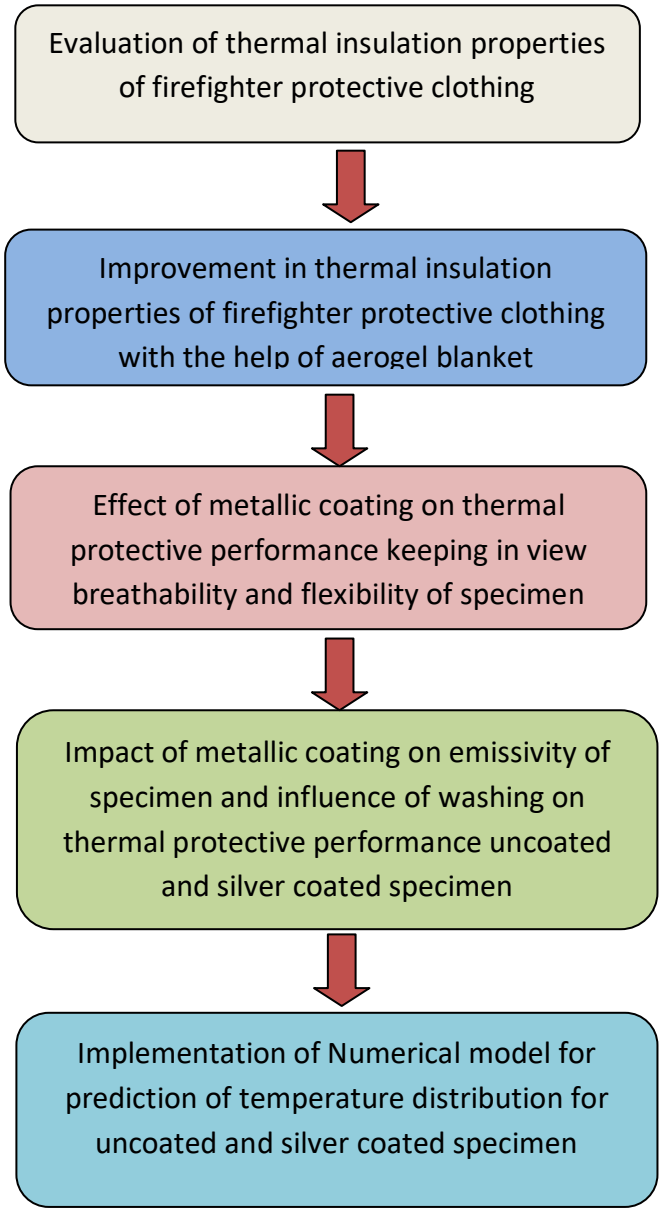

Figure 2: *Flow diagram of objectives*

CHAPTER 3: LITERATURE REVIEW

3.1 Background

Clothing not only serves as an obstacle to exterior atmosphere but also work as a channel of heat transmission from human body to surrounding atmosphere [33]. Heat exchange in clothing inculcates conduction by means of air gap and fabric layer, convection of air gap and radiation from the one fabric layer to another fabric layer [34]**.** The transference of heat means the rate of energy that is being exchanged from the medium of high temperature to low temperature medium and this transmission of heat continue until two medium reach the same temperature. Heat exchange through the conduction develops due to physical connection of two medium. Greater differentiation in temperature results in the swift flow of heat between two substrates. The mechanism of conduction inculcates transportation of energy from higher energy molecules to lower energy molecules. When clothing is worn by human being, the process of conduction takes place between two contact textile fabrics or between textile fabrics and human skin. The rate of energy being transmitted is dependent on temperature gradient and extent of resistance between two medium and is termed as thermal conductivity, which can be illustrated by the following equation [35][36]:

$$\dot{Q} = \frac{\lambda A \Delta T}{x} \quad (1)$$

In the above mentioned equation , $\dot{Q}$ is the rate of heat flow [W or J/sec], A is the area [m^2], λ is thermal conductivity [W/(m.K)]. ΔT is temperature difference [K] and x is thickness of the material [m].

The convective heat transmission in clothing is the consequence of movement of air in textile substrate which is contingent on the openness of the fabric. When contact is made by air with the warm surface, heat is absorbed due to which air becomes less dense. The gradient in density causes warm air to upsurge and as a result, natural convection takes place. However, wind can significantly influence convection and escalates heat transportation causing forced convection. In case of heat conduction, flow of heat is dependent on thickness of textile substrate. By increasing thickness of the textile substrate, more amount of air is confined in the fabric structure due to

which there is enhancement in thermal insulation. The rate of heat transmission due to convection can be calculated by Newton's law of cooling [35][36]:

$$Q = h_c A \Delta T \quad (2)$$

In the above mentioned equation, A is the heat transmitted surface area [m^2] and h_c is the coefficient of heat transmission from the surface to the fluid and is known as "convective heat transfer coefficient" [$W/m^2.K$] and ΔT is temperature difference [K]. This equation is true for the situation when the surface is heated due to movement of fluid having high temperature than the surface. Heat transmission through radiation does not require any material medium and textile substrates and it can be significant in low density textile substrates. The transfer of heat via radiation takes place in the form of electromagnetic waves. Transfer of heat by radiation from the body at temperature T is given by the following relation [35] [37]:

$$Q = A\, \varepsilon \sigma T^4 \quad (3)$$

Where ε is the emissivity of surface and σ is Stefan-Boltzman constant whose value is 5.67×10^{-8} W/m^2K^4 and T is the temperature of the body in [K] and A is area of surface [m^2].

3.2 Mechanism of thermal equilibrium of Human Body

Equation 4 illustrates summary of heat balance of human body [14][37][38][39]

$$M - W = C_{conv} + C_{cond} + R + E_s + E_{resp} + C_{resp} \quad (4)$$

M = Rate of metabolism (interior heat generation, W/m^2)

W= External work load (W/m^2)

C_{conv} = Heat loss due to convection (W/m^2)

C_{cond} = Heat loss due to thermal conduction (W/m^2)

R= Heat loss due to thermal radiation (W/m^2)

E_s= Heat loss due to evaporation from skin (W/m^2)

E_{resp} = Evaporative heat loss due to respiration (W/m^2)

C_{resp} = Sensible heat loss due respiration (W/m^2)

As human body persistently generates heat, therefore rate of metabolism is positive all the time. But, it differs with the amount of activity performed by human body [38]. External work load is negligible in most of circumstances [40]. Conduction permits the human body to evacuate heat from the soles of the feet or during sitting or lying on cooler place. However, the quantity of heat lost by conduction is generally negligible [41]. If the temperature of air is lesser than the temperature of skin, the convective heat term (C_{conv}) is positive and there will be discharge of body heat to surrounding atmosphere. On the other hand, (C_{conv}) is negative when the temperature of air is higher with respect to temperature of skin and the body acquires heat from the surrounding atmosphere [39].

When the ambient temperature exceeds skin temperature, evaporation of sweat is the only means by which human body can discharge heat from the skin [39]. Threkled [41] mentioned that evaporation heat loss is contingent on proportion of air humidity and mass transmission coefficient for specified individual surface temperature. At elevated temperature, when removal of heat due to conduction and radiation may not be possible then evaporation becomes the prime factor for heat evacuation from the human body [39]. However, when temperature of climate is very low, evaporation offers negligible influence in thermal equilibrium of human body [39].

Thermal radiation is being emitted by all the bodies and heat discharged via radiation takes place in the mode of infrared rays. A naked human body at normal temperature of room might give up approximately 60 percent of overall heat through radiation [39]. When radiation is confronted by a body, three possibilities might happen:

i. Transmission of radiation in continuous way without being affected
ii. Deflection or reflection of radiation from its path
iii. Absorption of radiation

Heat is acquired or lost by the body due to gradient between surface temperature of human body (apparel and naked skin) and mean radiation temperature (MRT) of surrounding atmosphere

[39]. In the absence of flow of air, radiation is the only mode of heat transfer between the body and surrounding climate [39].

3.3 SiO_2 aerogels and its application in firefighter protective clothing

The discovery of silica based aerogels in 1930s by Samuel Stephens Kistler was based on concept of substituting the liquid phase with the gaseous phase along with little amount of shrinkage and without crumpling of gel solid network. Aerogels are synthesized by Sol-Gel process [42]. In this method, a chemical reaction was carried out in a solution at low temperature to produce inorganic network or creation of an amorphous structure from the solution. The distinct feature of this reaction was conversion from colloidal solution to di-or multiphase gel. Silica based aerogels have 96 percent of air and 4 percent of silicon dioxide, making silica based aerogels as one of the lightest weight solid substrates [43]. A sol is a colloidal suspension of solid particulates in an aqueous medium in which range of dispersion phase is from 1 to 1000 *nm* [44]. Sol can be synthesized either by condensation or dispersion of particulates. Condensation occurs when nucleation development of particulates approaches adequate size. However, dispersion includes breaking of large particulates to colloidal sizes. In case of gelatin process, a free flowing sol is transformed into a three dimensional solid structure encapsulating the solvent media [44][45].

3.3.1 Structure of pore

Silica based aerogels are mostly mesoporous having interlocked pore size with range from *5 to 100 nm*. The diameter of average pore is between *20 to 40 nm* [46][47] . The specific surface range from *250 to 800* $m^2\ g^{-1}$ and can surpass *1000* $m^2\ g^{-1}$.

3.3.2 Thermal insulation, flame proof property

Silica based aerogels have very small portion of solid silica (nearly 1-10%) due to which they have lesser solid conductivity and thus exchange lesser thermal energy [45]. At ambient pressure, temperature and relative humidity, silica based aerogels have very low thermal conductivity of the order 0.015 [W/(m.K)] which is expressively lesser than thermal conductivity of air [0.026 W/(m.K)] under same circumstances [27]. Apart from having thermal insulation

property, silica aerogel has remarkable flame proof property [48]. By means of mass, aerogel is least dense man-made substrate [45]. Aerogel can abrogate all three modes of heat transfer. Conductive heat transfer is blocked because of nanometer pore size and porous structure of aerogel [49]. Convective heat transfer is averted because structure of aerogel does not allow circulation of air [50][51]. Infrared radiation that plays role in transference of heat can also be absorbed by aerogel [52][53][54]. As consequence, aerogel can function as outstanding thermal insulator [55] [56][57][58].

3.3.3 Sorption and Entrapment properties

Aerogels can be utilized to adsorb some chemical compounds i.e. waste water treatment for restricting radioactive waste or for filtration of gases. Silica aerogels soaked with $CaCl_2$, LiBr and $MgCl_2$ salts have also been confirmed to absorb water for retention of heat at low temperature [59]. It was suggested that hollow silica aerogel droplets can be employed for inertial entrapment of fluids, specifically blends of liquid deuterium and tritium [60].

3.3.4 Application of silica aerogel at high temperature

At present the most common utility of aerogel products are in oil and gas pipelines, building insulations along with aeronautics/aerospace and high temperature applications [61]. Aerogel is commercially available as Nanogel^{TM}, which can be employed as super insulating filling substrates. Moreover, aeogel is also available as Compression pack ^{TM} for special applications like pipe in pipe and cryogenic insulation systems. Apart from that, Aspen company is providing blanket-based products for insulation of building on commercial scale and also developing products for utility in acute hot and cold climates (pyrogel and cryogel) [62][61]. Novel advancements of aerogel science have made it viable to create more flexible aerogels in simplified ways. All these features make aerogel favorable prospects to be utilized for enhancing thermal protection and thermal insulation in fire fighter protective clothing. Firefighters are subjected to several threats with respect to their working atmosphere. In addition to numerous toxic ingredients in the surrounding atmosphere, extreme radiant heat fluxes and hot flames are probable hazards in fire extinguishing activity. Thermal protective performance of fire fighter protective clothing is of huge significance to the lives of firefighters [14].

The key purpose of fire fighter clothing is to decline the rate of heat accumulation in human skin so as to give time for the firefighter to respond and avert or reduce skin burn injury [5]. Jin et al [5] investigated thermal protective behavior of nonwovens employed with aerogels. It can be noticed that specimen coated with aerogels had greater limiting oxygen index (LOI) values than the untreated specimen. This might be due the fact that inorganic aerogel particles being attached on the surface of specimen might enhance the flame retardant characteristics [5]. For evaluation of effect of aerogel on thermal protective performance (TPP) of the whole fire fighter garment, aerogel treated firefighter clothing utilizing thermal liner in fighter protective garment was developed by Jin et al [63]. Instrumented manikin system was utilized under heat flux density of 84 kW/m^2 with 8 seconds of exposure time. For aerogel treated fire fighter clothing, total burn injury was 12.7 percent which was lesser than that of existing garment having 25.1 percent [63]. It was also witnessed that aerogel impregnated sample when utilized next to skin can absorb moisture and discharge it ambient surrounding with great ease. Moreover there was increase in the rate of moisture absorption when aerogel impregnated layer was employed next to skin [63]. Thus it was deduced that aerogel when coated on textile substrate can enhance thermal resistance of the fabric and delivers better thermal insulation properties.

3.4 Protection against Fire

In case of protection against thermal radiation and flame, two scenarios have been identified: In first case, heat and flame might crop up intermittently and unexpectedly, e.g. in accidents or in war; In second case, they are features of many work places, e.g. in rolling mills or smelting-works, during fire-fighting or rescue operations [10] [64].

Human skin starts to feel pain at 45^oC [10] and the skin completely burn at 72^oC [10], which indicates that human skin is very sensitive to heat. At temperature greater than 44°C [10] the cells get damaged by degradation of proteins tissues [10]; the rate and depth of this damage increases with escalation of temperature. Burns can be classified into three categories according to depth of damage [10][64] :

i. First degree burn
ii. Second degree burn
iii. Third Degree burn

i. First Degree Burn

It is a superficial burn or wound. This burn is an injury that affects the first layer of your skin. These burns are one of the mildest forms of skin injuries, and they usually don't require medical treatment. First degree burns might result into Scalds and Sun burn [64]. Temperature of first degree burn ranges from 44 ºC to 55 ºC [65].

ii. Second Degree Burn

Also known as partial thickness burns involving the epidermis and part of the dermis layer of skin. The burn site appears red, blistered, and may be swollen and painful. Blisters, deep redness and burned areas occur due to second degree burn [64]. For second degree burn, range of temperature varies from 55 ºC to 60 ºC [65].

iii. *Third Degree burn*

It is full thickness burn that goes through the dermis and affect deeper tissues. Third degree burn resulted in white or blackened, charred skin that may be numb. Figure 3 shows different degrees of burn [64]. Third degree burns occurs above 60 ºC [65].

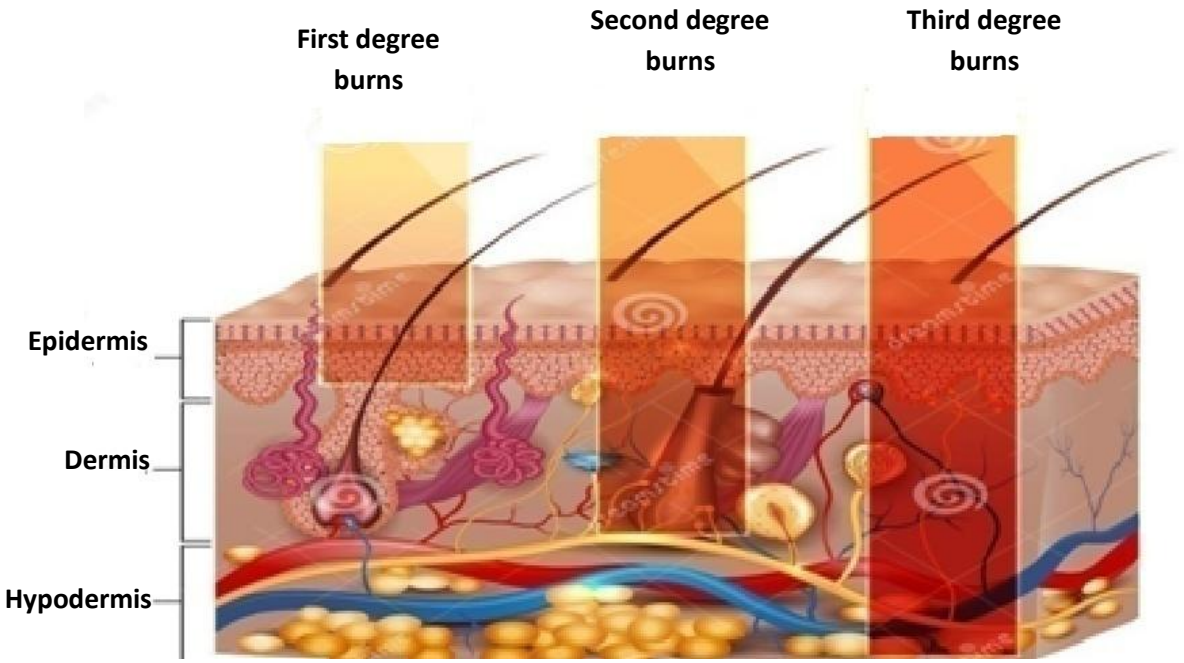

Figure 3: *Schematic diagram of categorization of burns [63]*

Generally, 3-10 seconds can be availed by person to get away from a place of fire with a heat flux of about 130 – 330 kW/m^2 [66]. Majority of the textile fibers are easier to burn or degrade.

Protective clothing must be able to resist flame and has capability to develop heat barrier. The latter is very pertinent if the wearer needs to withstand flames for a fairly long time [66]. It was observed that the main reason of death in a fire accident is not direct burning. Consequently, the use of non-toxic or low-toxic burning materials is very important for protection. Considering safety, the government regulations mention that some classes of garments and home textiles like carpets, upholstery fabrics, children's sleep wear and bedding should be made flame retardant or flame resistant [67].

Makinen [7] mentioned that most of the previous studies were performed under the conditions of acute heat fluxes, however emergency situations are not common and firefighters are most commonly subjected to routine and hazardous situations [6]. Table 1 shows range of heat fluxes and temperature linked to various firefighting situations.

Table 1: *Different conditions with respect to Heat flux and temperature [6] [7]*

Conditions	Heat flux (kW/m^2)	Air Temperature (^oC)
Routine conditions	0.42 to 1.26	10-60
Hazardous conditions	1.26 to 8.37	60-300
Emergency conditions	8.37 to 125.6	300-1000

Routine conditions are those in which firefighters are employing hoses or fighting fires from a distance, or standing in front of a small open fireplace.

Hazardous conditions are battled outside a burning room or a small burning building. The less severe hazardous condition regions are related to firefighters who are ventilating a fire without water support. The more severe hazardous conditions regions are associated to firefighters who are encountering these situations in a burning building. A "turnout uniform" is mandatory for delivering sufficient burn protection by declining the thermal stress withstands by the firefighters.

Emergency situations are generally not faced by civilian firefighters; such circumstances exist around a crashed aircraft when fuel is burning ferociously. This situation may also take place during "flashover" of a building fire. There is requirement of specialized equipment for very high levels of heat flux and temperature. Proximity suits are employed by firefighters working close

to the fire, and these suits must be engaged together with breathable equipment for working in the fire [10].

In case of thermal exposures the main concern for firefighter is thermal radiation from smoke, flames, hot gas convection, and conduction from high temperature surfaces [68]. Each of these modes of heat transmission might have deep influence on the thermal performance of fire fighters' protective clothing, and all of them can cause burn injuries. Nevertheless, in genuine firefighting situations these diverse components of heat transfer are likely to be pooled in varying fractions depending on the location and location of the fire fighter in relation to the fire's varying thermal environment. The fact that the constituent fractions of heat transfer differ during an exposure perplexes the evaluation procedure and enhances the measurement uncertainty [10].

3.4.1 Firefighter clothing

When body of firefighter is subjected to a heat stress, their body responds by activation of sweat glands through evaporative cooling mechanism. The protective clothing shields the firefighters from environmental heat and moisture but at the same time averts their flow in the opposite direction, away from the body to the environment. As a result, jeopardy of heat stress and steam burn injuries significantly enhances. In such hot climate, heat and moisture transfer properties of the protective clothing have strong influence on firefighters' performances and their safety. Escalation of these transportation procedure from the skin through the garment could increment comfort of the wearers and hence their performance. Efficient protective clothing should minimize heat stress while delivering protection [6]. For this reason, the firefighter protective clothing has to accomplish a variety of different demands according to the European standard EN 469 protection against thermal radiation and heat from flames, shield against hot liquids and other chemicals, resistance against abrasion and other mechanical stress, breathability, inflammable, unshrinkable, easy to wash, light and comfortable[17].

Firefighters are dependent on firefighter apparel made from DuPont™ Nomex® and Kevlar® fiber to satisfy the demands of a challenging and meticulous duty. Communally, these novel fibers help in fire resistance, strength and stability. The strength of Kevlar® is five times more than steel on an basis of equivalent weight, however fabrics can be thermally protective, light weight and comfortable. Intrinsically, Nomex fiber is flexible, tough and flame resistant [69].

Nomex® fiber carbonizes and thickens after being exposed to the intense heat of today's fires. This increases the protective barrier between the heat source and the user, helping to reduce burn injury and providing valuable time to work or escape.

When fabric constructed with Kevlar® fiber is combined with Nomex® fiber or utilized with another blend, it can help to further escalates tear strength and abrasion resistance of outer shells protecting the moisture barriers and thermal liners inside. DuPont™ Nomex® and DuPont™ Kevlar® brand fibers are extensively employed in firefighter clothing systems. These fibers will neither melt nor drip, nor will support combustion thus providing a stable barrier that helps minimize burn injuries. Each layer of flame resistant clothing delivers a protective obstruction from the heat source and entrapped insulating air. Multiple layers provide more thermal insulation but can also trap metabolic heat, increasing heat stress [69][10] .

3.5 Configuration of Firefighter clothing assembly

The structure of firefighter clothing assembly involves outer shell, moisture barrier and thermal liner.

Outer shell

The outer shell is developed for everyday utilization of firefighting. This outermost layer is configured to shield the interior components from thermal hazards, abrasion, sunlight and other parameters inculcating in fighting against hazardous fire. The outer shell defy ignition after being subjected to thermal radiation for a short period of direct flame contact. Normally only intrinsically flame-retardant fibers, such as aromatic polyamides (aramids) and polybenzimidazole (PBI) are employed for the outer layers of firefighters' turnout suits. On commercial scale there are class of aramids from different manufacturers, e.g. Nomex (DuPont), Fenilon (Russian), Conex (Teijin), and Apyeil (Unitika). Para-aramid fibers like Kevlar (DuPont), Twaron (Akzo Nobel) and Technora (Teijin) are employed in blends with meta-aramids to increase sturdiness, e.g., Nomex III (blend of Nomex and Kevlar (95/5%) and X-fire (blend of Teijin Conex and Technora). Especially in France, a polyamide-imide fiber called Kermel from Rhone-Poulenc is used for firefighters' protective clothing. Polybenzimidazole (PBI) fiber was developed by Celanese. Its advantage is that it absorbs more moisture than does cotton, and has a comfort rating from the wearers equivalent to that of 100% cotton. The fibers

on the market have the following trade names: Nomex®III, Nomex® Antistatic (IIIA), Nomex® Outer shell Tough (Delta T), Kermel® HTA, PBI®Gold (Ibena). Typical blends are PBI/aramid, Nomex with flame-retardant viscose and flame-retardant wool, Kermel with viscose. Furthermore, In addition to the above fibers, in the garments for wild land firefighting, some materials with flame-retardant finishes (FR) (e.g. Proban® and Pyrovatex® for cotton) are used. They must hold on to the FR properties after 50 launderings (ISO 15384:2003) [70][10][4].

Moisture Barrier

Moisture barrier includes moisture membranes which are vital element in protective clothing against heat and flame due to their dual role in preventing water penetration while permitting perspiration of water vapor to exit. Microporous moisture barriers are generally synthesized from expanded polytetrafluroethylene (e-PTFE) laminated to aramid fabric [71]. The moisture barrier provides defense against liquid water as well as against many common liquids such as chemicals. The moisture barrier can be a microporous or hydrophilic membrane or coating [66].

The moisture barrier in firefighters' clothing is:

i. a lightweight knitted substrate or web, placed in loosely between the outer fabric and thermal liner, or

ii. laminated or coated to the interior side of the outer shell fabric

Microporous moisture barriers are generally prepared from expanded polytetrafluroethylene (e-PTFE) laminated on an aramid fabric. The principle under the membrane breathable function is the enormous difference in size between water vapor molecules (~ 0.4 *nm* in diameter) and water droplets which usually exceed 100 μm in diameter which are larger than the size of membrane pores [71].

Thermal Liner

The thermal liner delivers the most thermal insulation by entrapment of air in either a conventional needle-punched batting or between multiple layers of fabric. The durability of this layer is enhanced by quilting these substrates to a woven facecloth fabric. The friction and adsorption of moisture parameters may influence the comfort and mobility of clothing as this layer is close to human body.

Generally, thermal liner is prepared from intrinsically flame-retardant fabrics or their combinations. When thermal liner and exterior shell substrate are made up of same or similar material, the washing of protective garment becomes easy. A newly developed thermal insulating barrier was developed WLGORE company to substitute conventional thermal barriers [72].

3.6 Test for evaluation of Thermal performance

There are two thermal performance tests in the NFPA 1971 standard: a fabric flammability test and the TPP test.

i. The thermal protective Performance (TPP) test evaluates how good a fabric defends the Firefighter against second-degree burns in a flash fire. The greater the TPP value, the better will be thermal protection the fabric provides as compared to other fabrics. A minimum TPP rating of 35 is the mandatory as per requirement of the NFPA standard

ii. The fabric flammability test has resulted in the configuration of protective garments that resist flaming ignition

At TPP of 35, a fire fighter would have about 17.5 seconds to get away from a flashover exposure before acquiring second degree burns. Most common misconception is that if 35 is good, a rating of 40, 50, or even 60 must be good but it is not like that. A greater value of TPP at expense of enhancement in weight is not considered good as it may result in heat stress for fire fighters [73][74][10].

3.7 Test standards for evaluation of performance of firefighter clothing

Most common standards used for evaluation of performance of firefighter protective clothing in accordance with EN 469 are:

3.7.1 EN ISO 15025

A distinct flame is applied to the surface or bottom edge of vertically oriented textile substrate from specific burner for 10 seconds. Observation about spread of flame, after glow, formation of debris, flaming debris or a hole is noted. Documentation of after flame time and afterglow is recorded [75].

Important terms

i. Application of flame time

Duration of time for which ignition flame is applied to textile specimen

ii. After flame time

Length of time during which textile substrate keeps on burning under specific test environment, after source of ignition has been taken away. This time is evaluated to nearest second.

iii. After glow

Determination of glowing combustion of textile substrate under specific conditions i.e. after termination of flame or elimination of ignition source.

iv. After glow time

Duration of time for which textile substrate persists to afterglow under specific test conditions after termination of flame or elimination of ignition source.

v. Char

Development of carbonaceous brittle residue when textile substrate is subjected to thermal energy source.

vi. Hole

A break in the sample of textile substrate in any direction having permanent perimeter caused by melting, glowing and flaming [75].

3.7.2 EN ISO 12127

The heating cylinder is heated to and kept at the contact temperature and a test substrate is positioned on the calorimeter. The heating cylinder is lowered onto the test specimen supported by the calorimeter or, on the other hand, the calorimeter with the textile substrate is raised up to the heating cylinder. The procedure is performed at a constant speed in both cases. The threshold time is evaluated by noting the temperature of the calorimeter [76].

Important Terms

i. Contact temperature (T_c)

Constant surface temperature of contact area of heating cylinder

ii. Start of timing

It is the instant when the upper surface of the calorimeter and the underside edge of the heating cylinder are 10 mm away from of each other

iii. Threshold time (t_t)

It is time between the start of timing and instant when the temperature of the calorimeter exceeds 10 °C above its starting value [76]

3.7.3 EN ISO 9151

Horizontally tilting test substrate is partly constrained from moving and subjected to an incident heat flux of 80 kW/m^2 from the flame of a gas burner placed beneath it. The heat flowing through the textile substrate is evaluated by means of a small copper calorimeter on top of and in contact with the specimen. The time, in seconds, for the temperature in the calorimeter to escalates (24 ± 0.2) ^oC is noted. The mean outcome for three test substrates is determined as the "heat transfer index (flame)"[77].

Important Terms

i. Incident Heat Flux density

Amount of energy incident per unit time on the exposed surface of the textile substrate, mentioned in kilowatts per square meter (kW/m^2).

ii. Heat transfer index

It is evaluated from the mean time in seconds to acquire a temperature escalation of (24 ± 0.2) ^oC by employing a copper disc having mass of (18 ± 0.05) g and initial temperature of (25 ± 5) ^oC.

3.7.4 EN ISO 6942

A textile substrate is affixed to the face of a calorimeter and subjected to a specific level of radiant heat. The times for which temperature escalates to 12 °C and 24 °C in the calorimeter are noted and outcomes are mentioned as a radiant heat transfer index and the percentage heat transmission factor [17].

Important terms

i. Percentage heat transmission factor (Percentage TF Q_o)

It is determination of the percentage of heat acquired by the calorimeter when test specimen is positioned in front of it. It is equivalent to the percentage ratio of the transmitted to the incident heat flux density.

ii. Radiant heat transfer Index (RHTI)

A whole number evaluated from the mean time in seconds to acquire a temperature rise of $(24 \pm 0.2)°C$ in calorimeter when evaluated by this method with a specific incident heat flux density [17].

3.8 Air Permeability

Air Permeability is defined as rate of flow of air through textile substrate under the gradient of pressure between the two surfaces of textile substrate.

$$A = \frac{V}{t(\Delta P).F} \tag{5}$$

V is the capacity of the flowing medium [m^3], t is the time flow [sec] and Δp is the drop in pressure of the medium [Pa], F is the area through which the medium is flowing [m^2]. Development of woven fabrics takes place due to interlacement of yarns. There exists free space between yarns and fibers which plays a role in configuration of air flow paths when pressure difference is employed. The permeation of air through textile substrate is indispensable for the estimation of comfort properties of fabric and the performance during drying process. Fabric properties like thermal insulation, transmission of moisture from human body to surrounding

environment, the rate of exclusion of liquid during drying of textile substrate and liquid removal during drying of textiles is dependent on permeation properties of textile substrate. Thickness of fabric and the applied pressure drop are one of prominent factors that influence permeability of air [78].

3.9 Thermal Resistance

Thermal resistance is defined as evaluation of temperature differentiation by which an object resists flow of heat. It indicates how well material insulates [79].

$$R = \frac{x}{\lambda} \tag{6}$$

Where x is thickness [m] and λ is thermal conductivity [W/(m.K)]. Thermal resistance is a determination of the resistance that a textile substrate delivers against heat loss from the human body of the wearer to the external climate [80]**.**

3.10 Clo

Clo is the determination of clothing insulation and one clo is defined as the insulation of a textile garment that kept a sitting–resting average male comfortable in a ventilated room of 0.1 m/s air velocity at temperature of air around 21°C along with relative humidity lesser than 50 percent. It is suggested that approximately 24 percent of the metabolic heat is lost due to evaporation from the skin and residual 38kcal/m^2h is exchanged through the clothing system by radiation, conduction and convection. The mean skin temperature at comfort level is 33°C. The total insulation of the clothing plus the ambient air layer is given by [15]:

$$I_T = \frac{33 - 21}{38} = 0.32\ m^2\ °\text{C h/kcal} \tag{7}$$

At above precise condition, insulation of air is 0.14 m^2 ^{o}C h/ kcal, the insulation of the clothing is 0.18 m^2 °C h/kcal, which is the differentiation between the total insulation of the textile garment along with the ambient air layer (i.e. 0.32 m^2°C h/kcal) and insulation of air layer (0.14 m^2 °C h/kcal). Thus, 1 clo is mentioned as 0.18 m^2°C h/kcal, which is equivalent to 0.155 m^2°C/W [15]. This insulation of clothing is termed as effective insulation. A warm garment assembly delivers approximately 1 clo of insulation for the entire body [81].

3.11 Tog

Unit of thermal resistance is Tog. It is illustrated as the thermal resistance capable of maintaining temperature difference of 0.1 ℃ with a heat flux of 1 W/m^2 [82]. A light summer suit provides 1 tog insulation.

3.12 Met

It is used to compute metabolism of man taking rest in sitting post under the situation of thermal comfort. One met is equal to 50 kcal/m^2h (i.e. 58.2 W/m^2) [83]

3.13 Thermal Absorptivity

Flow of heat between textile substrate and human skin is always due to temperature gradient. If skin temperature is higher than the textile substrate, heat will be transported from human body to fabric and person will endure cool feeling. This procedure is called warm cool feeling. Thermal absorptivity [84][85][86][87][88][89][90] is a characteristic of textile substrate which is related to warm/cool feeling of fabric at the instant of contact with surface of human skin. The greater the value of thermal absorptivity, the cooler will be the feeling. It was reported, thermal absorptivity is dependent on thermal conductivity, density and specific heat capacity of textile substrate. Thermal absorptivity is explained by following equation [84][85][86][87][88][89][90].

$$b = \sqrt{\lambda \rho c} \tag{8}$$

Here, λ is thermal conductivity [W/(m.K)], ρ is density [Kg/m^3] and c is specific heat capacity of textile fabric [J/Kg.K].

3.14 Thermal Diffusivity

It is used to determine ability of textile substrate to conduct thermal energy relative to its capability to store thermal energy. It is the thermal conductivity divided by density and specific heat capacity at constant pressure [89].

$$\alpha = \frac{\lambda}{\rho . c} \tag{9}$$

λ = Thermal conductivity , ρ = density and c = specific heat capacity of textile substrate

3.15 Water Vapor Permeability

It is also known as "breathability" and is defined as capability of textile substrate to transmit water vapour from surface of skin through the fabric to the exterior climate. Diffusion of water vapor should take place instinctively due to the vapour pressure difference through textile substrate. The water vapour disperses from the region of high vapour pressure (surface of human body) to the region of lower vapour pressure (exterior drier climate). The diffusion of water vapour takes place through fabric interstices and air spaces between the skin and the textile substrate [10].

3.16 Water vapor resistance

Water vapour permeability has inverse relation with water vapour resistance which is illustrated as amount of resistance against the transmission of water vapour through textile substrate. As liquid water has an excellent conductivity of heat, the thermal resistance of a garment is directly affected by quantity of moisture present in the fabric. Consequently, the more occurrence of water in textile substrate, either due to normal absorption from the air or absorption of water due to perspiration, the greater will be the rate of conduction of heat [10].

3.17 Permeability Index

Woodcock established [91] permeability index which displays evaporative performance of clothing. The permeability index (i_m) can be explained by the following equation:

$$i_m = \frac{R_t}{R_{et} . LR} \tag{10}$$

where R_t is the total thermal resistance of the clothing including surface air layer (m^2°C/W), and R_{et} is the total evaporative resistance of the clothing along with the air layer (m^2kPa/W) and LR

is Lewis relation which shows relationship between convective heat transfer and convective mass transfer.

3.18 Limiting oxygen Index (LOI)

Limiting oxygen Index is the concentration of oxygen (in vol %) that is essential to maintain a steady combustion of the samples after ignition. The higher the LOI of a polymer material, the lower the heat flux provided by its flame and the higher the flammability resistance [92].There are two reasons for polymers having different LOI values.

i. When there is higher ratio of hydrogen to carbon ratio in polymer, there will be greater propensity for burning.
ii. There are some polymers which emit blanketing gases which restrain burning.

Those polymers whose LOI values are greater than 25 are considered flame retardant polymers [93].

3.19 Surface Emissivity

Surface emissivity is denoted by ε which means relative ability of material to emit energy by radiation.

$$\varepsilon = \frac{Energy\ radiated\ by\ particlular\ material}{Energy\ radiated\ by\ black\ body} \tag{11}$$

A true black body ε = 1, whereas any real object would have emissivity value less than 1, for polished metal surfaces emissivity is nearly equal to 0. Emissivity is a dimensionless quantity [94].

CHAPTER 4: MATERIALS AND EQUIPMENT

All fabric layers utilized in firefighter protective clothing for the experimental work were supplied by Kivanc group turkey and Vochoc company Czech republic. Aerogel blanket was supplied by Ayvaz Yalitim company, Turkey.

4.1 Nomex [Conex]

These are made of aramid fibers which are available on commercial scale from different manufacturers like Nomex [Dupont] or Conex [Teijin]. They are utilized in outer shell because of excellent heat and flame resistance properties. When heat is absorbed by Nomex fabrics it carbonizes and forms protective char barrier. In this way it prevents the heat from entering into body of firefighter. Nomex degrade at 480 ºC [4][95][96]. Limiting oxygen index varies from 28 ~31 [97] .

4.2 Kevlar [Twaron]

These are para-aramid fibers commercially available as Kevlar (Dupont), Twaron (Akzo Nobel) and Technora (Teijin). Kevlar fibers are used as blends with blends with meta-aramids for enhancement in durability like Nomex III which is blend of Nomex and Kevlar and X-fire which is blend of Conex and Technora. Addition of Kevlar provides extra tensile and tear strength [4] [96]. The decomposition temperature is 590 ^{o}C. Limiting oxygen index is between 29~31 [97].

4.3 Kermel

Kermel is polyamide-imide fiber used in firefighter protective clothing. They are inherently inflammable because of high proportion of aromatic structure. They are employed in firefighter clothing because they are inherently non-flammable due to chemical structure having high proportion of aromatic structure and combined double bonds. They might also be used in the form of blends with fire retardant viscose. Kermel is smooth surface fiber with an almost circular cross section. These fibers have very high resistance to abrasion and thermal conductivity as low as any other aramid fiber. It has excellent resistance to chemicals [4] [98].

4.4 Lenzing FR or Fire retardant viscose

They are inherently flame resistance fibers which are contingent on high wet modulus cellulosic fiber. Lenzing FR is environment friendly and biodegradable fiber. Lenzing FR is speciality viscose fiber i.e. the fiber which is build up from natural raw material. These fibers have high moisture regain of almost 13 %. Therefore, they are used in blends with Nomex fiber to increase comfort properties. Lenzing FR fiber has flame retardant substrate inculcated throughout cross section of fiber to ensure permanent heat protection [99] .

4.5 Polytetraflouroethylene [PTFE]

It is a synthetic flouropolymer, which can be expanded to thin porous membrane having 1.4 billion pores per cm^2. This membrane is permeable to water vapor but impermeable to liquid water. In firefighter protective clothing PTFE membrane act as water barrier and it is laminated to fire retardant aramid or fire retardant viscose. This membrane is located within firefighter clothing assembly to protect from thermal impacts. By employing these membranes, water vapor is able to flee away from clothing. Due to this reason, evaporation of sweat from skin enhances. However, inner layers of clothing are shielded against liquid water which is coming from outside. Density of PTFE varies from 2.1-2.3 g/cm^3. Moisture regain is 0.01 % [100]. These PTFE membranes are laminated to non-woven web of Nomex or fire retardant viscose fibers. Apart from PTFE membrane, polyurethane membrane (PU membranes) are also used as moisture barrier in firefighter protective clothing.

4.6 Oxidized Polyacrylonitrile polymer [PANOX]

Oxidized polyacrylonitrile (PANOX) was developed for flame and heat resistant properties in textile substrates. Moreover it can be utilized in industrial, automotive and air craft industry. Limiting oxygen index (LOI) varies from 45 to 55. This fiber is electrically non conductive and have very good thermal stability. It has excellent chemical resistance. It has very low thermal conductivity of 0.030 [W/(m.k)]. They are excellent thermal insulators. They deliver excellent protection against flame. PANOX fibers do not melt and burn and they don't even shrink, when exposed to 1250 ºC for 30 seconds. Density varies from 1.37 g/cm^3 to 1.40 g/cm^3. Moisture regain is 9 percent. Decomposition temperature is greater than 450 ºC [101]. They are also

available in the form of non woven felts embedded with aerogel particles from Aspen aerogel companies.

4.7 Fire retardant chemical Proban

Proban is a chemical employed to cellulosic fibers and blends for making them flame retardant [102]. Proban coated materials are used for wild land firefigther's clothing [4]. The reason for utilizing proban coated fabric was to compare their thermal protective performance with inherent flame and heat resistance materials like Nomex when they are subjected to different levels of radiant heat flux density. Proban coated fabrics are commercially available as Proban.

Proban is a low molecular weight, polymeric chemical developed around a phosphonium salt (tetrakis-hydroxymethyl phosphonium chloride, THPC). At first, THPC is reacted with sodium hydroxide solution and transformed to Tetrakis- hydroxymethyl phosphonium hydroxide (THPOH). The Proban method inculcates impregnation of chemical, followed by drying and curing with ammonia gas, oxidation and finally neutralization. Flame retardant behavior is acquired by the development of a cross-linked inert polymer within the fiber. As there is no chemical reaction within the fiber, hence the textile substrate stays unaffected. Brief procedure is that, textile substrate like cotton fiber is immersed in Proban chemical solution and dried to precise moisture content. Afterwards, it is subjected to a high concentration of ammonia gas followed by oxidization with hydrogen peroxide, washing, drying, softening with high density polyethylene textile softener [102].

4.8 Belltron

Belltron is high performance antistatic conductive fiber. Static control is managed by blending small amount of belltron in primary fiber. Belltron is made up of polymer matrix and conductive layer. Polymer matrix consist of nylon 6, nylon 66 or polyester and conductive layer have embedded carbon black or white metal compound as conductive particles [103][104].

4.9 Characterization of thermal properties of firefighter clothing

4.9.1 Sweating guarded hotplate

Sweating guarded hot plate M259 B by SDL Atlas company was employed to evaluate thermal resistance R_{ct} [m²K/W] and water vapor resistance R_{et} [m²Pa/W] of textile substrate in steady state conditions. Sweating guarded hot plate works on principle of "skin model". This test replicate heat and mass transportation process taking place next to skin of human being. This machine evaluates flow of heat and moisture transportation from a test plate (calibrated), heated to surface temperature of human skin at temperature of 35 ºC, through test specimen. This equipment is constructed in climate chamber to make sure that testing of samples takes place accurately. Humidity guard and hotplate are made of (sintered) porous bronze which delivers perfect replication of human skin. This instrument work as per standard of ISO 11092 [105].

4.9.2 Thermal Manikin

A thermal manikin "Maria" from University of Minho, Portugal in figure 4 was used to measure the thermal insulation values of firefighter protective clothing samples as per ISO 9920 standard. The manikin is built up of fiber glass armed polyester shell covered with a thin nickel wire enveloped around the body to ensure the heating and temperature measurement. The design of shoulder, hip and knee joints was made of a circular cut to make the sitting and standing positions normal.

Figure 4: *Thermal manikin Maria with left forearm covered with sample of firefighter protective clothing*

During the testing, the manikin was positioned at the centre of the climatic chamber and was kept in a supporting frame, hung from the head and with the feet 0.15 m away from the floor. The manikin had 20 independent parts managed by a computer according to the association between dry heat losses and skin temperature of the human body for the conditions close to thermal comfort [106]. In experimental work, the forearm limb portion of the manikin was covered with a forearm sleeve, since the forearm limb area was much lesser as compared to the other parts of the manikin where less fabric was used.

Global Method

The global method is a general formula for defining the whole body resistance. It is a conventional method which performs an overall calculation and defines whole body resistance. In equation 12, f_i is the relationship between the surface area of the segment *I* of the manikin, A_i, and the total surface area of the manikin, *A*. T_o is the temperature of the operating environment in degrees centigrade (°C). $\overline{T}_{sk}$ is the mean skin temperature in °C and $\bar{\dot{Q}}_{s,i}$ [W/m^2] is the sensible heat flux of manikin.

$$I_T = \frac{\sum\left(f_i \times \bar{T}_{sk,i}\right) - T_o}{\sum\left(f_i \times \bar{\dot{Q}}_{s,i}\right)} \tag{12}$$

After subtracting I_a from I_T, the effective clothing insulation, I_{cle} ,(m^2 °C/W) was acquired.

$$I_{cle} = I_T - I_a \tag{13}$$

Intrinsic thermal insulation, I_{cl} was calculated with equation 14.

$$I_{cl} = I_T - I_a / f_{cl} \tag{14}$$

Where f_{cl} is the ratio of the outer surface area of a clothed body to the surface area of a nude body.

4.10 Determination of thermal protective performance of firefighter clothing

4.10.1 Transmission of heat by contact heat plate

The contact heat plate test was used to characterise the thermal protective performance of firefighter protective clothing. An experimental setup was made, the basic principle was derived with a slight modification of ISO standard 12127 [76] and this set up was arranged in University of Minho, Portugal.

The hot plate was heated to and maintained at constant temperature, and a thermocouple was placed on the top of a test sample. The sample was lowered down towards the heated cylinder. The operation was conducted at constant speed. The threshold time was evaluated by monitoring the temperature rise of the thermocouple.

The specimen of FFC were cut to 15 cm diameter and then attached on to a ring shape frame. The latter was made fixed on a circular clamp with the help of a magnet and thermocouple on the top and middle of a sample. The clamp was attached to a dynamometer. The heated plate (heat source) was maintained at constant temperature of 150°C. A schematic diagram is shown in figure 5. The samples were raised to the height of 60 mm above the heated plate with the help of a dynamometer and afterwards brought down towards the heated plate. When the distance between the heat plate and the specimen was 10 mm, time was recorded and temperature of the sample was noted until there was a 10°C rise in temperature. Afterwards, the heat source was removed away from the specimen and the thermocouple along with clamps was allowed to cool down for the next sample to be evaluated. The specimens were brought towards the heated plate at the constant speed of 5mm/min [30]. The test procedure had to be performed on three samples to get the average value. The arrangement of the contact heat test is depicted in figure 6.

The apparatus consists of a heat plate, digital multimeter, T type thermocouple, clamps and a dynamometer:

i. Heat plate which is VWR® professional hot plate developed for applications requiring exceptional accuracy, stability, and repeatability are equipped with an exclusive safety system that helps protect both the operator and sample [107].

ii. Digital multimeter Velleman DVM 345DI was employed to evaluate the temperature changes in the sample. This device enables the user to measure AC and DC voltages, AC and DC currents, resistance, capacitance and temperature. The device can be interfaced with a computer and the user can also test diodes, transistors and audible continuity.

iii. T type thermocouple "UT-T" with the temperature probe test range from –40 to +260 °C with the accuracy of ±0.75% was utilized. Circular clamps were employed to hold the sample.

iv. Dynamometer was used to move the test sample at the constant speed of 5 mm/min from fixed distance.

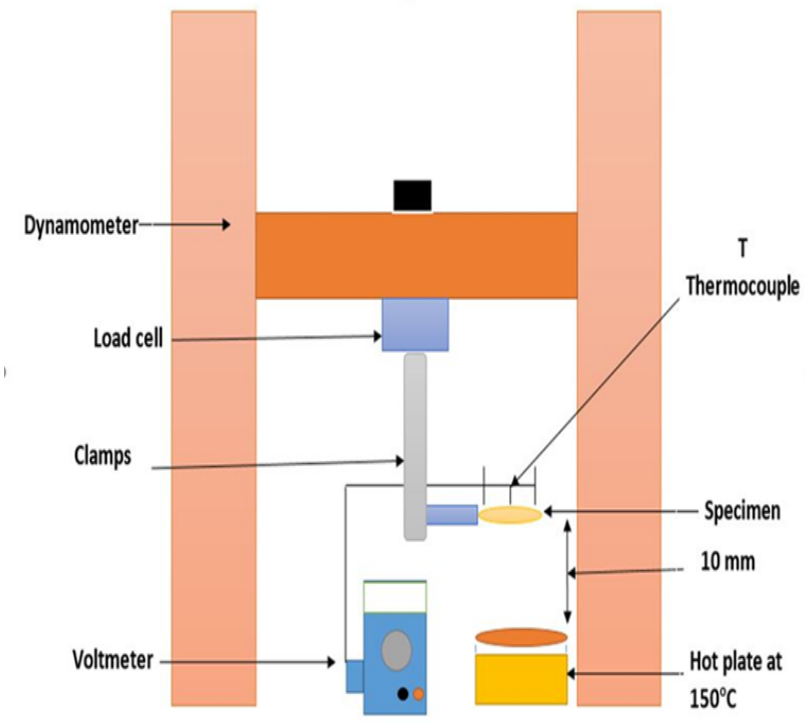

Figure 5: *Schematic diagram of contact heat test arrangement*

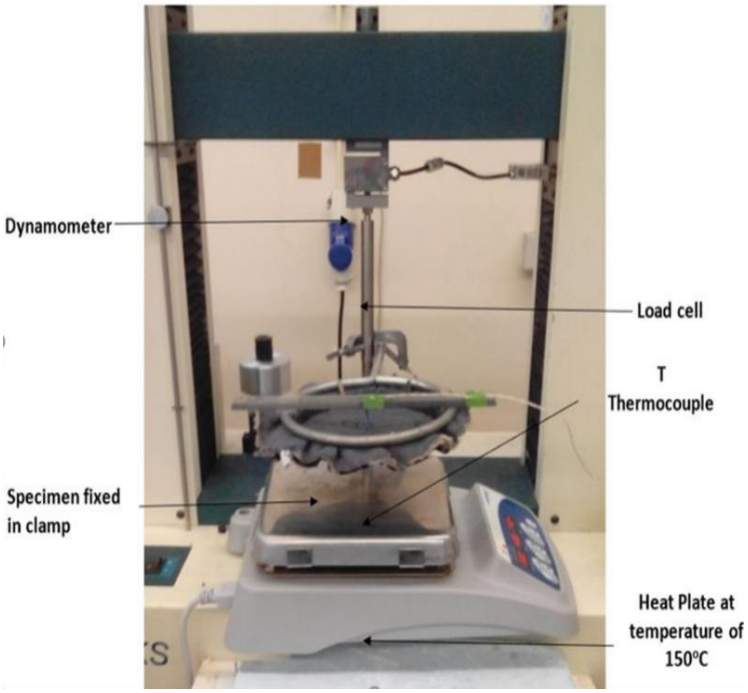

Figure 6: *Arrangement of Contact heat test*

4.10.2 Transmission of heat through radiant heat flux density equipment

This X637 B radiant heat transmission machine uses ISO 6942 standard to measure transmission of heat through material or material assembly. The temperature of room shall be maintained between 15 °C and 35 °C.

The radiant heat testing equipment was employed to investigate radiant heat flux density through material or material assembly according to ISO 6942 standard. The apparatus consists of six carbide rods serving as radiation heat source, a small curved copper plate calorimeter, a moveable test frame having cooling device and specimen holders as shown in figure 7. At first, calibration is performed when moveable screen is withdrawn and reverted to point when rise of temperature was reached to 30°C and incident heat flux density Q_o is measured. Afterwards, specimen is affixed to one side plate of specimen holder and held in contact with the face of the calorimeter, applying a mass of 200 g. The movable screen is withdrawn, and the starting point of the radiation is recorded. The movable screen is returned to its closed position after a temperature rise of about 30°C has been reached. The size of the sample was 230 mm × 80 mm. The time for temperature acceleration of 12^{o}C and 24^{o}C in the calorimeter was determined and

conclusions are mentioned in the form of radiant heat transmission index (*RHTI 12 and RHTI 24*) and the percentage heat transmission factor (*percentage TF* Q_o) and transmitted heat flux density Q_c [108]. Before experimentation, all specimens were pre-conditioned for 24 hours at temperature of 20°C and have relative humidity of 65 percent [108]. Three specimens are required for testing at each level of heat flux density. Incident heat flux density is evaluated from the following equation.

$$\mathrm{Q_o} = \frac{\mathrm{C_p RM}}{\mathrm{a.A}} \tag{15}$$

A = Area of the copper plate in m^2, a = the absorption coefficient of the painted surface of calorimeter, M = Mass of copper plate in kg, C_p = Specific heat of copper 0.385 (kJ/Kg°C), R = Rate of rise of the calorimeter temperature in the linear region in °C/s.

The transmitted flux density, Q_c in kW/m^2 is evaluated by the following equation

$$Q_c = \frac{MC_p}{A} \times \mathrm{K} \tag{16}$$

$$K = \frac{12}{(RHTI\ 24 - RHTI\ 12)} \tag{17}$$

K = Mean rate of escalation of the calorimeter temperature in °C/s in the region between a 12°C and 24°C rise.

RHTI 12= threshold time in (sec) when temperature of calorimeter increases in 12°C

RHTI 24= threshold time in (sec) when temperature of calorimeter increases in 24°C

Percentage age heat transmission factor, [Percentage TF Q_o] for incident heat flux density level is explained by equation 18 [108]:

$$\%\ TF\ Q_o = 100.\frac{Q_c}{Q_o} \tag{18}$$

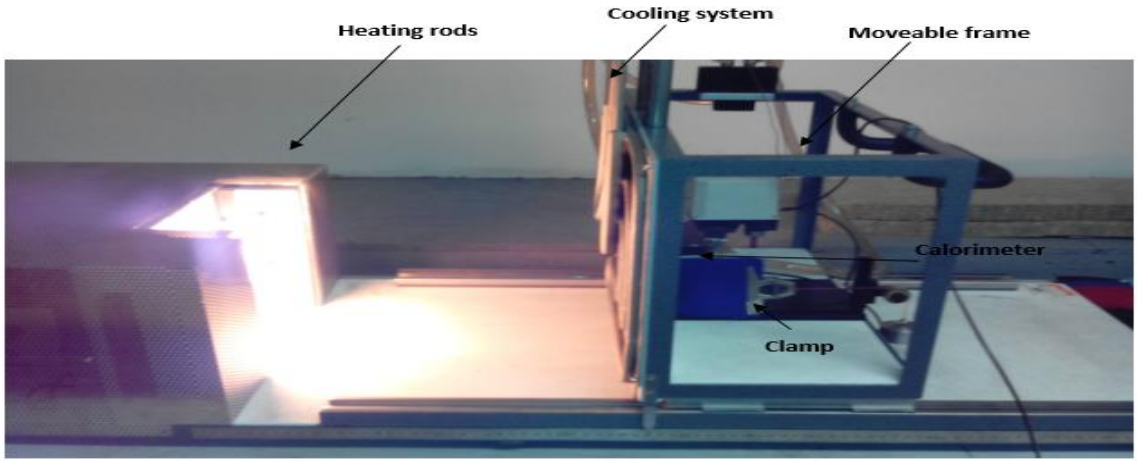

Figure 7: *Radiation heat testing equipment*

4.11 Evaluation of air permeability of firefighter specimen

Air permeability tester FX 3300 Labotester III (Textest Instruments) at pressure of 200 pascals was employed to evaluate air permeability as per CSN EN ISO 9237 standard. The Air Permeability Tester tests permeation of air with ease of convenience, efficiency and reliability. It evaluates the flow of air through a given area of a textile substrate (set by a selected standard orifice) at a certain pressure drop over this test area during the time period mentioned by the recognized standard. The main features inculcate recognition of the test head size and an automatic ranging system that diminishes the requirement for a pretest to find out and then maintain the range of instrument. The 50 cm test arm permits for simple testing on a large substrate without having to cut multiple small specimens [10][109].

4.12 Determination of water vapor permeability values

Permetest was employed to determine relative water vapor permeability. It was developed by Sensora company. It was designed for the swift evaluation of relative water vapour permeability (RWVP % age) and water vapor resistance R_{et} (m^2Pa/ W). Evaluations are based on the principle of heat flux sensing. The reason for using this equipment was limitation in size of silver coated specimens. The test is carried out under isothermal conditions; the temperature of the measuring head is regulated at room temperature. When water passes through measuring head, some heat is lost due to evaporation. The instrument evaluates the evaporation of the “uncovered” head as well as that of the head when sheltered with the test fabric. The full test is accomplished when

the exchange of water from the measuring head to the atmosphere reaches steady-state (usually within two to three minutes) [110][111][88].

4.13 Characterization of surface morphology

Scanning electron microscopy (SEM) images are taken by using Zeiss Ultra plus scanning electron microscope utilized to study surface morphology of firefighter specimens inculcating silver deposited layer. Scanning Electron microscope generates images of specimen when it is scanned by focused beam of electrons. In scanning electron microscope, interaction of electrons with atoms present in specimen takes place. As a result, secondary and backscattered electrons are generated which can be identified and thus they deliver information about surface topography of specimen and its configuration [112].

4.14 Evaluation of bending moment

TH-4 (Tuhomer) was utilized to measure the bending moment of uncoated and silver coated firefighter protective clothing specimen. This instrument evaluates the bending moment of textile substrates by CSN 80 0858 standard. The size of specimen was 5 cm × 2.5 cm [113]. Bending properties describes stiffness of fabric. Stiffness is the ability of material to resist deformation when force is applied on it. The instrument TH-4 (Tuhomer) measures force required to bend specimen by 60 degree. This can be explained by following equation:

$$M_o = F \times K \tag{19}$$

M_o is the bending moment [mN.cm]
F is the force applied in mN
K is constant whose value is 0.52 [113]

4.15 Measurement of emissivity

Emissivity of specimen was evaluated by ASTM E 1933 – 99a standard (non-contact method) through Fluke Ti 25 Infrared camera. It is a non contact methodology for measurement of emissivity [94].

4.16 Determination of washing resistance

Washing was done in Miele washing machine in accordance with NFPA 1851 standard. The temperature was maintained at 30 ºC along with 400 RPM for two hours and 10 minutes.

4.17 Evaluation of abrasion resistance

Abrasion resistance of silver coated specimen was determined with the help of Martindale abrader M235 as per standard of ISO 5470-2: 2015. Pressure was kept at (12 ± 0.2) kPa between abrader and specimen holder [114]. In this device, specimens were hold tightly in sample holder and are abraded by utilizing specimen of specific abradant under by applying constant pressure. There are two cases in which test can be stopped i.e. after completion of fixed cycles (assessment of specimen is performed to analyze damage) or when test samples acquired specific degree of abrasion (number of cycles are recorded) [114].

4.18 Determination of reflectivity

PIKE technology Mid-IR INTEGRATIR connected with FTIR spectrometer Nicolet 380 from Thermo Electron Corporation was employed in this study to investigate reflectivity of specimens from 2 μm to 18 μm wavelength [115]. The integrating sphere is a device for evaluating reflectance properties of solids for measurement of scattering and absorption of light and gathering of spectral data which is very complicated to acquire with standard sampling methodologies. Integrating spheres are highly reflective enclosed space that are positioned very close to the specimen in such a way that the reflected light enters the sphere, leaps around the highly reflective diffuse substrates of the sphere wall and finally falls upon the detector. Integrating sphere spatially integrates the light flux. The main portion of the equipment is a sphere with a very highly reflecting inner surface. The surface should be employed as the ideal Lambertian scatterer, which illustrates that the light falling on the surface is uniformly scattered in all directions and the scattered light intensity is proportional to the cosine value of the angle of observation [115].

CHAPTER 5: RESEARCH METHODOLOGIES

For investigation of thermal protective performance of firefighter protective clothing, three different type of research studies are performed:

I. Evaluation of thermal insulation properties of firefighter protective clothing specimen
II. Improvement in thermal insulation properties of firefighter protective clothing with the help of aerogel blanket
III. Effect of metallic coating on thermal protective performance, emissivity, washing resistance, breathability and flexibility of firefighter protective clothing specimen

5.1 Evaluation of thermal insulation properties of firefighter protective clothing specimen

The aim of this research was to investigate the thermal protective performance of different firefighter clothing (FFC) samples. Each clothing items consisted of three layers, i.e. outer layer, moisture barrier and thermal liner. Four different clothing specimens with different material combinations were used in this research. The material specification of different firefighter clothing items are mentioned in table 2 and their arrangement in the clothing assembly are listed below in table 3. Thickness of specimen was evaluated by digital thickness tester SDL Atlas M034A.

Table 2: *Material Specifications*

Material code	Material Specification	Material Function	Weave Design	Mass per unit area [g/m^2]	Thickness [mm]
O1	50% Conex, 43% Lenzing FR, 5% Twaron, 2% Beltron	Outer shell	Rip stop	215 ± 1.8	0.42±0.01
O2	70 % Nomex, 23% Kevlar, 5 % Twaron, 2% P-140	Outer shell	Rip stop	195 ± 2.8	0.40±0.02
O3	55% Conex, 38% Lenzing FR, 5% Twaron, 2% Belltron	Outer shell	Rip Stop	215 ± 1.5	0.43±0.01
O4	75% Conex, 18 % Lenzing FR, 5% Twaron, 2% Beltron	Outer shell	Rip stop	225 ± 2.7	0.44±0.01
MB1	Fabric part: 100 %polyester Membrane: Polyurethane membrane	Moisture Barrier	Single jersey	145 ± 2.5	0.416±0.02
MB2	Fabric: 50% Kermel, 50% viscose FR	Moisture Barrier	Non Woven	120 ± 1.3	0.503±0.01

	Membrane: PTFE membrane (PTFE membrane is laminated to face fabric part)				
MB3	Fabric: 50% Kermel, 50% viscose FR Membrane: PTFE membrane (PTFE membrane is laminated to face fabric part)	Moisture Barrier	Non woven	120 ± 1.7	0.529±0.01
MB4	Fabric: 50% Kermel, 50% viscose FR Membrane: PTFE membrane (PTFE membrane is laminated to face fabric part)	Moisture Barrier	Non Woven	120 ± 1.8	0.53±0.01
TB	Thermal part: para-aramid Liner: 50% meta-aramid, 50% FR viscose	Thermal Liner	Non Woven	120 ± 1.5	1.8±0.02

Table 3: *Arrangement of specimens*

Specimen No	Sample assembly	Thickness [mm]	Mass per unit area [g/m^2]
1	O1 + MB1 + TB	2.636 ± 0.02	560 ± 2.3
2	O2 + MB2 + TB	2.73 ± 0.03	515 ± 2.1
3	O3 + MB3 + TB	2.709 ± 0.01	535 ± 2.9
4	O4 + MB4 + TB	2.77 ± 0.01	545 ± 2.5

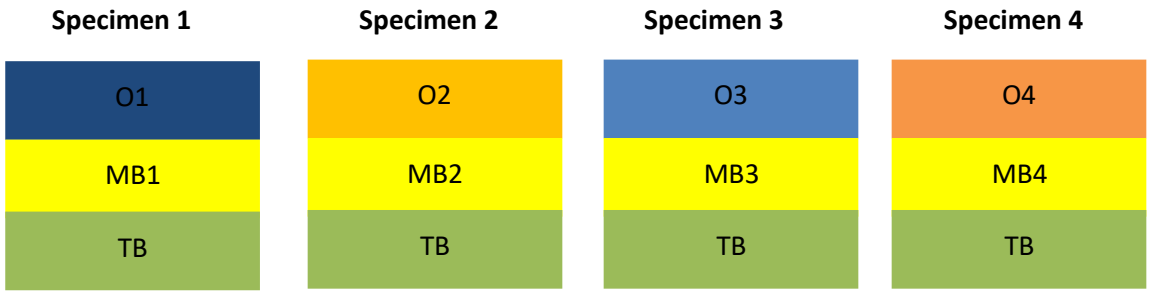

Figure 8: *Schematic diagram of fabric arrangement*

These specimens were tested with Sweating guarded hot plate, thermal manikin and air permeability tester. The threshold time, *t* (s), was measured in accordance with the ISO 12127 standard. Afterwards, these specimens were characterized with a radiant heat transmission machine (ISO 6942 method) to determine the heat transmission through a specimen at 10 kW/m^2 and 20 kW/m^2. Moreover, transmitted heat flux density, Q_c (kW/m^2), percentage transmission factor, *percentage TF* Q_o and radiation heat transmission index (*RHTI12* and *RHTI24*) were determined.

5.2 Improvement in thermal insulation properties of firefighter protective clothing with the help of aerogel blanket

In this experimental work, Improvement in thermal insulation properties of firefighter protective clothing with the help of aerogel blankets. Aerogel layer was used as substitute layer to thermal barrier. Two different outer shells, one moisture barrier and one thermal liner were employed as stated in table 4. Four different combinations of clothing assemblies were prepared as mentioned in table 5 and figure 9 respectively.

Table 4: *Specifications of multilayer clothing arrangement*

Layer	Fabric Code	Component	Weave type	Fabric weight [g/m^2]	Thickness [mm]
Outer layer 1	O(1)	75 %Nomex-23% Kevlar -2 %Antistatic P-140	Twill	240 ±2.4	0.84±0.02
Outer layer 2	O(2)	Proban (100 % cotton)	Twill	300 ± 3.4	0.98±0.02
Moisture barrier	M	PTFE membrane laminated to non woven Nomex	Nonwoven	128 ± 1.5	0.94±0.01
Thermal liner	T	Liner:50/50 Nomex /FR Viscose Thermal part: Para-aramid	Nonwoven	380 ± 2.9	3.424±0.03
Aerogel blanket	P	Silica based aerogel emebedded in oxidized polyacrylonitrile nonwoven sheet	Nonwoven	400 ± 3.5	2.85±0.02

Table 5: *Combinations of clothing assemblies*

Sr #	Fabric arrangement in multilayer clothing assembly	Fabric Code	Thickness (mm)	GSM (g/m^2)
1	Outer shell (1) + Moisture barrier+ Thermal liner	A	5.20 ± 0.05	748 ± 3.1
2	Outer shell (2) + Moisture barrier + Thermal liner	B	5.34 ± 0.07	808 ± 3.5
3	Outer shell (1) + Moisture Barrier + Aerogel sheet	C	4.63 ± 0.06	768 ± 2.9
4	Outer shell (2) + Moisture Barrier + Aerogel sheet	D	4.77 ± 0.04	828 ± 2.8

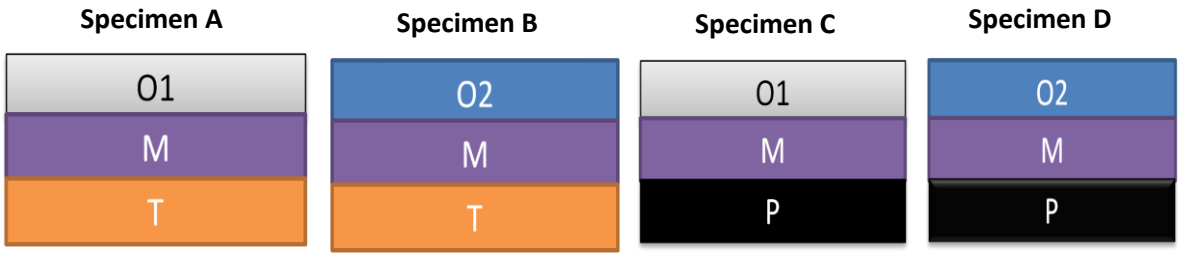

Figure 9: *Schematic diagram of clothing arrangement assemblies*

Temperature on surface of fabric when placed at certain distance from heating source is given by following table.

Table 6: *Incident temperature on surface of specimen when exposed to different heat flux density*

Heat flux density	10 kW/m^2	20 kW/m^2	30 kW/m^2	40 kW/m^2
Incident temperature on surface of specimen	220 ^oC	292 ^oC	390 ^oC	495
Distance of specimen from heating source	37.1 cm	25.1cm	19.7cm	16.5 cm

The main purpose of this experimental work was to enhance thermal protective performance of firefighter protective clothing. For this purpose four combinations of high performance fabrics were made. Each corresponding combinations were characterized by Sweating guarded hot plate. Afterwards, these combinations were evaluated by X637 B machine (ISO 6942 standard) for determining transmission of heat through multilayer protective clothing assemblies at 10 kW/m^2, 20 kW/m^2, 30 kW/m^2 and 40 kW/m^2 to evaluate the thermal protective performance in terms of transmitted flux density Q_c and percentage transmission factor (percentage TF Q_o).

5.3 Effect of metallic coating on thermal protective performance, emissivity, washing resistance, breathability and flexibility of firefighter protective clothing specimen

In this research, outer shell of firefighter clothing was coated silver particles through magnetron sputtering. Each specimen combination consists of three layers i.e. outer layer, moisture barrier, thermal barrier. The exterior portion of outer layer of each specimen was coated with silver particles at 1 μm, 2 μm and 3 μm thickness. There are 4 different combinations and their specification along with arrangement is mentioned in table 7 and table 8 respectively.

Table 7: *Specification of samples*

Sr #	Name of Sample	Code	Material specification	Weave Design	Fabric weight [g/m^2]	Thickness [mm]
1	Outer shell	O	70% Conex, 23 % Lenzing FR, 5% Twaron, 2 % Beltron	Rip stop	225 ± 2.1	0.44±0.01
2	Outer shell (1 μm thickness)	O (1)	70% Conex, 23 % Lenzing FR, 5% Twaron, 2 % Beltron	Rip stop	234± 1.8	0.441±0.02
3	Outer shell (2	O (2)	70% Conex, 23 %	Rip stop	246 ± 2.2	0.442±0.03

	µm thickness)		Lenzing FR, 5% Twaron, 2 % Beltron			
4	Outer shell (3 *µm* thickness)	O (3)	70% Conex, 23 % Lenzing FR, 5% Twaron, 2 % Beltron	Rip stop	255 ± 2.1	0.443±0.02
5	Moisture Barrier	MB	Face fabric, 50 %/50 % Kermel / viscose FR, PTFE membrane	Non-woven	120 ± 1.8	0.55±0.01
6	Thermal Lining	TB	Thermal: Para Aramid Inner futter: 50% Meta aramid, 50% viscose	Non-woven	200 ± 2.3	1.8±0.02

Table 8: *Arrangement of Fabric assemblies along with their code*

Sr #	Fabric assembly	Fabric code	Fabric weight [g/m^2]	Thickness [mm]
1	Outer shell (O) + Moisture Barrier (MB) + Thermal barrier (TB)	A	545 ± 3.1	2.79±0.01
2	Outer shell (O1) + Moisture Barrier (MB) + Thermal barrier (TB)	A1	554 ± 3.5	2.791±0.02
3	Outer shell (O2) + Moisture Barrier (MB) + Thermal barrier (TB)	A2	566 ± 2.9	2.792±0.03
4	Outer shell (O3) + Moisture Barrier (MB) + Thermal barrier (TB)	A3	575 ± 2.7	2.793±0.03

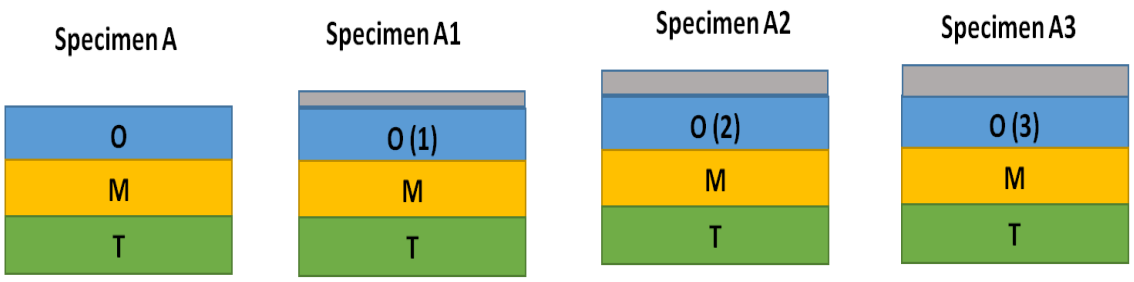

Figure 10: *Schematic diagram of arrangement of fabric assemblies along with their codes*

5.3.1 Coating of Samples through Magnetron Sputtering

Magnetron sputtering is physical vapour deposition process, where magnetically confined plasma is generated near the surface of target metal. Highly energetic ions with positive charge collide with surface of negatively charged target metal. As a result, atoms are ejected from the target material which then deposit on surface of substrate. Magnetron sputtering employs strong

magnetic field to confine electrons near surface of target material (metal). In consequence, efficiency of ionization process and deposition rate is enhanced and plasma is created at lower pressure [116][117].

A schematic diagram of magnetron sputtering is shown in figure 11. Coating of silver particles on outer shell of firefighter specimen was done by DC reactive Magnetron Sputtering equipment "Prevace". At first, deposition chamber was evacuated at 4 Pascals. The distance between specimen holder and target (silver metal) was maintained at 15 cm. Later on, these specimens were placed in Physical Vapor Deposition (PVD) chamber. The silver particle layer was acquired by sputtering of pure 99.99 percent silver (*Ag*) in the presence of 100 percent Argon gas floating at speed of 10 sccm (standard cubic centimeter per minute).

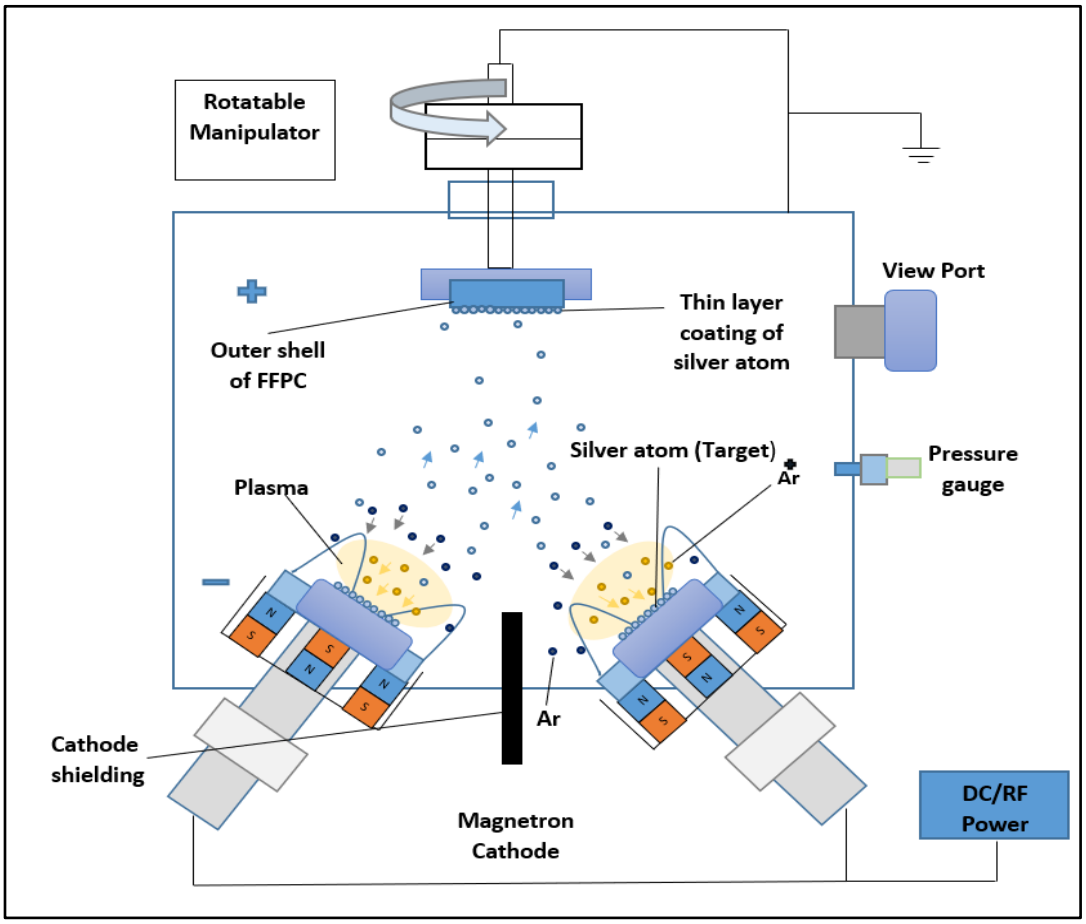

Figure 11: *Schematic diagram of magnetron sputtering* [118]

At the time of sputtering, the working pressure was maintained at pressure of 1.3 Pascals. The power of magnetron supply was maintained at 615 watt and negative substrate bias voltage was maintained at 300 volts. Physical appearance of uncoated and silver coated specimen after magnetron sputtering is shown in figure 12.

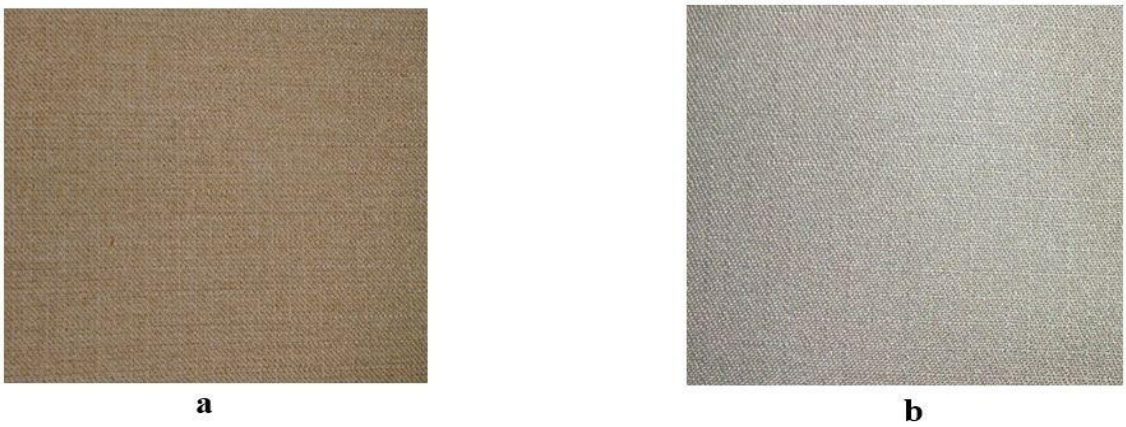

Figure 12: *Physical appearance of a. uncoated specimen and b. silver coated specimen*

Previously, magnetron sputtering was utilized to coat films or simple textile fabrics with metallic particles. Sputtering is the method in which atoms are expelled from a target or source material which is to be deposited on a substrate like textile fabric, such as a silicon wafer, solar panel or optical device due to the bombardment of the target by high energy particles [118]. In consequence, the layer of metallic coating was certain micrometer thick, thermal comfort issue was balanced as thermal barrier was not blocking dissipation of human body heat to surrounding climate and unlike PCM [25], the impact for enhancement was witnessed for longer duration of time and arrangement of clothing assembly was easy as compared to that of arrangement of clothing assembly involving increment of air gap size.

All the uncoated and silver coated specimens were then characterized on air permeability tester, Permetest and radiant heat transmission machine. Afterwards, bending moment, emissivity and reflectivity values were evaluated and thermal protective performance was evaluated before and after washing. Later on, abrasion resistance of silver coated specimens was evaluated for different abrasion cycles.

CHAPTER 6: RESULTS AND DISCUSSION

6.1 Evaluation of thermal insulation properties of firefighter protective clothing specimen

The thermal insulation of protective clothing plays a very important role in the thermal protective performance of firefighter protective clothing. The main purpose of firefighter protective clothing is to delay the increase in temperature of the human body when they are exposed to a heat source and consequently to enhance the firefighters' working time when saving lives and valuables. The ability of a textile substrate to conduct heat is called thermal conductivity of a textile material. A greater value of thermal conductivity indicates a greater amount of heat exchange passing through that substrate. However, the thermal conductivity of a textile substrate is determined by the physical and chemical properties of the textile substrate [119]. An increment in the relative humidity absorbed by the substrate is followed by an increase in the thermal conductivity of the textile substrate [120]. Consequently, the more a material is hygroscopic, the better is thermal conductivity. Thermal resistance is associated with thickness, surface weight and density. For thickness, it can be explained that at equivalent surface weights, increasing the thickness leads to an increase in the amount of air entrapped in the fabric. This is confirmed by the fact that thermal resistance decreases by increasing density as higher density means less air entrapped in the textile. In consequence, a thick fabric has higher thermal resistance as compared to a light and thin textile substrate [78]. This is also described by the mathematic formula: $R = h/\lambda$, where R is thermal resistance, h is thickness and λ thermal conductivity. Moreover, it is influenced by the fabric construction parameters. Thus, a thick and heavy fabric is more insulative than a thin and light one [21]. Table 3 from section 5.1 of chapter 5 reveals that *specimen 4* had slightly greater thickness than other samples, which might be one reason for better thermal insulation and increased thermal resistance as compared to other samples. As the thickness of *specimen 1* was smaller than the rest of samples, therefore *specimen 1* had significantly lower values of thermal resistance and total thermal insulation values as compared to the rest of samples. This was also evident by the ANOVA test as the *p*-value was 3.87×10^{-6}, i.e. less than 0.05, indicating a significant difference among the samples. Furthermore, the constituent material of the substrate plays a very important role in the thermal insulation/thermal resistance of firefighter protective clothing [121]. The results of thermal

resistance evaluated from sweating guarded hot plate in figure 13 also support the outcomes (thermal insulation values) in figure 14 respectively for the thermal manikin, i.e. greater thermal insulation, which results in lower thermal conductivity and enhanced thermal resistance.

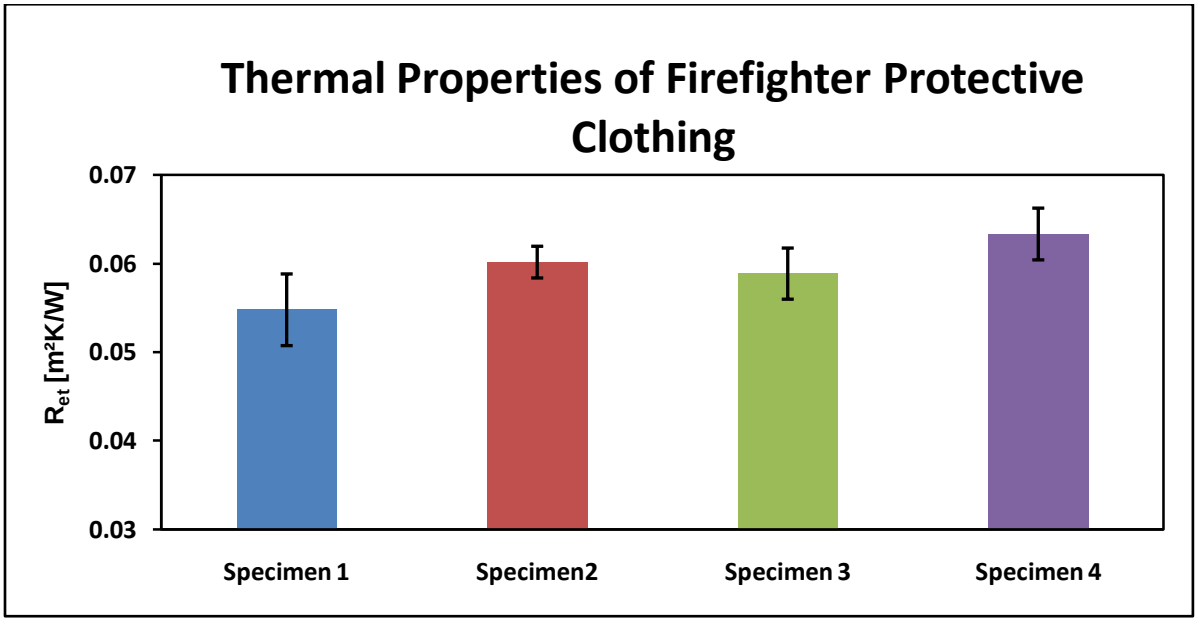

Figure 13: *Analysis of thermal characteristics with Sweating Guarded hot plate*

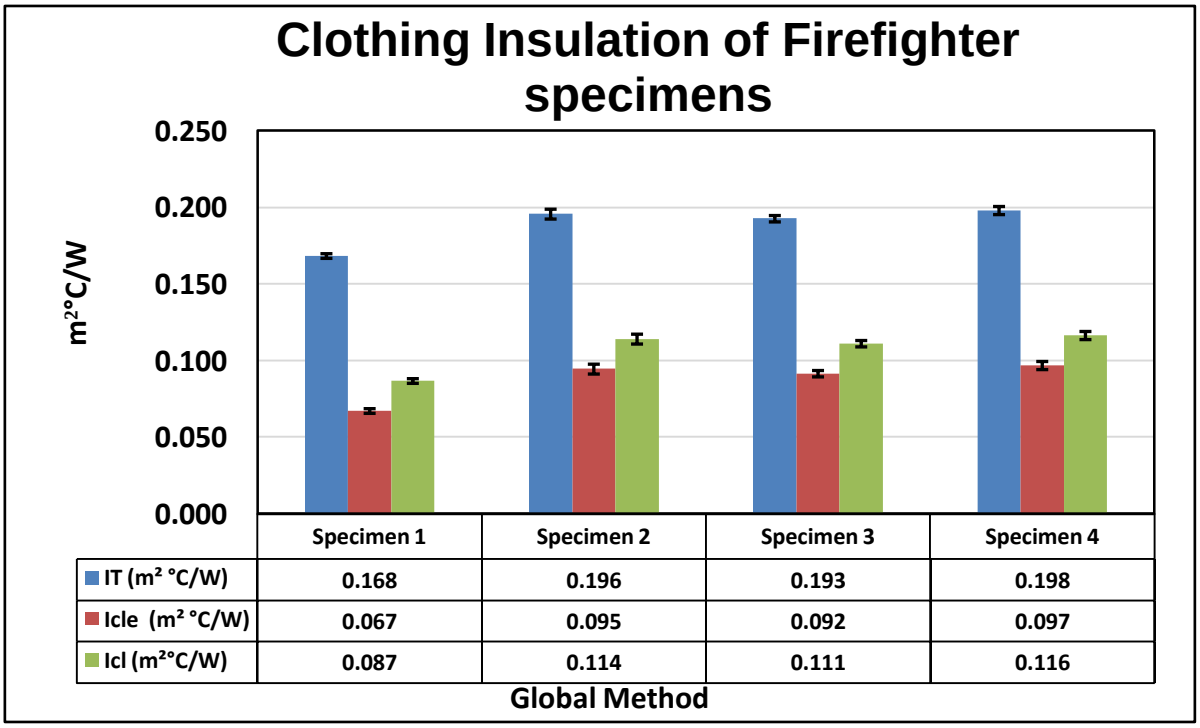

Figure 14: *Total thermal insulation (I_T), effective clothing insulation (I_{cle}) and basic insulation (I_{cl}) of firefighter protective sample*

6.1.1 Determination of air permeability values

The evaluation of the air permeability of the outer shell was carried out with the help of air permeability tester. The air permeability of firefighter protective clothing is very low, since the main task of firefighter protective clothing is to protect the firefighter's body from the heat in the form of radiation, convection and conduction. If the value of air permeability is very high, it decreases the thermal protective performance of firefighter clothing as it allows the air to pass through the sample resulting in the temperature increase of the human body within a shorter period of time. It can be seen in figure 15 that the outer shell (O4) of *specimen 4* exhibited lower air permeability values as compared to the outer shell of *specimens 1, 2 and 3*. This low value of outer shell (O4) of *specimen 4* is supported by the high value of thermal insulation evaluated by the thermal manikin respectively.

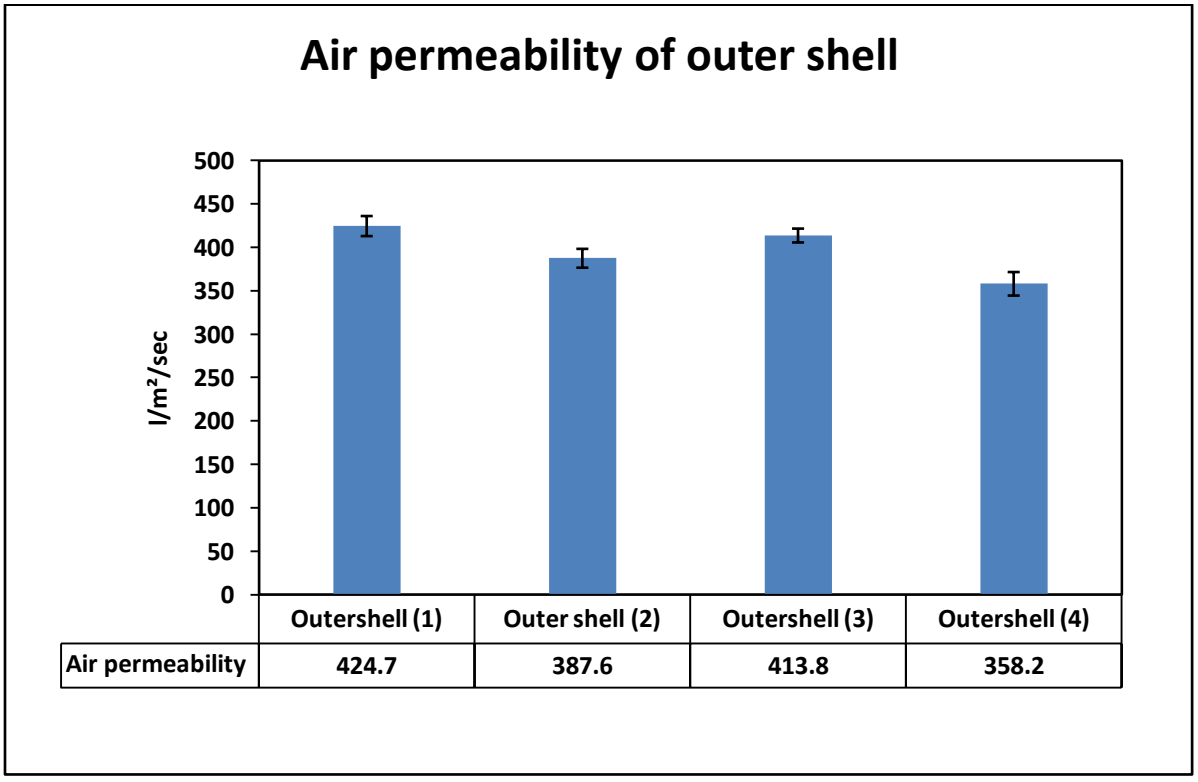

Figure 15: *Air permeability of outer shell of firefighter protective samples*

6.1.2 Determination of thermal protective performance of firefighter clothing

Transmission of heat through Contact heat plate

In table 9 and figure 16, it can be seen that *specimen 4* took more time for the increment of 10 ℃ rise in temperature when exposed to the heat source (150℃) at the constant speed of 5mm/min. Furthermore, when the sample was at 10 mm distance from the heat source, the temperature at the back of *specimen 4* was lower as compared to other samples at the same distance. Threshold time for rise of 10 ºC was greater in case of specimen 4 as compared to other specimens. There are two possible reasons for better thermal protective performance of the clothing. One is the thickness and the other is the physical and chemical properties of constituent fibers in the fabric. In the case of *specimen 4*, thickness was slightly higher as compared to the rest of samples; the sample had a higher percentage of Nomex fiber in the outer shell, enhancing the thermal protective performance and delaying the rate of the temperature rise. The greater the delay in the heat transmission towards the human body, the greater is the thermal protective performance of the clothing, enabling the firefighters to spend more time on duty. In figure 16, the best fitted curves and highest R^2 values for all the specimens were acquired through exponential equations.

Table 9: *Threshold time in contact heat test at exposing speed of 5mm/min*

Specimen	***T_c*** **(°C)**	***T1*** **(°C)**	***T2*** **(°C)**	***t*** **(s)**
Specimen 1	150	49±1	60.3±1.53	91
Specimen 2	150	44.3±1.15	54.7±0.58	106
Specimen 3	150	46.7±1.53	58.3±1.53	101
Specimen 4	150	41.7±0.58	52.7±1.15	111

T_c – contact temperature of hot plate

T1 – initial temperature at the back of sample when at the distance of 10 mm from hot plate

T2 – final temperature at the back of a sample when there is at 10 ℃ rise in temperature

t– Threshold time for increase of 10℃

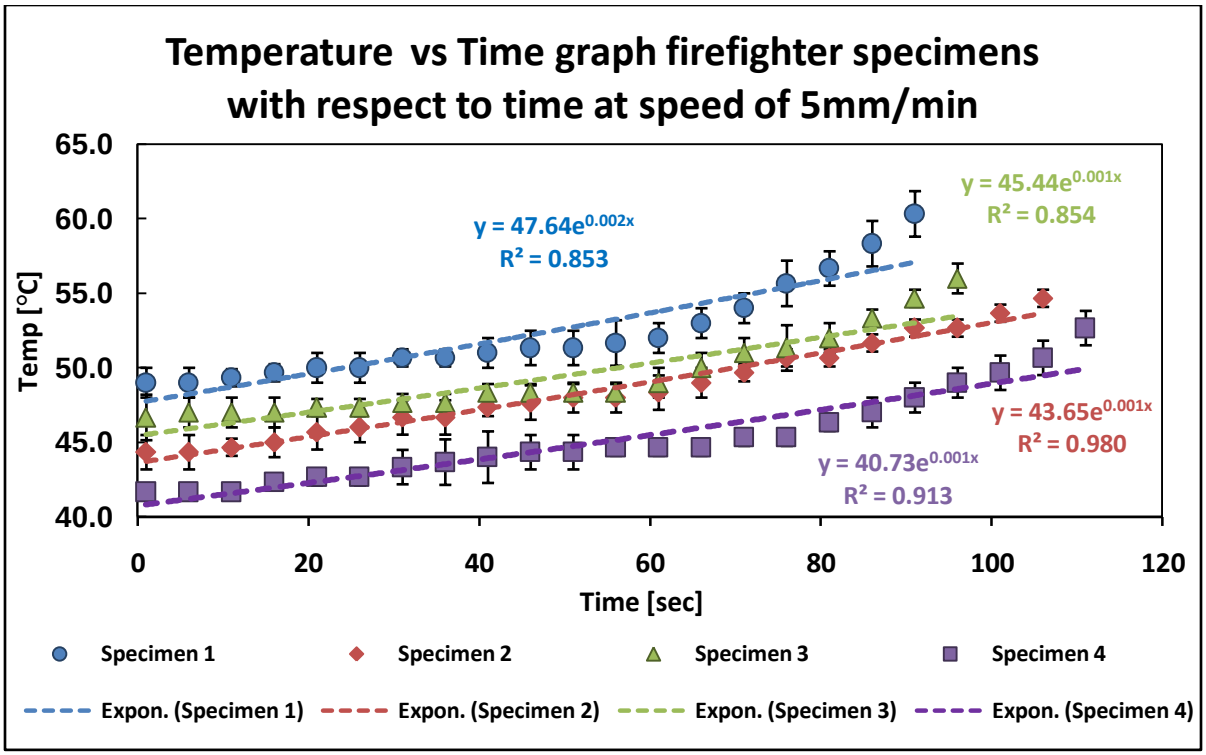

Figure 16: *Temperature of firefighter specimens with respect to time at speed of 5mm/min when exposed to 150ºC*

Transmission of radiant heat flux through multilayer protective clothing

Radiant heat transmission machine X637 B machine was used to evaluate transmission of radiant heat flux density through firefighter protective clothing. A generic overview of table 10 reveals that with the increase in the value of the incident heat flux density from 10 kW/m^2 to 20 kW/m^2, the values of transmitted heat flux density, Q_c (kW/m^2) and percentage transmission factor *percentage TF* (Q_o) increase successively at all samples. On the other hand, a reverse trend was observed for the values of the radiant heat transmission index *RHTI 24 – RHTI 12* (s). The smaller the values of transmitted heat flux density, the lesser the amount of heat flowing through the FFC sample towards the calorimeter. In consequence, fire fighters are able to continue with their activities for a lengthier period before acquiring skin burn injuries. Table 10 also illustrates that a greater difference between *RHTI 24* (s) and *RHTI 12*(s) shows that the sample is able to withstand the respected incident heat flux density for a longer duration before having burn wounds.

Table 10: *Comparison of transmitted heat flux density and incident heat flux density at 10 and 20 kW/m^2*

Sr #	Sample	Q_o (kW/m^2)	RHTI12(s)	RHTI24(s)	RHTI24 – RHTI12(s)	Q_c(kW/m^2)	Percentage TF(Q_o)
1	Specimen 1	10	34.35±0.919	53.9±0.697	19.55	3.38 ± 0.02	33.8
2	Specimen 2		37.4±0.282	61±0.424	23.6	2.80 ± 0.06	28.0
3	Specimen 3		37.6±0.981	59.4±0.939	21.8	3.03 ± 0.02	30.3
4	Specimen 4		44.25±0.495	72.9±0.848	28.65	2.30 ±0.03	23.0
1	Specimen 1	20	21.95±0.070	31.35±0.141	9.4	7.03 ± 0.07	35.1
2	Specimen 2		25.9±0.682	38.65±0.353	12.75	5.18 ± 0.02	25.9
3	Specimen 3		26.7±0.979	38.35±0.757	11.65	5.67 ± 0.04	28.3
4	Specimen 4		28.95±0.574	43.3±0.676	14.35	4.60 ± 0.01	23.0

At Q_o of 10 kW/m^2, *specimen 1* and 3 depicted higher values of Q_c (kW/m^2) as compared to *specimens 2 and 4,* respectively. Q_c (kW/m^2) values of *specimens 1 and 3* were very close to each other. A slightly different pattern was witnessed for FFC samples at Q_o of 20 kW/m^2. *Specimen 1* depicted very high values of Q_c and *percentage TF* (Q_o) as compared to all samples. *Specimens 2 and 3* exhibited very close values of Q_c and *percentage TF* Q_o. However, the lowest value of Q_c and *percentage TF* Q_o was witnessed at *specimen 4.*

Specimen 1 had relatively smaller thickness as compared to all other samples due to which it delivered higher values of Q_c and *percentage TF* Q_o at both 10 kW/m^2 and 20 kW/m^2. In the case of *specimen 2,* it had slightly less thickness as compared to *specimens 3* and *specimen 4.* Nevertheless, it had a lower value of Q_c and *percentage TF* Q_o as compared to *specimen 3*. This might be due to the fact that *specimen 2* had higher percentage of Nomex fiber in the outer shell, assisting the endurance against radiant heat flux density for a longer period of time, and delivered lower values of Q_c and *percentage TF* Q_o.

Specimen 4 had slightly higher thickness and greater percentage of Nomex fiber in the outer shell as compared to the rest of samples due to which the transmission of heat was delayed, and smaller values of Q_c and *percentage TF* Q_o were observed at both 10 kW/m^2 and 20 kW/m^2.

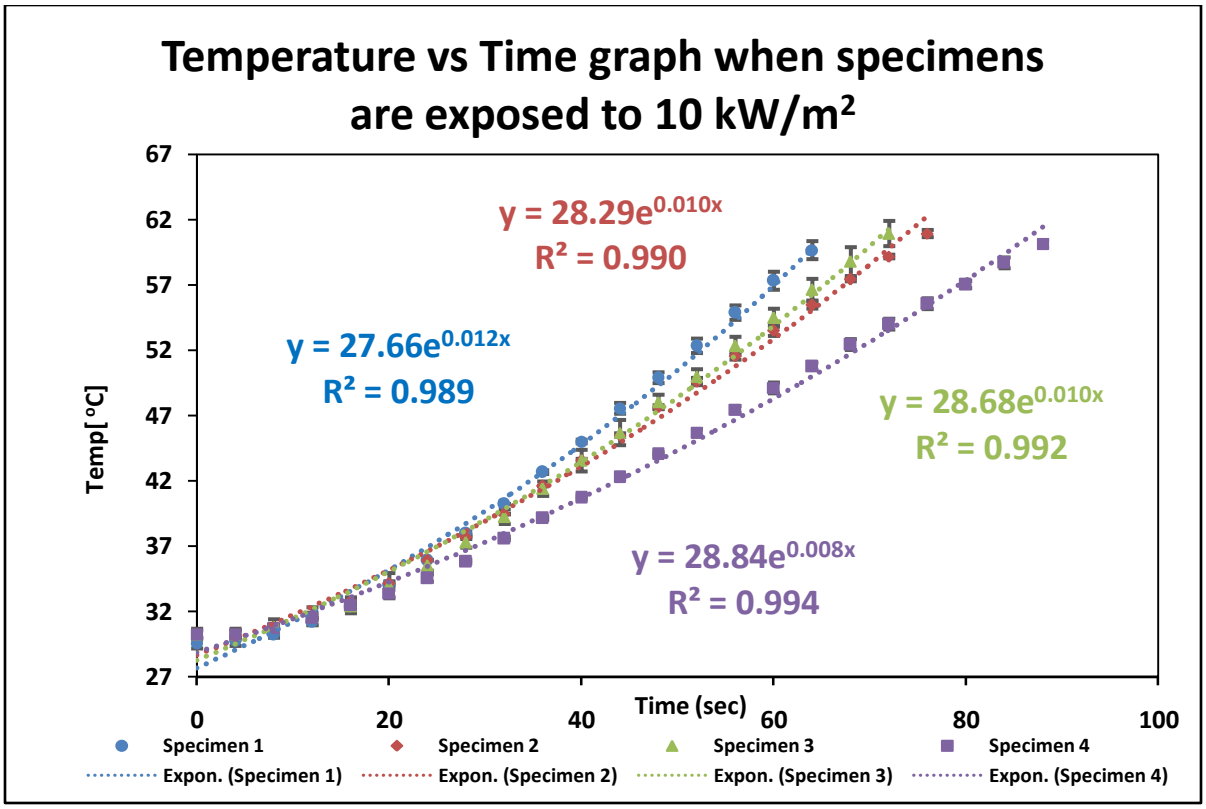

Figure 17: *Temperature of firefighter specimens with respect to time when specimens are exposed to 10 kW/m²*

Figure 17 shows that in the first 12 seconds, the rate of temperature rise in all samples was almost equal. However, afterwards, the rate of temperature rise of *specimen 4* occurred at a much slower rate; therefore, a flatter curve was seen. In the case of *specimen 1*, a steeper curve was observed, which indicated that the rate of temperature rise was greater as compared to the rest of samples. For *specimens 2 and 3*, the curve pattern was very similar until the 35th second. Afterwards, the curve of *specimen 2* became slightly flatter as compared to the curve of *specimen 3*, indicating a slightly better thermal protective performance of *specimen 2* as compared to *specimen 3*. The flatter the curve, the more time was required to raise the temperature on the other side adjacent to the calorimeter, due to which the amount of heat was delayed and lower values of Q_c(kW/m^2) and *percentage TF* Q_o were noted by the calorimeter. As a result, firefighters are able to endure the heat for a longer period of time and perform their activities before acquiring any harmful injuries. *Specimen 4* has increased value of radiant heat transmission index *RHTI 24* as compared to *specimen 1* by 35.25 percent and highest value of R^2 and best fitted curve was acquired through exponential equations. The higher the value of RHTI

24, the greater will be the time for rise of 24 ºC. As a result, flatter curve will be obtained for specimen and greater will be thermal protective performance of firefighter clothing specimen.

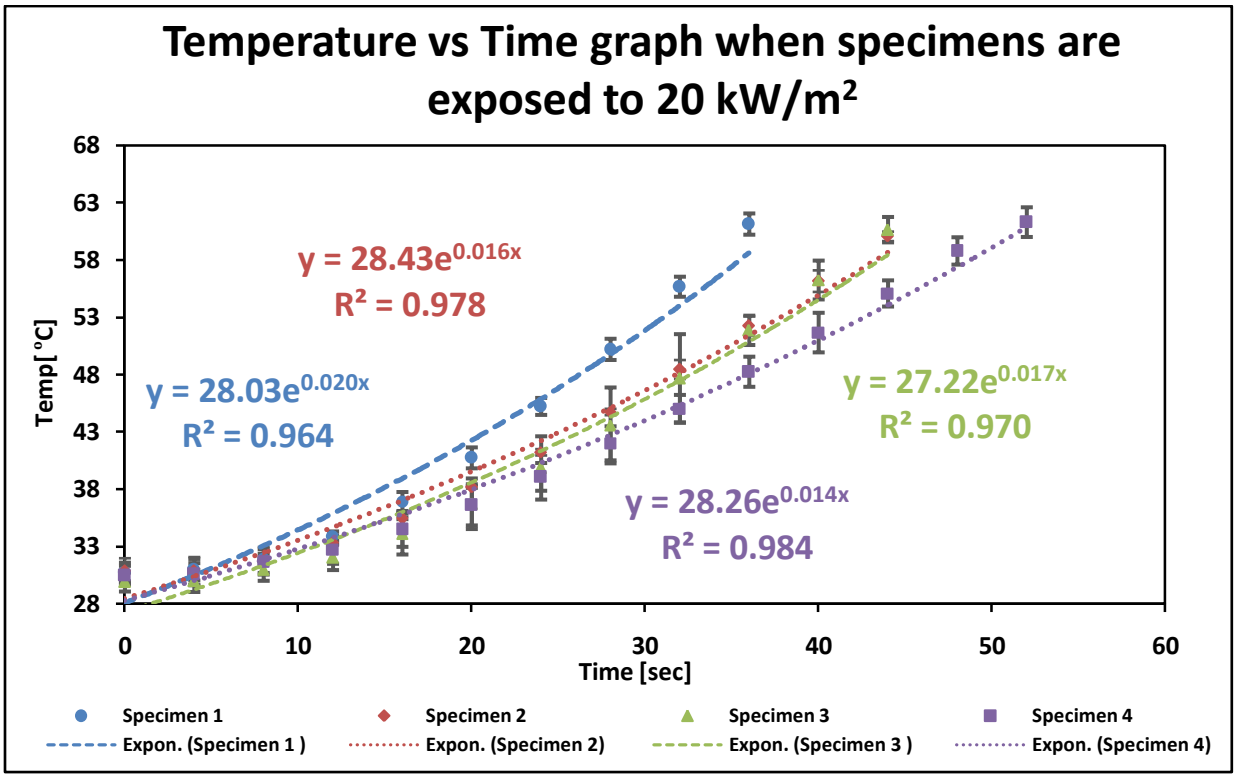

Figure 18: *Temperature of firefighter specimens with respect to time when specimens are exposed to 20 kW/m²*

At 20 kW/m², the curve pattern of *specimen 4* was flatter as compared to curves of other specimens. However, this time, the curve of *specimen 3* was slightly flatter as compared to the curve of *specimen 2* and both curves were overlapping each other from the time of 40–57 seconds. It was also noticed that in table 10, at 20 kW/m², the value of Q_c relatively increased for each sample as compared to the value of Q_c for 10 kW/m² due to which steeper curves were acquired indicating the rate of temperature rise occurring at a faster rate. Radiant heat transmission index *RHTI 24* value of *specimen 4* was higher than *specimen 1* by 38 percent. More over best fitted curves and highest value of R^2 was delivered by exponential equations.

6.2 Improvement in thermal insulation properties of firefighter protective clothing with the help of aerogel blanket

Thermal resistance values were evaluated by Sweating guarded hot plate for monolayer and multilayer protective fabric assemblies and their comparison was made in figure 19. Thermal resistance R_{th}, of textile substrate is a function of the actual thickness of the textile fabric and its thermal conductivity. This thermal resistance is inversely proportional to thermal conductivity [21]. Thermal conductivity and thermal resistance are not only contingent on thickness of the fabric assemblies and but also on physical and chemical properties of textile substrate [119]. Greater the thickness, greater will be the thermal resistance of the material. However, this is not only the whole scenario, the porosity and density of the textile substrate also plays a vital role in thermal behavior of the medium. Textile substrates with closed and small pores are able to trap air inside the substrate. The illustration of this phenomenon is the due to fact that air has a lower thermal conductivity than materials constituting the sample [78].

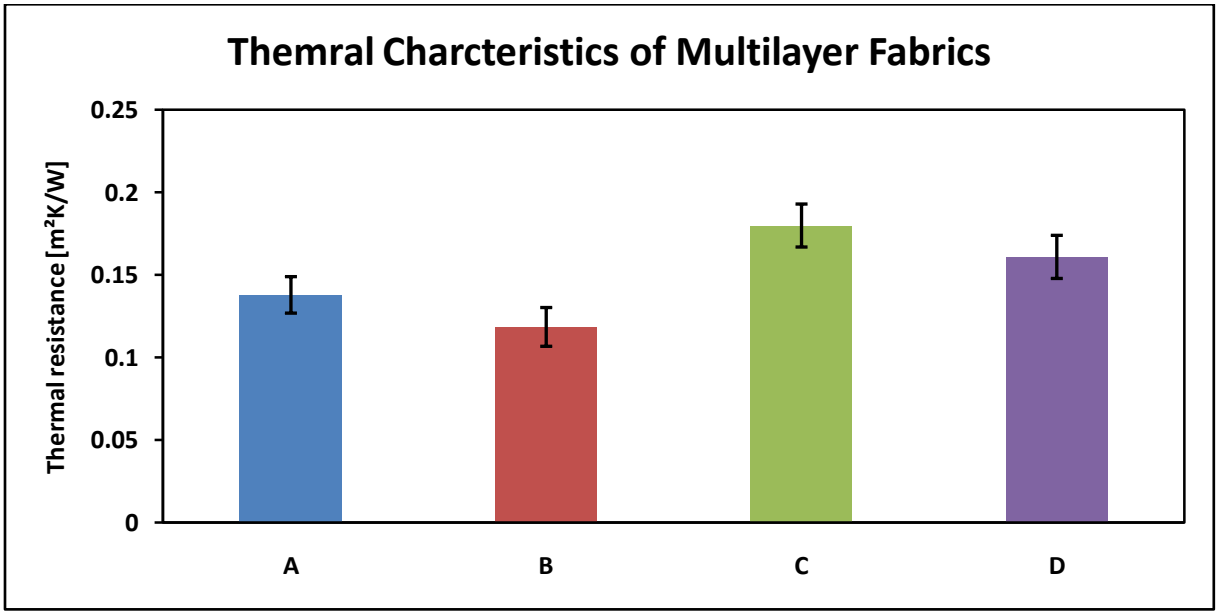

Figure 19: *Thermal resistance values of multilayer protective clothing*

On the other hand, thermal conductivity enhances with the relative humidity absorbed by the material [120][122]. Consequently, the thermal conductivity of highly hygroscopic material is more as compared to less hygroscopic substrate. From figure 19, it can be noted that a high value of thermal resistance was witnessed in arrangement of multilayer protective clothing having

aerogel layer as an alternate to thermal liner *(sample C and D)*. There might be several reasons. One reason might be that this substitute layer encloses silica based aerogel which has very less thermal conductivity even lower than still air. By means of mass, aerogel is 96 percent of air making it least dense man-made substrate [45]. Because of porous and nanometer pore size, silica based aerogels are highly insulating materials and transmit low thermal energy [49][123].

Convective heat transfer is deterred because construction of aerogel does not allow circulation of air [50][51][55]. The other reason is that this aerogel blanket also contains oxidized polyacrylonitrile fiber which has very low thermal conductivity (0.030 W/mK). Consequently, *specimen C and D* which employ aerogel layer as an alternate to thermal barrier offers more thermal resistance as compared to *specimen A and B*. On the other hand, thermal resistance of *specimen A* was slightly greater than *specimen B*. This might be due to the fact that *specimen A* has outer shell O (1) containing 75 percent and 23 percent of Nomex and Kevlar fibers respectively which have inherent flame retardant and better insulation characteristics as compared to *specimen B* in which the main ingredient of outer layer is cellulosic material (cotton) which offers more thermal conductivity and less thermal resistance as compared to outer layer of *specimen A*.

6.2.1 Evaluation of water vapor resistance

Water vapor resistance R_{et} (m^2Pa/W) was determined by Sweating guarded hot plate equipment.

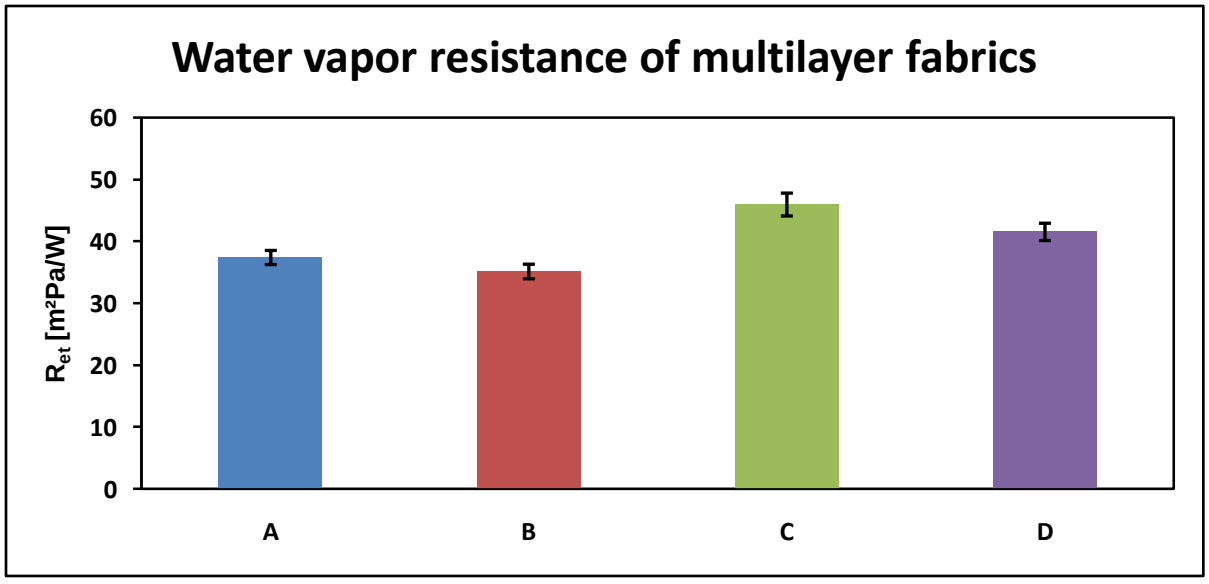

Figure 20: *Water vapor resistance of multilayer protective clothing*

A careful analysis of figure 20 revealed that more water vapor resistance was witnessed in *specimen C and D* utilizing aerogel blanket. This might be due to hydrophobic nature of aerogel and presence of closed pores inside the structure of aerogel blanket [51][52][53][58][124]. Barker et al [121] mentioned that the influence of moisture on thermal protective performance is a function of exposure conditions, amount of moisture in the turnout system and its permeability and insulation properties [121].

6.2.2 Transmission of radiant heat flux through multilayer protective clothing

This X637 radiant heat transmission equipment comprises of a radiation heat source which can generate heat flux density up to 80 kW/m^2. The outcomes of this test are the two threshold times i.e. Radiant heat transfer index *(RHTI 24 and RHTI 12)* respectively, incident heat flux density *(Q_o)* and transmitted heat flux density *(Q_c)*and percentage heat transmission factor *(percentage TF Q_o).*

Table 11: *RHTI 12 and RHTI 24, Q_o, Qc and %age TF through multilayer firefighter protective clothing specimen*

Sr #	Name of material	Q_o [kW/m^2]	RHTI12	RHTI24	RHTI24-RHTI12	Q_c [kW/m^2]	Percentage TF Q_o
1	P	10	54.55 ± 2.828	102.6 ± 2.969	48.05	1.36±0.006	13.6
2	A		58.2 ± 0.424	101.0 ±, 0.015	42.8	1.55±0.014	15.5
3	B		74.1±.707	128.65 ± 2.757	54.55	1.212±0.045	12.1
4	C		84.55 ± 0.777	163.35 ± 3.181	78.8	0.839 ± 0.026	8.3
5	D		97.4±6.929	195 ± 2.5738	97.6	0.677±0.132	6.7
1	P	20	33.25 ± 5.727	54.15 ± 8.273	20.9	3.164 ± 0.390	15.8
2	A		36.7 ± 0.989	57.05 ± 1.343	20.35	3.249±0.056	16.2
3	B		46.7±6.081	58.55 ± 6.293	11.85	5.580±0.100	27.9
4	C		44.6 ± 0.457	70.8 ± 2.596	26.2	2.524±0.050	12.6
5	D		58.15±.919	79.95 ± 1.484	21.806	3.033±0.079	15.1
1	P	30	33.3 ± 0.141	48.75 ± 0.353	15.45	4.280 ± 0.058	14.2
2	A		27.85 ± 0.070	40.35 ± 0.494	12.5	5.290±0.181	17.6
3	B		31.4±2.121	38.15 ± 2.474	6.75	9.79±0.516	32.6
4	C		41.5 ± 1.272	61 ± 2.969	19.5	3.391±0.297	11.3
5	D		44.15±1.626	59.8 ± 1.272	15.65	4.225±0.096	14.0
1	P	40	25.9 ± 0.172	36.1 ± 0.452	10.2	6.522 ± 0.154	16.3
2	A		24.8 ± 0.258	31.3 ± 0.389	6.5	10.235 ± 0.245	25.9
3	B		23.7 ± 0.121	28.9 ± 1.35	5.2	12.794 ± 0.489	32.4
4	C		41.4 ± 1.378	57.1 ± 1.14	15.7	4.237 ± 0.354	10.7
5	D		38.2 ± 1.48	52.2 ± 1.25	14	4.752 ± 0.158	11.88

A perusal of table 11 reveals that values of transmitted heat flux density Q_c and percentage Transmission factor *(percentage TF* Q_o*)* of all specimens increases sequentially with increase in level of incident heat flux density. It was also noted that minimum values of transmitted flux density Q_c *(kW/m*^{2}*)* were observed for the samples having aerogel blanket *(P)* as substitute to thermal liner. A similar pattern was also noted in *percentage TF* Q_o values for the specimen having aerogel sheet *(P)*. This might be due to fact that silica based aerogel blanket contains almost 96% of air and air is a good insulator blocking the amount of heat passed through the specimen [45]. Moreover, these aerogel samples consist of oxidized polyacrylonitrile polymer which have very good thermal stability and can withstand higher amount of heat flux [101]. The lower the value of transmitted heat flux density, the lesser will be amount of heat passed through fabric assemblies towards calorimeter allowing more time to firefighter to perform their duties before acquiring burn injuries. Table 11 also depicts that greater difference between *RHTI 24* and *RHTI 12*, lesser will be the value of transmitted flux density Q_c (kW/m^2) and *percentage TF* Q_o respectively, which indicates that specimen can withstand respected heat flux for longer time period allowing firefighters to perform their duties for longer duration before getting burn injuries. At 10 kW/m^2, the lowest values of Q_c and *percentage TF* Q_o were witnessed for *specimen C* and *D* utilizing aerogel blanket *(P)*. These values were higher for *specimen A* and *B* having no aerogel blanket. It was also noted that there was minor difference in the values of Q_c and *percentage TF* Q_o values for aerogel sheet *(P)*, *sample A and specimen B* respectively. At 20 kW/m^2, the situation was slightly different i.e. the Q_c and *percentage TF* Q_o values of *specimen B* was significantly higher than rest of the samples and negligible difference for the values of Q_c and *percentage TF* Q_o was witnessed for aerogel sheet (*P), specimen A and specimen D* respectively. The lowest value of *percentage TF* Q_o and Q_c for 20 kW/m^2 was observed for *specimen C.* At 30 kW/m^2, a trend similar to that of 20 kW/m^2 was noted i.e. the least value of Q_c and *percentage TF* Q_o was observed for *sample C* and highest value was observed *sample B*. However, this time there was significant difference in values Q_c and *percentage TF* Q_o for *specimen A* and aerogel sheet (*P)*. At 40 kW/m^2, the orientation of Q_c and *percentage TF* Q_o values was not very different than those witnessed at 30 kW/m^2. *Specimen C* displayed least values of Q_c and *percentage TF* Q_o and again a pertinent differentiation in the values of Q_c and *percentage TF* Q_o for *specimen A* and aerogel blanket (*P)*.

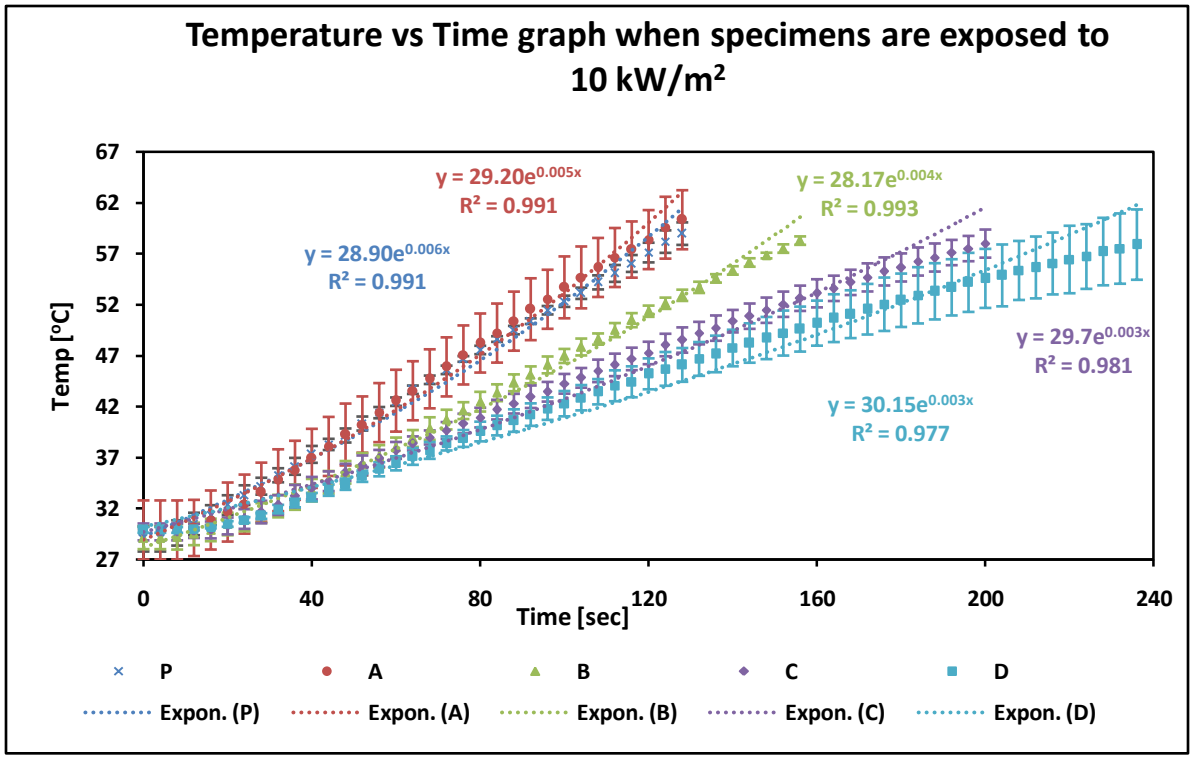

Figure 21: *Temperature of firefighter specimens with respect to time when specimens exposed to 10 kW/m²*

A glance at figure 21 reveals that at 10 kW/m² the curves of *specimen D and specimen C* are much flatter as compared to the curves of *specimen B*, *specimen A* and aerogel layer *(P)* respectively. The flatter the curve, the slower will be rate of increase in temperature, which will give more time of exposure to specimen when subjected to radiant heat flux. The flatter curve also indicates less damage to the corresponding fabric layers of the specimen. However, there was no gap in the curves of aerogel blanket *(P)* and *specimen A*, which have very close values of Q_c and *percentage TF* Q_o. Figure 21 also depicts clear gap between curves of *specimen B* and curves of *specimen A* and aerogel blanket (P), which is also highlighted from the values of Q_c and *percentage TF* Q_o from table 11. *Specimen C* has improved thermal protective performance as comparison to *specimen A* in terms of radiant heat transmitted index *RHTI 24* by *61.7 percent*. Whereas *specimen D* has improved *RHTI 24* values in comparison with *specimen B* by *51.5 percent*. The maximum value of R^2 and best fitting curves of all specimens was achieved by exponential equations.

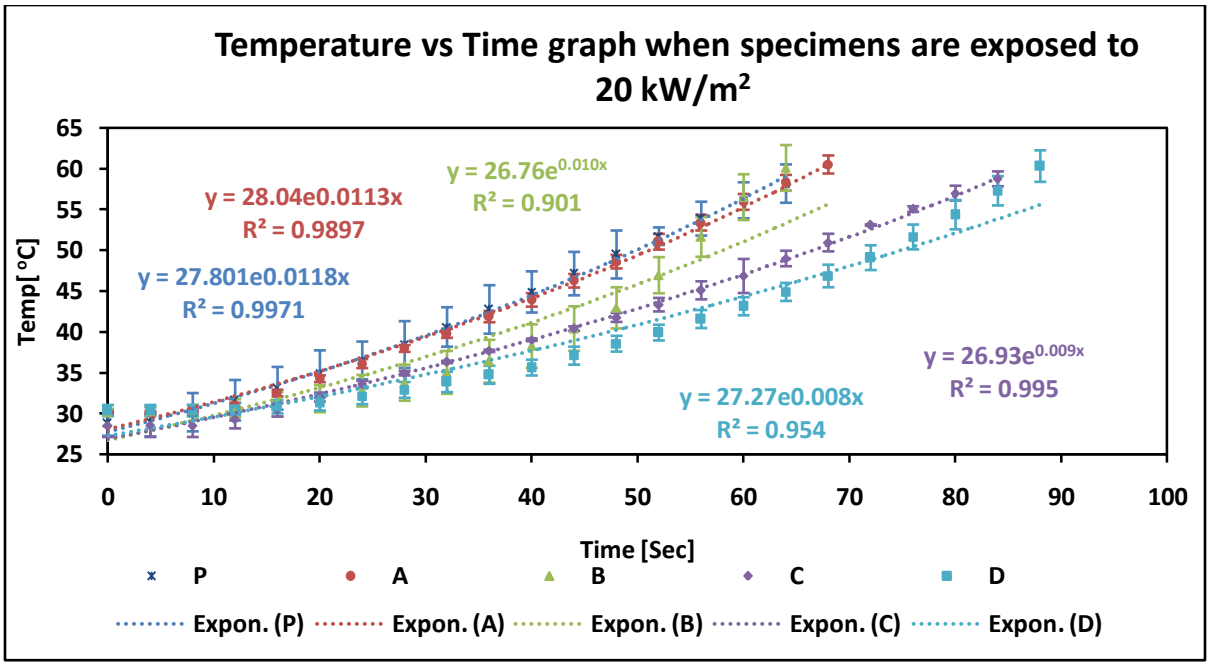

Figure 22: *Temperature of firefighter specimens with respect to time when specimens exposed to 20 kW/m²*

From figure 22, it can be seen that at 20 kW/ m^2, there was quite similarity between the curves of *specimen A* and aerogel sheet *(P)*. The pattern of the curve of *specimen B* at 20 kW/ m^2 was different than that of the curve of *specimen B* at 10 kW/ m^2. The rate of increase of temperature was smooth till 50 seconds for *specimen B* but after wards there was sharp increment in the rate of rise of temperature which might indicates sudden structural changes or deterioration of outer shell of *specimen B* as the time of exposure increases. The outer shell of *specimen B* consists of cellulosic fibers. At incident heat flux density of 20 kW/ m^2, the incident temperature on surface of outer shell was 292^{o}C and at this temperature the decomposition of cellulosic fibers occurs at spontaneous rate. The curve of *specimen C* was much flat and there was no unusual variation. However, in case of *specimen D*, the pattern of the curve was flat till 70 seconds but later on it becomes very steep indicating certain damage to layers of specimen especially the outer layer. This is also evident from values of Q_c and percentage *TF* Q_o which are higher than that of *specimen C*. *RHTI 24* value of *Specimen C* was enhanced as compared to *specimen A* by 24 percent. *Specimen D* depicts better *RHTI 24* values as compared to *specimen B* by 36.5 percent. The greatest value of R^2 and curves with best fittings for all specimens was attained through exponential equations.

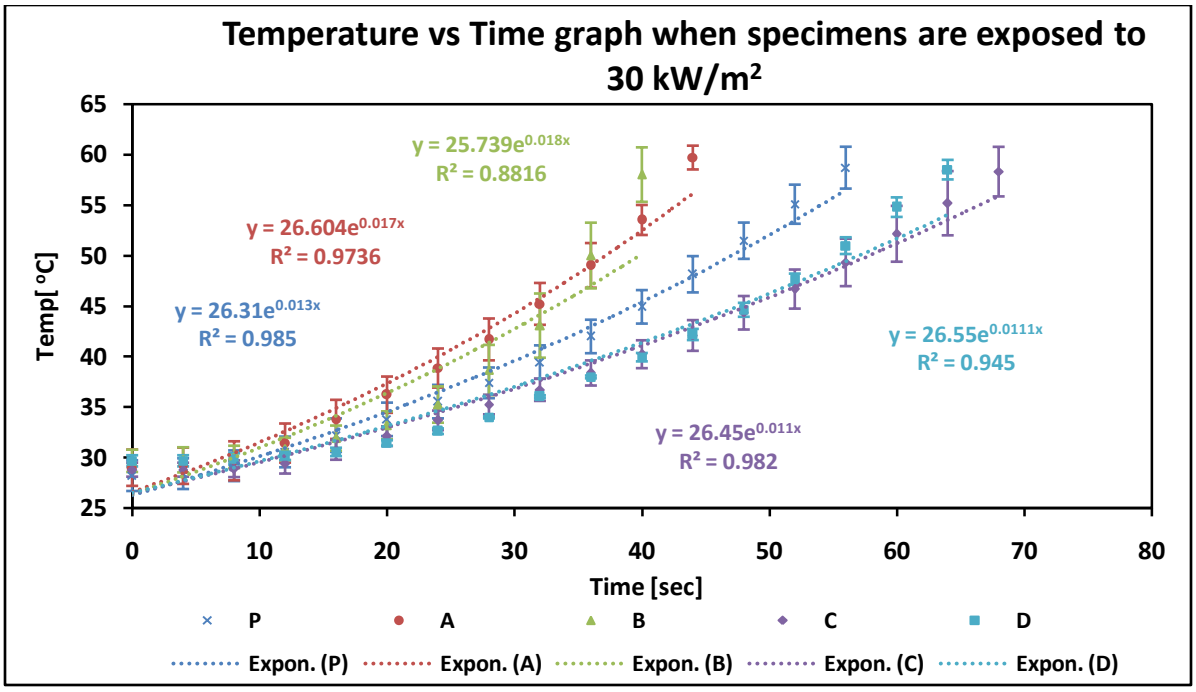

Figure 23: *Temperature of firefighter specimens with respect to time when specimens are exposed to 30kW/m²*

In case of 30 kW/m^2 from figure 23, there was dissimilarity in the pattern of the curves for *aerogel blanket (P)* and *specimen A* showing loss of thermal stability of fibers at higher flux density as compared to *aerogel blanket (P)*. But the curve of *specimen B* depicts irregular behavior after 30 seconds showing sudden sharp increment in the temperature, which is clear indication of decrease in thermal protective behavior of specimen because structural changes or deterioration of outer shell of specimen *B* due to swift rate of decomposition of cellulosic fibers as the incident temperature at surface of specimen for Q_o of 30 kW/ m^2 is 390 ^{o}C. This allows swift passage of heat after 30 seconds causing increase in values of Q_c and percentage *TF* Q_o. For *specimen D*, after 70 seconds, there was irregular increase in temperature due to which greater values of Q_c and percentage *TF* Q_o was witnessed in table 11 for *specimen D*. The curve of *specimen C* was regular, flat and long showing better thermal protective behavior of *specimen C* at 30 kW/ m^2. *Specimen C* has better *RHTI 24* value with respect to *specimen A* by 51 percent. *Specimen D* has enhanced *RHTI 24* values in comparison to *specimen B* by 56.74 percent. The maximum value of R^2 and best fitting curves for all specimens was accomplished through exponential equations.

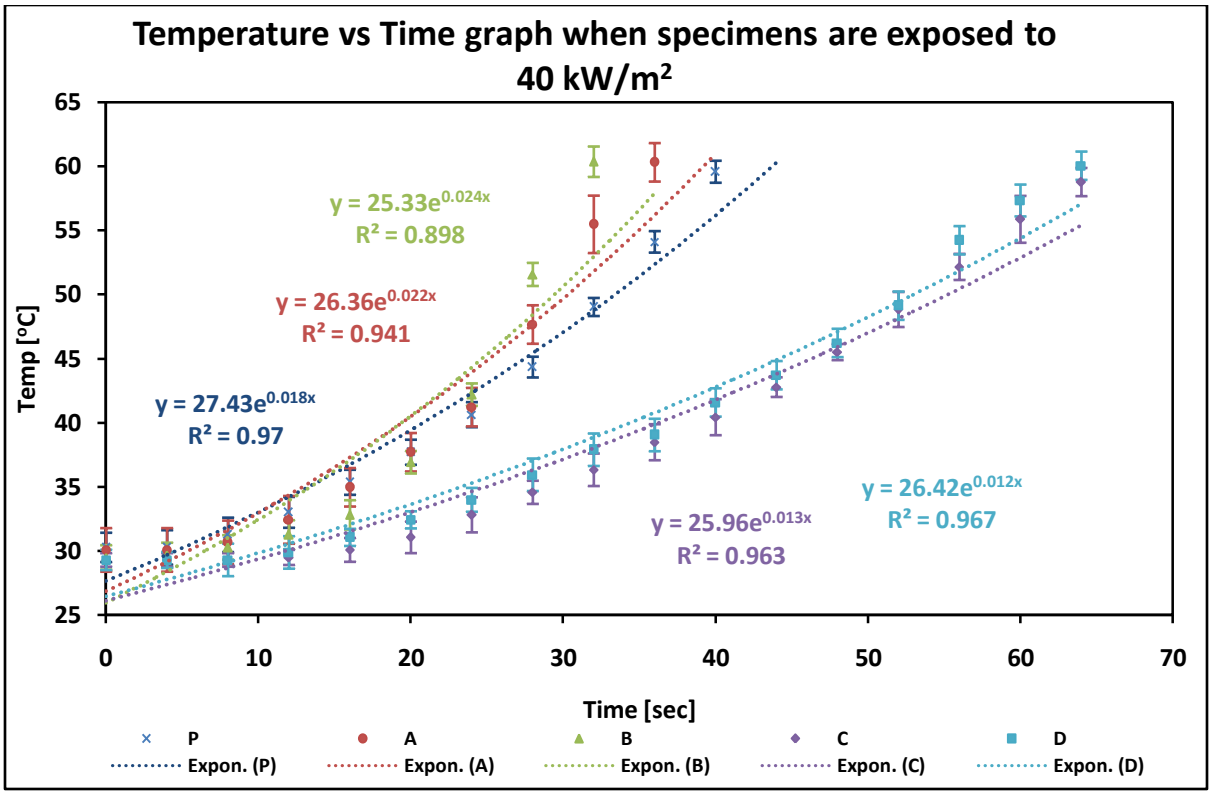

Figure 24: *Temperature of firefighter specimens with respect to time when specimens are exposed to 40 kW /m²*

It can be witnessed from figure 24 that at 40 kW/m^2, the pattern of curves for all specimens was quite similar to behavior of curves at 30 kW/m^2. *Specimen C* curve displays better thermal protective performance as compared to all other curves as curve of *specimen C* was flatter as compared to all curves of other specimen. Thus the fabric assembly having aerogel sheet *(P)* as alternate to thermal barrier has better thermal protective behavior as compared to other samples. This might be due to fact that Infrared radiation that plays a significant role in transference of heat can also be absorbed by aerogel [52][53][58] due to which aerogel blanket offers better thermal stability and insulation as compared to other specimens. *RHTI 24* value for *Specimen C* was increased as compared to *specimen A* by *82.4 percent*. In case of *Specimen D, RHTI 24* value was enhanced by *80.6 percent* in comparison with *specimen B*. The maximum value of R^2 and best fitting curves for all specimens was accomplished through exponential equations.

6.3 Effect of metallic coating on thermal protective performance of firefighter clothing specimens

6.3.1 Evaluation of water vapor permeability

Permetest was utilized to determine relative water vapor permeability and water vapor resistance of uncoated (O) specimen and silver coated O (1), O (2) and O (3) specimens. During operational activities, firefighter generates lot of sweat which must be evacuated. Therefore, the permeability of water vapor should not be neglected.

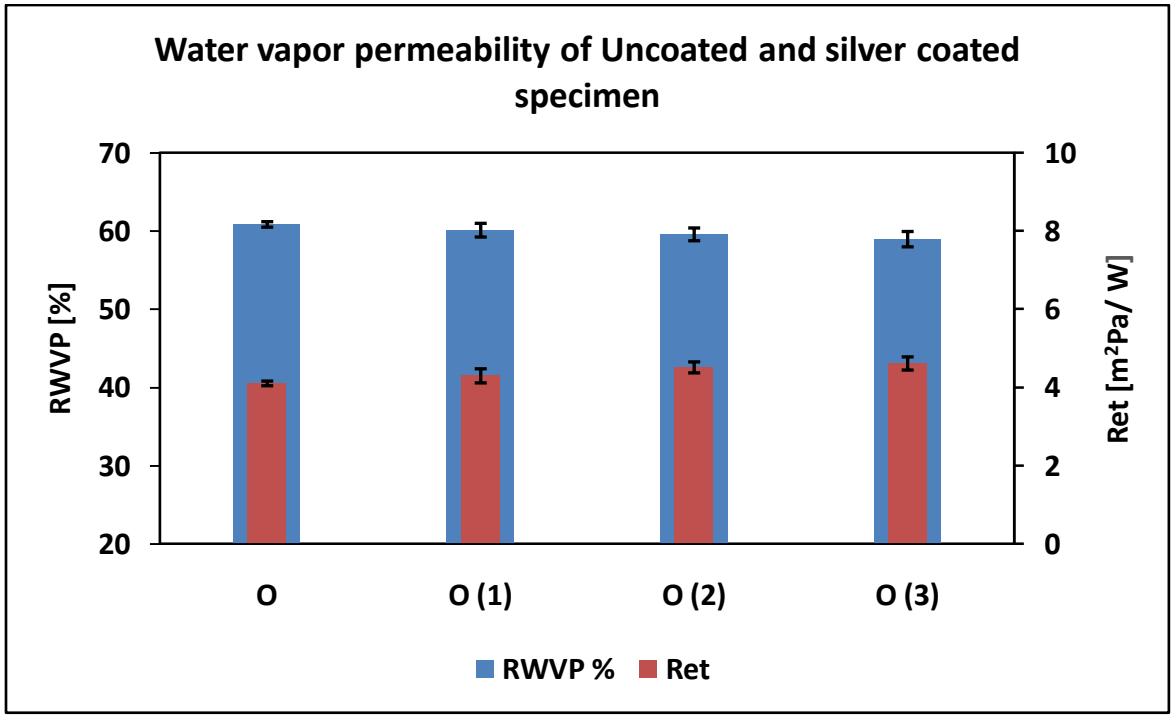

Figure 25: *Relative water vapor permeability percentage and Water vapor resistance of firefighter protective clothing specimen*

From figure 25, it was revealed that that outer shell coated with deposition layer of silver particles have slightly less values of relative water vapour permeability percentage and slightly highly values of water vapour resistance. However, this difference was not very conspicuous, which indicates that after coating of silver particles, there is still permeation of water vapour through outer shells and porous structure is not completely blocked by coating of silver particles.

6.3.2 Evaluation of Air Permeability

Evaluation of air permeability of outer shell of uncoated (O) and silver coated O (1), O (2) and O(3) specimen was carried out with the help of air permeability tester. Air permeability of firefighter protective clothing is very low because the main task of firefighter protective clothing is to protect the body of firefighter from the heat in the form of radiation, convection and conduction. If the value of air permeability is very high, it will decrease the thermal protective performance of firefighter because it will allow air to pass through the specimen resulting in increase in the temperature of human body within short duration of time [10].

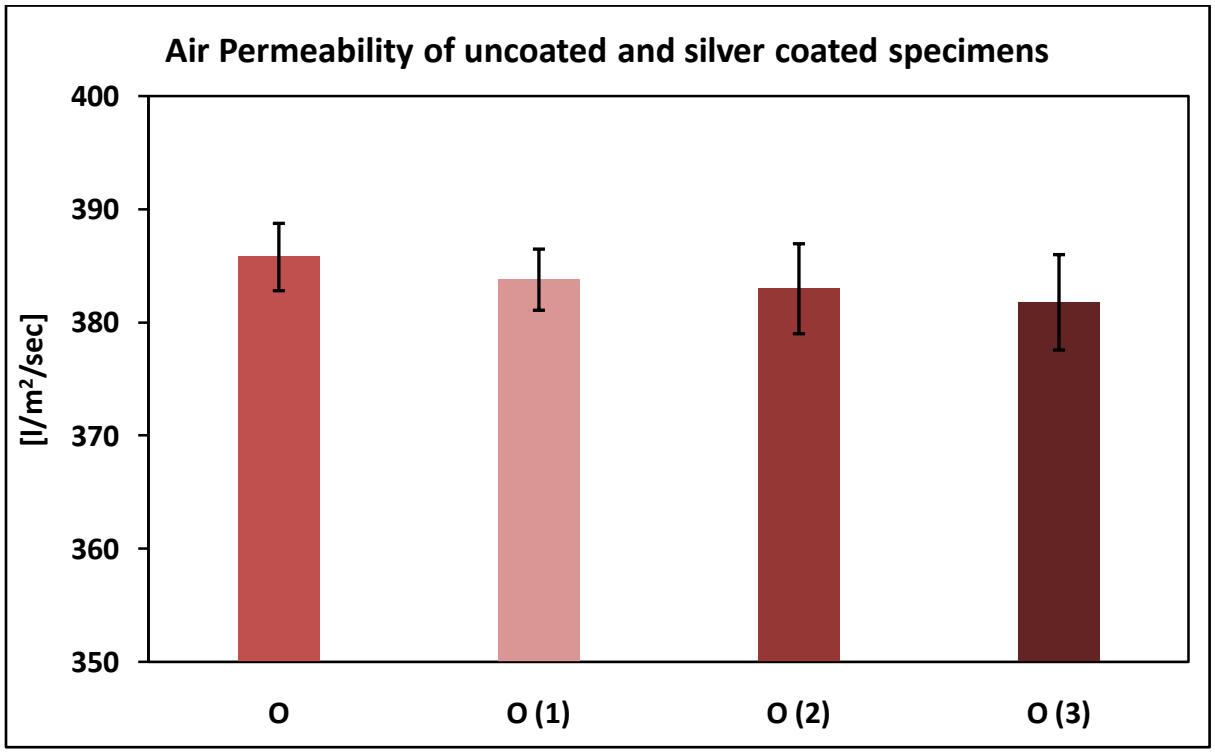

Figure 26: *Air permeability of uncoated and silver coated outer shell O(1), O(2) and O(3)*

A perusal of figure 26 revealed that there was negligible difference between the air permeability of uncoated and silver coated specimen. This might indicates that porous structure of textile substrate was not completely blocked by silver particle coating even at 3 μm thickness level for O (3) outer shell. Due to which the breathability and thermal comfort properties of protective clothing specimen was not affected to significant extent.

6.3.3 Transmission of radiant heat flux through multilayer protective clothing

The behavior of coated and uncoated specimen when subjected to respective heat flux densities are shown schematically in figure 27 a and 27 b respectively. It is evident from figure 27 a and 27 b that uncoated specimen is transferring more amount of heat through specimen towards calorimeter and less amount of heat towards surrounding environment climate due to absence silver particle layers. In case of silver coated specimen, less amount of heat Q_c *[kW/ m^2]* was transmitted via specimen towards calorimeter. Furthermore, greater amount of radiant heat flux density was dissipated to surrounding climate due to high reflective property of silver particles.

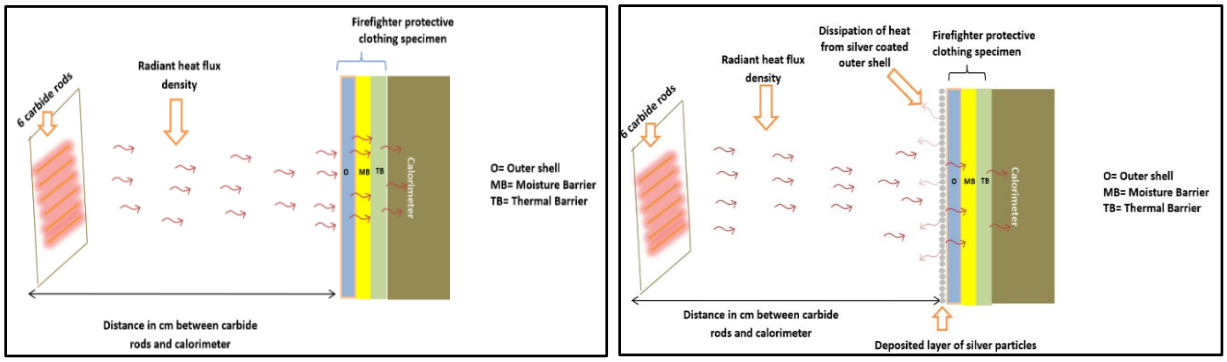

Figure 27: *a. Uncoated sample* *b. silver coated specimen*

Table 12: *RHTI 12, RHTI 24, Q_c and [%] TF Q_o values of specimen when exposed to 10 kW/ m^2, 20 kW/ m^2, 30 kW/m^2 and 40 kW/m^2*

Sr #	Specimen	Q_o [kW/ m^2]	*RHTI 12* [sec]	*RHTI 24* [sec]	*RHTI24-RHTI 12* [sec]	Q_c [kW/ m^2]	[%] *TF Q_o*
1	A	10	46.3 ± 0.94	77.2 ± 0.92	30.9	2.153 ± 0.001	21.6
2	A1	10	63.3 ± 0.86	110.5 ± 0.72	47.2	1.415 ± 0.003	14.2
3	A2	10	63.5 ± 0.72	113.6 ± 0.79	50.1	1.323 ± 0.001	13.3
4	A3	10	69.0 ± 0.73	124.3 ± 0.62	55.3	1.203 ± 0.002	12.1
1	A	20	28.6 ± 0.84	42.5 ± 0.86	13.9	4.786 ± 0.006	23.93
2	A1	20	35.6 ± 0.74	55.4 ± 0.89	19.9	3.343 ± 0.025	16.71
3	A2	20	35.8 ± 0.87	56.0 ± 0.91	20.2	3.293 ± 0.006	16.46
4	A3	20	37.5 ± 0.81	59.1 ± 0.75	21.6	3.080 ± 0.008	15.4
1	A	30	23.9 ± 0.93	33.2 ± 0.98	9.3	7.154 ± 0.038	23.84
2	A1	30	27.4 ± 0.82	38.9 ± 0.89	11.5	5.785 ± 0.035	19.28
3	A2	30	30.4 ± 0.75	42.5 ± 0.80	12.1	5.498 ± 0.022	18.32
4	A3	30	31.6 ± 0.82	44.2 ± 0.88	12.6	5.280 ± 0.024	17.6
1	A	40	19.3 ± 0.94	26.9 ± 0.89	7.6	8.754 ± 0.05	21.88
2	A1	40	25.2 ± 0.85	34.5 ± 0.88	9.3	7.154 ± 0.022	17.88
3	A2	40	26.1 ± 0.81	35.7 ± 0.79	9.6	6.930 ± 0.58	17.32
4	A3	40	27.7 ± 0.88	38.2 ± 0.91	10.5	6.29 ± 0.018	15.80

An overview of table 12 depicts that silver coated *specimen A1*, *A2* and *A3* have high *RHTI 12* and *RHTI 24* values and low values of transmitted heat flux density and percentage Transmission Factor *[%] TF* Q_o at 10 kW/m^2, 20 kW/m^2, 30 kW/m^2 and 40 kW/m^2 respectively as compared to uncoated *specimen A*. There was further decrease in the values of Q_c and percentage *TF* Q_o with the increase in thickness level of silver deposited layer on outer shell of firefighter protective clothing specimen. This might be due to fact that outer shell has coating of silver particles having high melting point and highly reflective property which not only slow down the amount of heat passing through the specimen but also reflect radiant substantial amount of radiant heat flux density. The lower the values of transmitted heat flux density Q_c *[kW/ m^2]* and percentage transmission factor, better will be thermal protective performance as less heat will be transmitted towards human body for given period and great time will be required for rise of temperature of 12 ^oC and 24 ^oC in the form of *RHTI 12* and *RHTI 24* allowing greater amount of time to firefighters to perform their duties without enduring injuries.

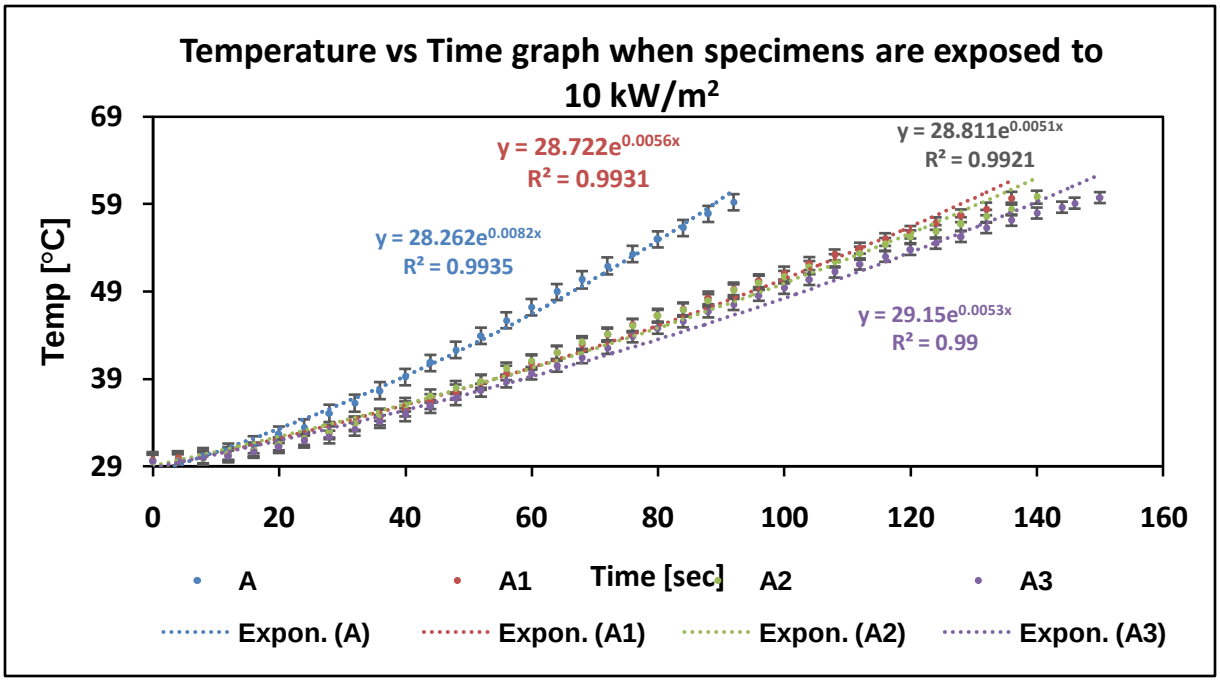

Figure 28: *Temperature of firefighter specimens with respect to time when specimens are exposed to 10 kW/m^2*

Figure 28 reveals that curves of all specimens were at same position till 15 seconds. Afterwards, curve of *sample A* started to move in upward position and a slight gap appeared between curve of *specimen A* and rest of specimen curve at 20 seconds which keep on increasing with the passage of time as the curve of *specimen A* becomes steeper than the rest of the curves. The curves of

specimen A1 and *A2* follow same path in almost superimposed position. After 100 seconds, the curve of *specimen A1* becomes slightly upward as compared to curve of specimen *A2* and it remains in upward position till end. The curve of *specimen A3* remains in flat position and gap between curves of *specimen A3* and *A2* started to widen off after 40 seconds and keep on widening till the end. *Specimen A1* has improved *RHTI 24* values with respect to *specimen A* by 43 percent and highest value of R^2 along with best fitting curves were gained through exponential equations.

A perusal of figure 29 reveals, when uncoated and silver particle coated specimen were subjected to 20 kW/m^2, almost similar pattern of time versus temperature curve was acquired when exposed to 10 kW/m^2. All specimens in figure 29 follows same pattern till first 5 seconds. Afterwards, curves of *specimen A1*, *A2* and *A3* remains flatter than that of curve of *specimen A*. After 15 seconds, the pattern of curve of *specimen A3* takes flatter path with respect to curves of *specimen A1*and *A2* respectively. The curves of *sample A1* and *A2* remains neck to neck till 52 seconds, then *specimen A2* curves remained slightly flatter than *A1* curve. *RHTI 24* values for specimen *A1* was increased by 30.35 percent as compared to *specimen A*. The best fitting curves and maximum value of R^2 for all specimens was acquired by exponential equations.

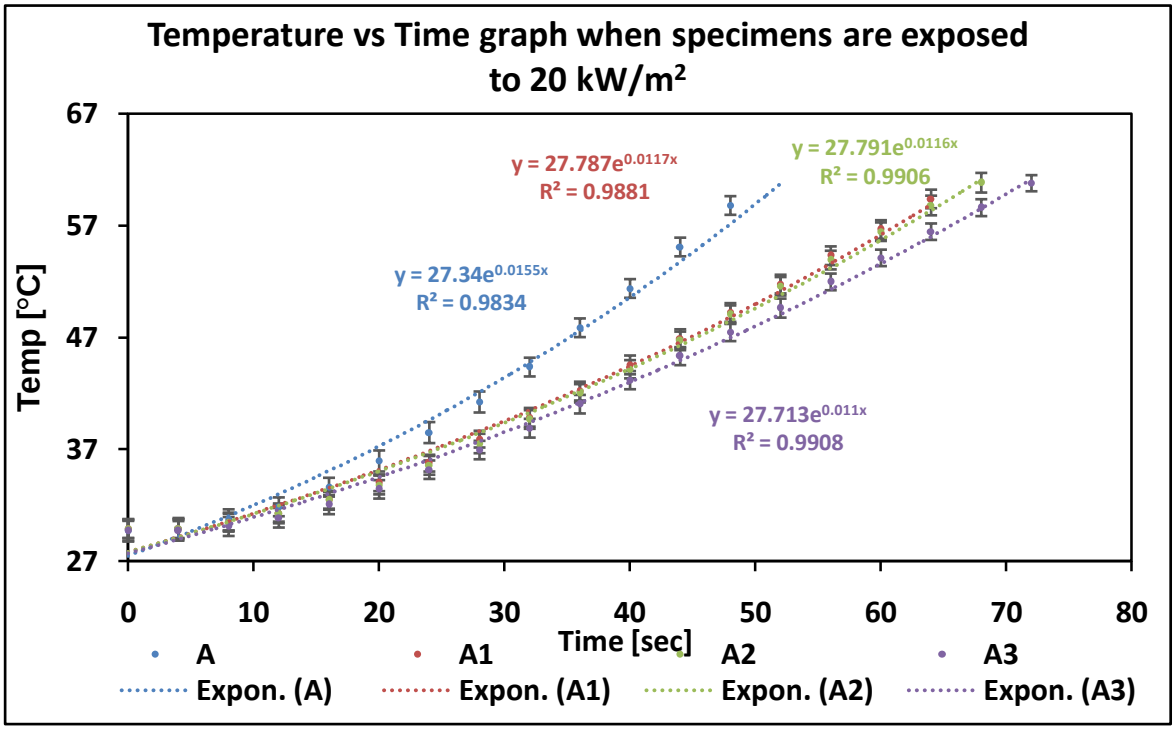

Figure 29: *Temperature of firefighter specimens with respect to time when specimens are exposed to20 kW/m^2*

A careful analysis of figure 30 reveals that at 30 kW/m^2 the behavior of curves of all specimen was not very different from pattern of the curves when subjected to 20 kW/m^2.

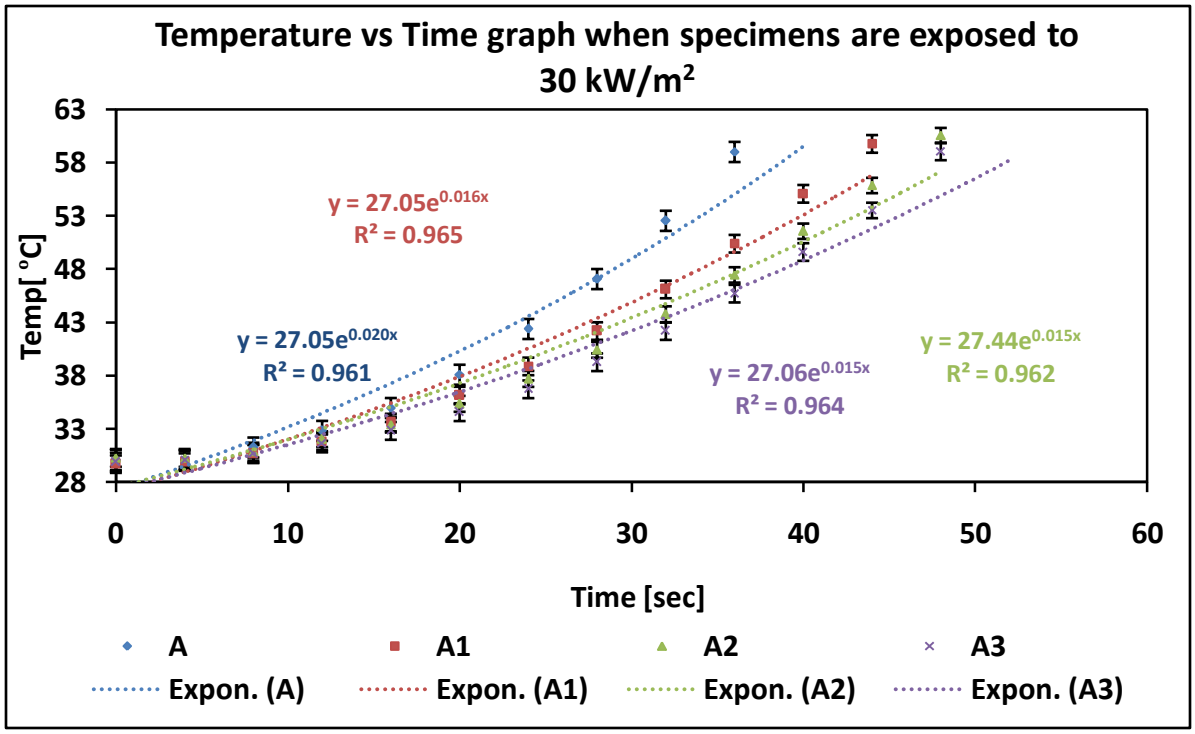

Figure 30: *Temperature of firefighter specimens with respect to time when specimens are exposed to 30 kW/m^2*

Almost similar pattern was displayed by specimen till initial 5 seconds. Afterwards, curve of *specimen A* becomes steeper and curves of *specimen A1, A2 and A3* remains in flat position. After 15 seconds, the gaps between the curves of *specimen A* with respect to curves of *specimen A1, A2 and A3* started to increase. The curves of *specimen A2 and A3* are very close to each other till initial 12 seconds. Afterwards the curve of *specimen A3* remains in flatter position which shows better thermal protective performance. *RHTI 24* values for curve of *specimen A1* was incremented by 17 percent as compared to curve of specimen *A*. The best fitting curves and highest value of R^2 for all specimen in figure 30 was acquired by exponential equations.

A perusal of figure 31 reveals that till first 5 seconds, all the curves of *specimen A, A1, A2 and A3* are very close to each other. Later on, the curve of specimen *A* moves upward and the gap of curve *A* increases against other curves with increase in time. Till initial 10 seconds, the curve of *specimen A1, A2 and A3* are neck to neck. Afterwards, the curve of *specimen A1* remains slightly

upward and this gap increases with the passage of time. The curves of *specimen A2 and A3* were very close to each other till first 12 seconds and then curve of *specimen A3* remains in flat position for the rest of experimentation. Curves of *specimen A1* has improved RHTI 24 values as compared to curve of *specimen A* by 28.2 percent. Highest R^2 and best fitted curves for all specimens was accomplished by exponential equations.

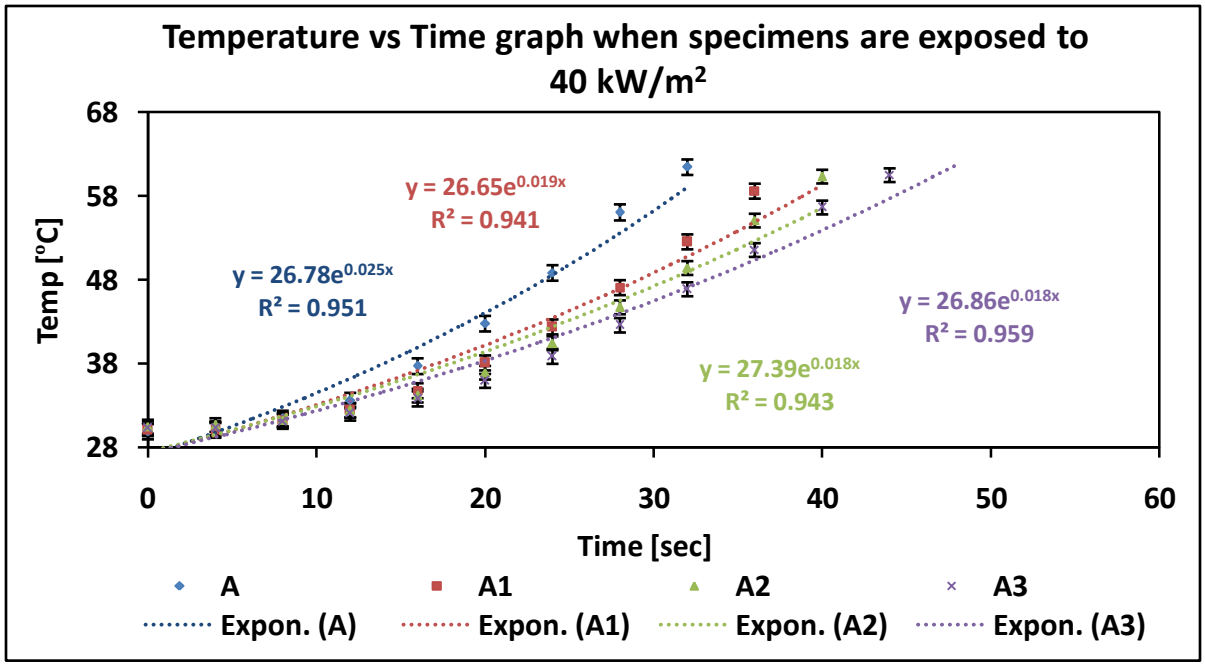

Figure 31: *Temperature of firefighter specimens with respect to time when specimens are exposed to 40 kW/m²*

It can be summarized from figure 28 to figure 31 that all curves of uncoated *specimen A* when exposed to 10 kW/m2, 20 kW/ m^2, 30 kW/m^2 and 40 kW/m^2 deliver very steep curve as compared to the curves of silver particles coated specimen. The steeper curves mean rate of rise of temperature per second is very fast. This means specimen are transferring the heat towards the calorimeter at swift rate and time to achieve second degree burns occur at very fast rate. As a result, less time will be spent by firefighter on their duties. The point where curve started to become steep might be indication of certain amount of damage in the FFPC specimen. It was noticed that the curves of silver coated *specimen A1, A2* and *A3* specimen were very close to each other. However, there was significant gap between the curve of uncoated *specimen A* and curves of silver coated specimen. This indicates the enhancement of thermal protective performance due to presence of silver coated film deposited through magnetron sputtering.

6.3.4 Analysis of surface morphology

In order to determine impact of radiant heat flux density on surface morphology of uncoated and silver coated specimen, scanning electron microscopic images were taken.

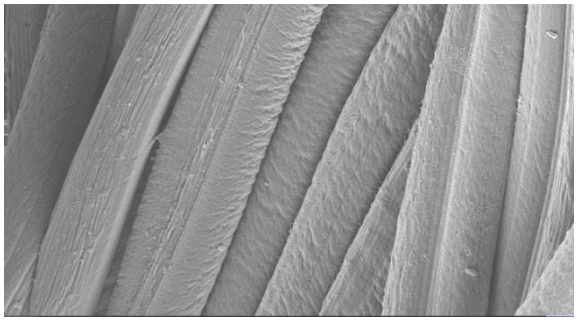

a. Uncoated specimen O

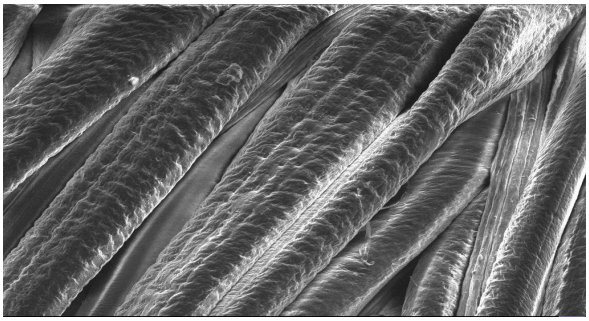

b. Uncoated specimen O exposed to 40 kW/m^2

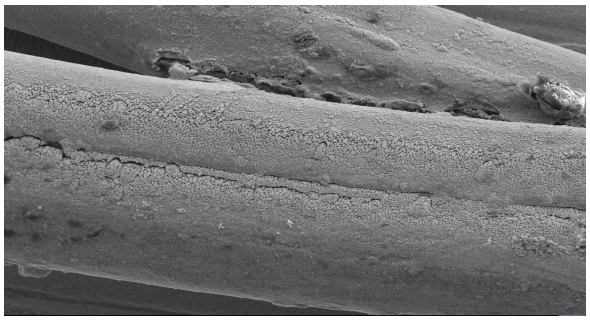

c. 3 *um* silver coated specimen O3

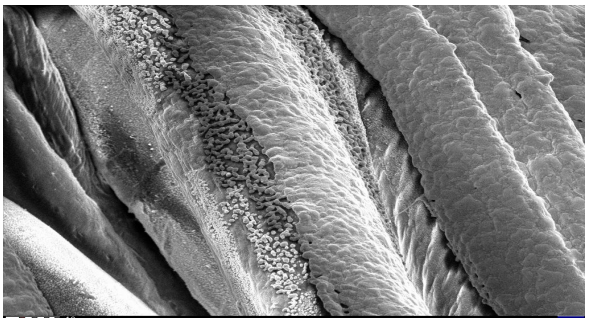

d. 3 *um* silver coated specimen O3 exposed to 40 kW/m^2

Figure 32: *Scanning electron microscopy images of coated and uncoated samples*

From figure 32 b and d, it was noted that uncoated specimen on being exposed to 40 kW/ m^2 has much darker surface as compared to 3 μm silver coated specimen. This might indicates better thermal stability of silver coated specimen as this specimen is reflecting/dissipating incident radiant heat flux density to surrounding environment. Also the presence of silver particles can be witnessed even after exposure to 40 kW/m^2 as shown in figure 32 d.

6.3.5 Determination of Stiffness/ Bending moment

Bending moment was evaluated with the help of TH4 (Tuhomer) device. The greater the bending force *F* required to bend the textile substrate at particular angle, greater will be the bending moment which ultimately results into greater stiffness of textile substrate. From above figure 33,

it can be witnessed that with increase in thickness level of silver deposition layer, there was slight increase in bending moment values of silver coated specimen.

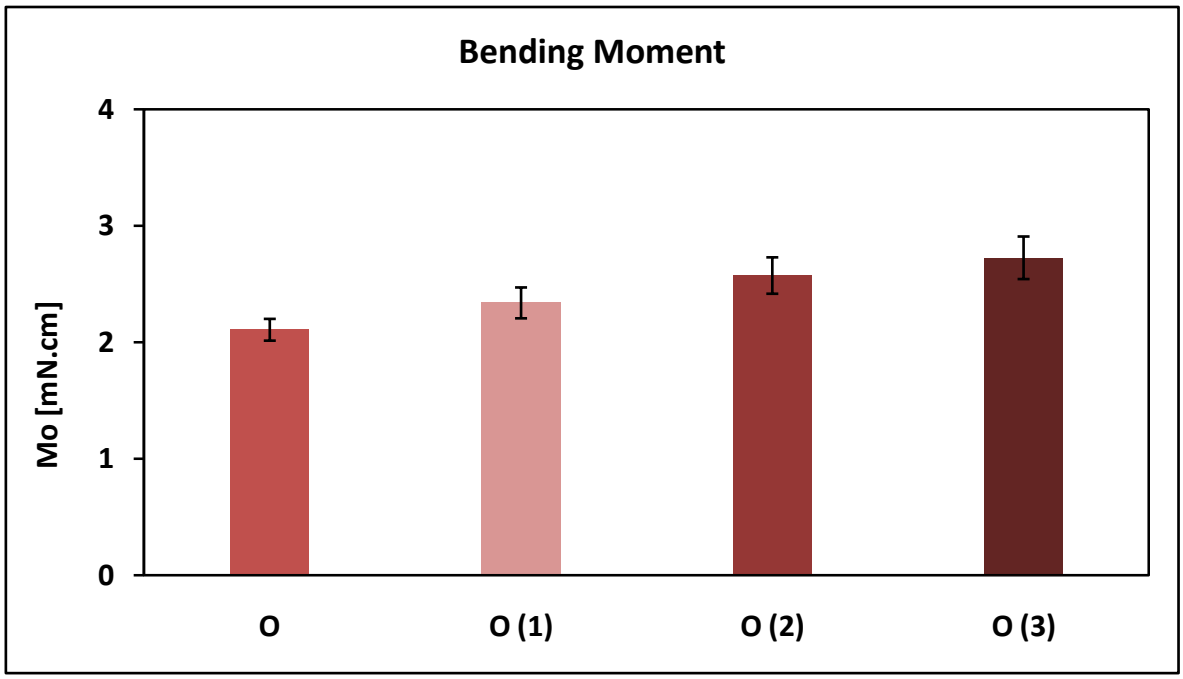

Figure 33: *Bending rigidity of uncoated and silver coated specimen*

This difference occurs due to coating of silver particles which eventually increases weight of outer shell due to which slightly greater amount of force was required to bend specimen through certain angle.

6.3.6 Evaluation of Emissivity

Emissivity of specimen was evaluated with Fluke Ti 25 Infrared camera. Emissivity of surface depends not only on the material but also on the nature of surface i.e. polished and clean metal surface have low emissivity values as compared to rough, oxidized metal surface having high emissivity values.

Table 13: *Emissivity values of hot plate, uncoated specimen and silver coated specimen*

Hot plate	Uncoated specimen	Silver coated specimen
0.98	0.86	0.52

Emissivity is dimensionless number having values between 0 (perfect reflector) and 1 (perfect emitter). Emissivity is also dependent on temperature of surface along with its wavelength and angle. Understanding of emissivity is pertinent for non-contact temperature measurement and transmission of heat calculations [125].

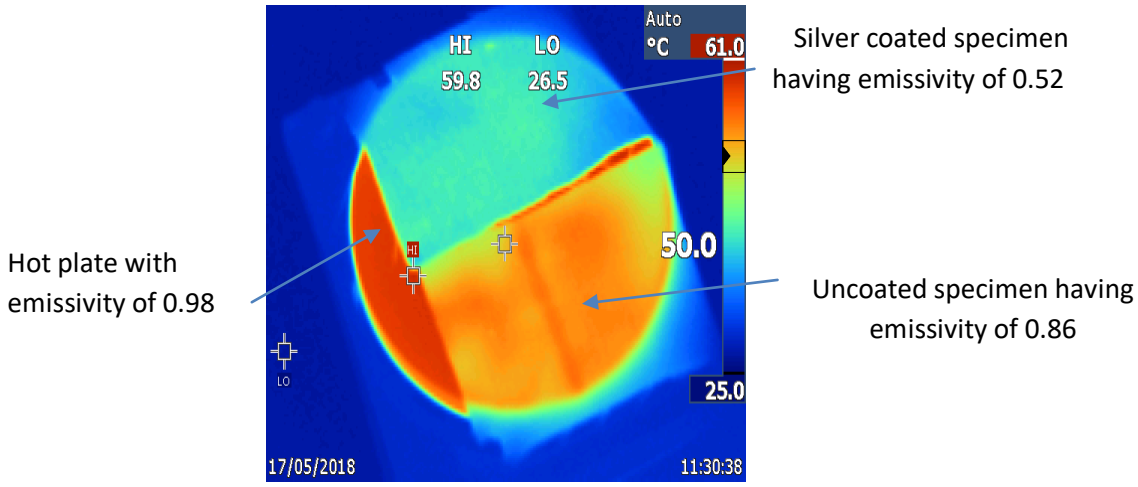

Figure 34: *Thermal images of hot plate, uncoated and silver coated specimen*

The brighter yellow color in the figure 34 shows emission of more thermal radiation and therefore have higher emissivity values. On the other hand, the light bluish dull colors depict less emissivity values and thus endure good reflective properties. Figure 34 shows, silver coated specimen have good reflective property due to which it is able to dissipate greater amount of radiant heat flux density to surrounding temperature.

6.3.7 Thermal Protective Performance after washing

In order to investigate stability of metallic coating on surface of substrate, silver coated specimens were washed for five cycles in Miele washing machine and their thermal protective performance was investigated at 40 kW/m^2. Comparison of Q_c and radiant heat transmitted index is shown in table 14.

Table 14: *RHTI 12, RHTI 24, Q_c and [%] TF Q_o values of specimen when exposed to 40 kW/m^2 before and after washing cycles*

Sr #	Specimen	Q_o [kW/m^2]	*RHTI 12* [sec]	*RHTI 24* [sec]	*RHTI24-RHTI 12* [sec]	Q_c [kW/ m^2]	Percentage *TF* Q_o
1	A1 (Before washing)	40	25.2± 0.79	34.5± 0.84	9.3	7.15±0.05	17.88
2	A1 (after one cycle)	40	24.12± 1.01	33.3±1.16	9.18	7.20±0.117	18.00
3	A1 (After two cycle)	40	24.0 ±1.44	33.12±1.58	9.12	7.25±0.111	18.17
4	A1 (after three cycle)	40	23.8± 1.26	32.65±1.36	8.85	7.47±0.084	18.68
5	A1 (after four cycle)	40	23.5±1.74	32.32±1.84	8.825	7.49±0.085	18.73
6	A1 (after five cycle)	40	23.1±1.69	31.72± 1.79	8.625	7.66±0.089	19.16

From table 14, it was witnessed that silver coated *specimen A1* has slightly high value of *RHTI 12* and *RHTI 24* before washing. It was also observed that value of Q_c before washing for *A1* specimen was a little less. With increase in number of washing cycle, there was minor decline in values of *RHTI 24*. On the other hand the value of Q_c, started to slightly increment in sequence with increase in number of washing cycles. This might indicates that coating of silver particles remains almost stable during washing cycles and no considerable damage was done to coating layer after several washing cycles.

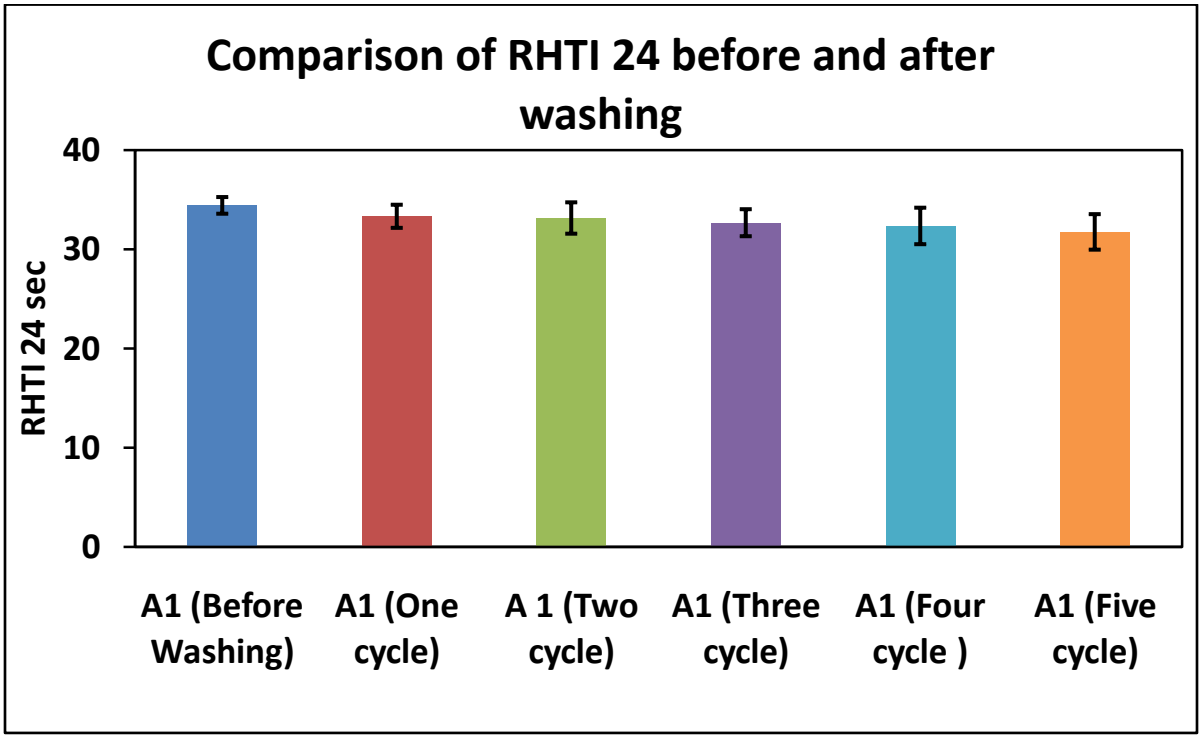

Figure 35: *Comparison of RHTI 24 before and after washing for specimen A1*

A comparison was made for *RHTI 24* before and after washing in order to quantify decrease in *RHTI 24* for specimen *A1* when exposed to 40kW/m^2 in figure 35. It can be witnessed that there was 3.4 percent and 4 percent decline in *RHTI 24* values after one and two washing cycles respectively. However, after three and four washing cycles the decrease in *RHTI 24* was 5.36 percent and 6.3 percent. After five washing cycle there was almost 8.05 percent decrement in *RHTI 24*.

6.3.8 Analysis of SEM images before and after washing

SEM images were taken for further verification of minor decrease in TPP for silver coated specimen.

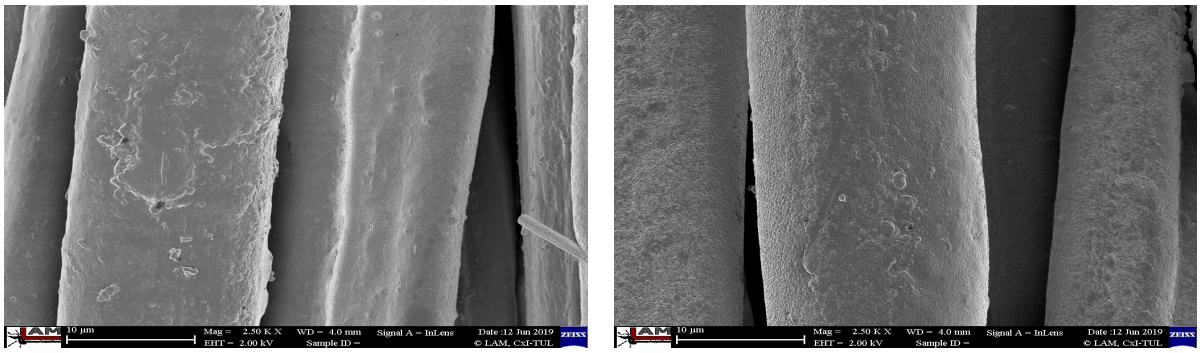

a. SEM images of O1 silver before washing

b. SEM images of O1 after five washing cycles

Figure 36: *SEM images before and after washing*

It can be clearly seen From SEM images given in figure 36 b that there is retention of metal coating even after five cycles of washing. No evidence of substantial removal of silver coating was witnessed for specimen *A1* in figure 36 b.

6.3.9 Thermal Protective Performance after abrasion

For further verification of stability of silver coating on outer shell substrate, Martindale abrader was utilized. Q_c and *RHTI 12* and *RHTI 24* values were mentioned in table 15 for different cycle of abrasion for specimen A1 when subjected to 40 kW/m^2. An overview of table 15 depicts, silver coated *specimen A1* has greater value of *RHTI 12* and *RHTI 24* before abrasion. It was noted that value of Q_c before abrasion for *specimen A1* was less. As the number of abrasion cycles increase, the values of *RHTI 12* and *RHTI 24* began to decrement.

Table 15: *RHTI 12, RHTI 24, Q_c and [%] TF Q_o values of specimen when exposed to 40 kW/m^2 before and after abrasion cycles*

Sr #	Specimen	Q_o [kW/ m^2]	*RHTI 12* [sec]	*RHTI 24* [sec]	*RHTI24-RHTI 12* [sec]	Q_c [kW/ m^2]	Percentage *TF* Q_o
1	A 1 (Before abrasion)	40	25.2 ± 0.79	34.5± 0.84	9.3	7.15±0.05	17.88
2	A1 (after twenty abrasion cycle)	40	23.1 ± 0.85	32.2 ± 0.95	9.1	7.31±0.08	18.27
3	A1 (After fifty abrasion cycle)	40	22.7 ± 0.79	31.1 ± 0.97	8.4	7.58±0.65	18.95
4	A1 (after hundred abrasion cycle)	40	21.2 ±0.81	29.5 ± 0.99	8.3	7.97±0.172	19.99
5	A1 (after five hundred cycle)	40	20.5 ± 0.85	28.7 ± 1.08	8.2	8.06±0.22	20.1

With increase in number of abrasion cycles, value of *RHTI 12* and *RHTI 24* started to decrease substantially. The value of Q_c increases in sequence with increase in number of abrasion cycles. This might indicates possible damage to silver coating on *specimen A1* which result in decline of thermal protective performance. Figure 37 reveals a comparison for *RHTI 24* before and after abrasion for quantification of reduction in *RHTI 24* for specimen *A1*.

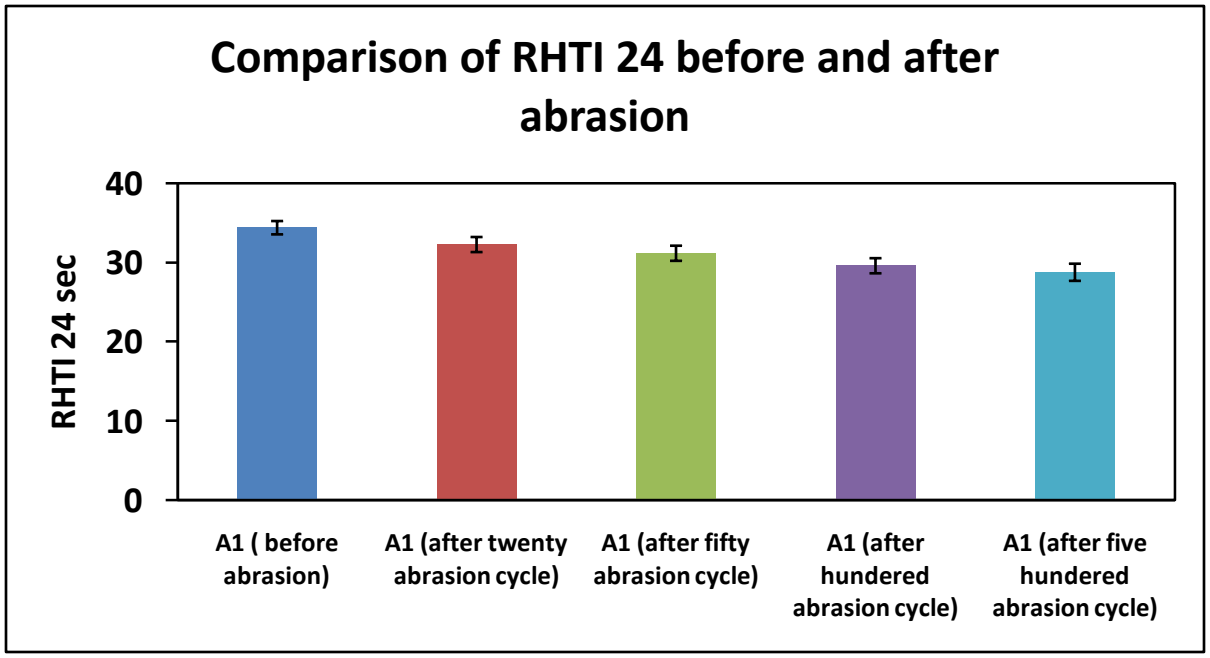

Figure 37: *Thermal Protective performance before and after abrasion*

A perusal of figure 37 depicts, for twenty and fifty abrasion cycles the decline in *RHTI 24* was 6.66 percent and 9.85 percent respectively. Whereas, decline in *RHTI 24* value was 14.49 percent

and 16.81 percent respectively. This indicates certain deterioration of metallic on coating on surface of substrate layer.

6.3.10 Analysis of SEM images before and after abrasion

For investigation of decline in TPP, SEM micrographs were examined. A careful look at SEM images reveals certain removal of metallic coating at certain points in figure 38 c and d respectively. This indicates that as number of abrasion cycles increases there was certain deterioration of metallic coating. As a result, there was substantial decline in TPP.

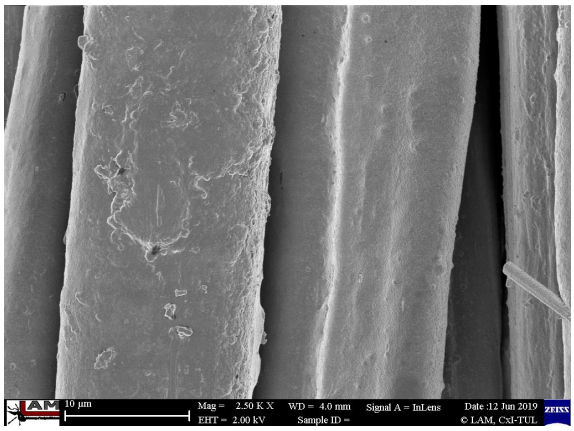

a. SEM images of O1 (1 µm silver coating) before abrasion

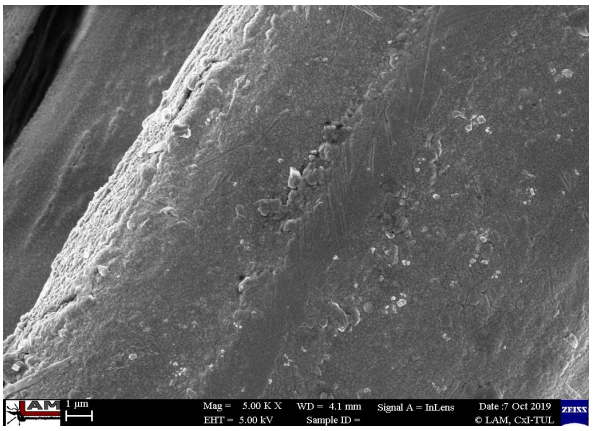

b. SEM images of O1(1 µm silver coating) after 20 abrasion cycle

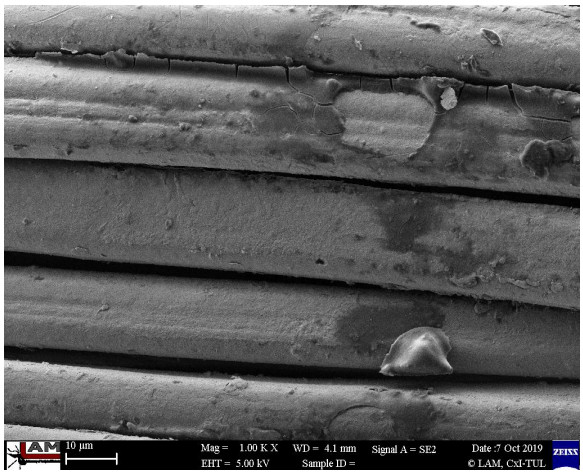

c. SEM images of O1(1 µm silver coating) after 50 abrasion cycle

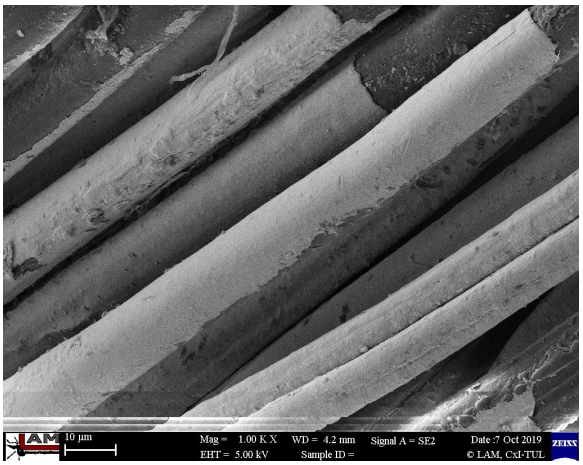

d. SEM images of O1 (1 µm silver coating) after 100 abrasion cycle

Figure 38: *SEM micrographs before and after abrasion*

6.3.11 Evaluation of Reflectance and transmissivity

Mid Infrared Integrator with FTIR spectrometer was used for evaluation of reflectivity and transmissivity. It can be witnessed from table 16 that uncoated specimen O has lower value of reflectance as compared to silver coated specimens O1, O2, and O3 respectively. This might be due to better reflective property of silver particle which reflects the incident radiant heat flux towards ambient surrounding and in consequence less amount of radiant heat flux was transmitted towards calorimeter. The greater the reflectivity, the lesser will be emissivity and better will be thermal protective performance of multilayer clothing specimens.

Table 16: *Reflectivity for uncoated and silver coated specimen*

Layers	O	O1	O2	O3
Reflectivity	0.09 ±0.01	0.46± 0.01	0.50 ± 0.02	0.53 ± 0.01

From table 17, it was witnessed that uncoated specimen has greater transmittance value as compared to silver coated specimen. Due to this reason greater amount of heat flux was transmitted towards calorimeter highlighting greater rate of rise in temperature at the back of calorimeter in uncoated specimen.

Table 17: *Transmissivity values for uncoated and silver coated specimen*

Layers	O	O1	O2	O3
Transmissivity	0.01±0.01	0.007± 0.02	0.006 ± 0.01	0.004 ± 0.01

CHAPTER 7: NUMERICAL MODEL FOR PREDICTION OF TEMPERATURE DISTRIBUTION

In the previous chapters, experimental investigations for rate of rise in temperature for uncoated and silver coated firefighter clothing specimens were performed. It has been observed that rate of rise in temperature was low for those specimens in which outer shell was coated with silver particles. This chapter deals with the Numerical model for prediction of temperature distribution at several positions along with thickness of uncoated and silver coated specimen at different intervals of time. Numerical model implemented by Su et al [126][127] was used with slight modification for estimation of temperature distribution in uncoated and silver coated firefighter protective clothing specimen. In the end, a comparison was made for uncoated and silver coated specimens for rate of rise in temperature at different positions with respect to time interval with the help of Numerical solutions. Radiant heat transmission equations mentioned by Su et al [126][127] and Torvi et al [128] were employed to illustrate radiant heat flux density transmitted towards the firefighter clothing assembly from heat source.

7.1 Materials and Methodology

The firefighter clothing specimens used in this study were consisted of outer shell, moisture barrier and thermal barrier. These specimens were provided by Vochoc Company, Czech Republic. The specifications of these specimens are given in table 18 below. The outer shell of these specimens was coated with 1 μm coating of silver particles through magnetron sputtering. Two arrangement of fabric assemblies as given in table 19 were made from these samples.

Table 18: *Specification of samples*

Sr #	Name of Sample	Code	Material specification	Weave design	GSM [g/m^2]	Thickness [mm]
1	Outer shell	O	70% Conex, 23 % Lenzing FR, 5% Twaron, 2 % Beltron	Rip stop	225±2.1	0.44±0.01
2	Outer shell (1 µm thickness)	O (1)	70% Conex, 23 % Lenzing FR, 5% Twaron, 2 % Beltron	Rip Stop	234±1.8	0.441±0.02
3	Moisture Barrier	MB	Face fabric, 50 %/50 % Kermel / viscose FR, PTFE membrane	Non-woven	120±1.8	0.55±.01
4	Thermal Barrier	TB	Thermo: Para Aramid Inner futter: 50% Meta aramid, 50% viscose	Non-woven	200±2.3	1.8±0.02

Table 19: *Arrangement of Fabric assemblies along with their code*

Sr #	Fabric assembly	Fabric code	Fabric weight [g/m^2]	Thickness [mm]
1	Outer shell (O) + Moisture Barrier (MB) + Thermal barrier (TB)	A	545±3.1	2.79±0.02
2	Outer shell (O1) + Moisture Barrier (MB) + Thermal barrier (TB)	A1	554±3.5	2.791±0.03

These specimens were exposed to a 10 kW/m^2 heat flux. In order to determine temperature distribution between multilayer clothing assembly, two K-type thermo couples were placed between outer shell and moisture barrier, and moisture barrier and thermal barrier as shown in figure 39. Thermocouple 1 measures temperature of outer shell and thermocouple 2 measures temperature of the moisture barrier.

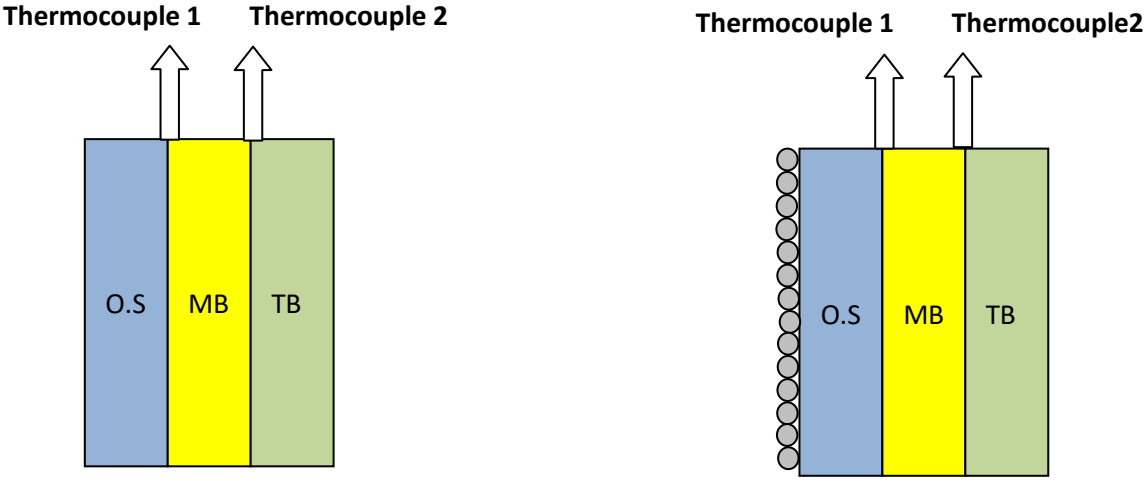

Figure 39: *a. Uncoated specimen* *b. silver coated specimen*

In order to simplify explanation with theoretical equations, following assumptions have been made:

i. Transmission of heat takes place in one dimension only.
ii. Transfer of mass is negligible
iii. Radiation only penetrates through exterior shell of multilayer assembly as almost 95% of incident energy is in the form of radiation that is absorbed after covering a distance equivalent to the outer shell thickness
iv. Optical characteristics like transmissivity, reflectivity and absorptivity are assumed constant [126][127] [128].

Initial temperature of room was 301.45 K ± 3 K. Temperature versus time graph for uncoated and silver coated specimens are shown in figure 40 and figure 41 respectively.

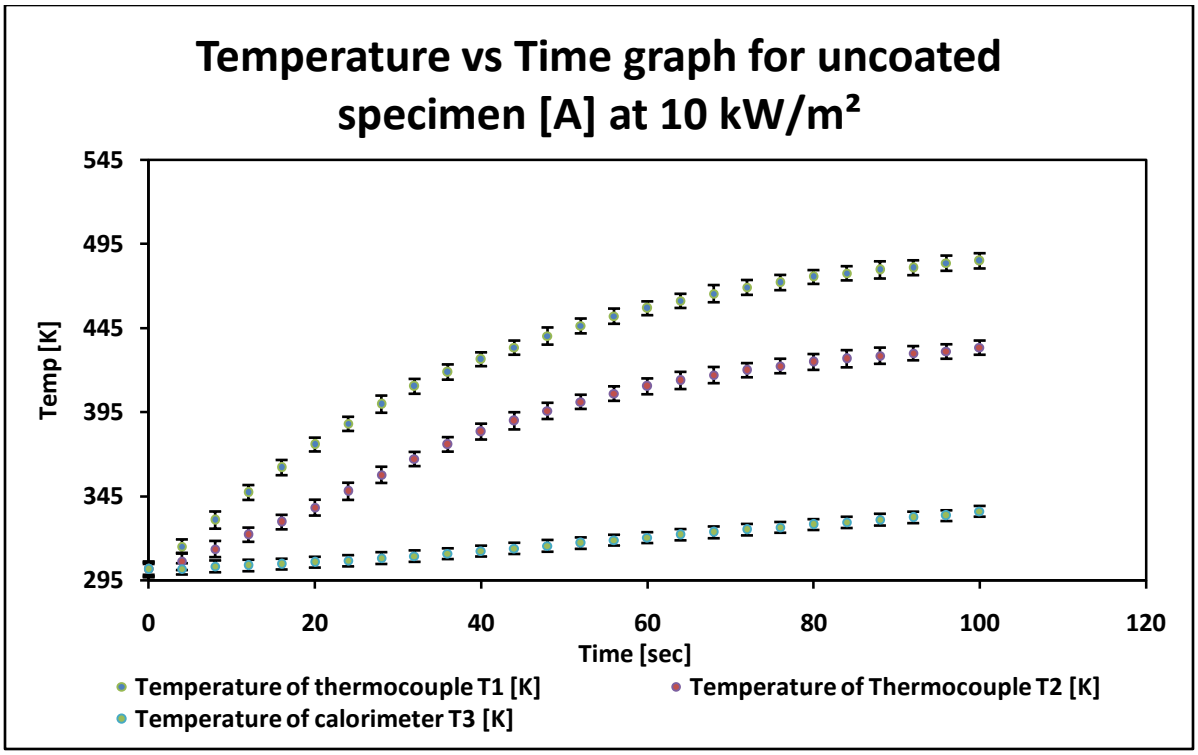

Figure 40: *Temperature of uncoated specimens with respect to time when specimens are exposed to 10 kW/m²*

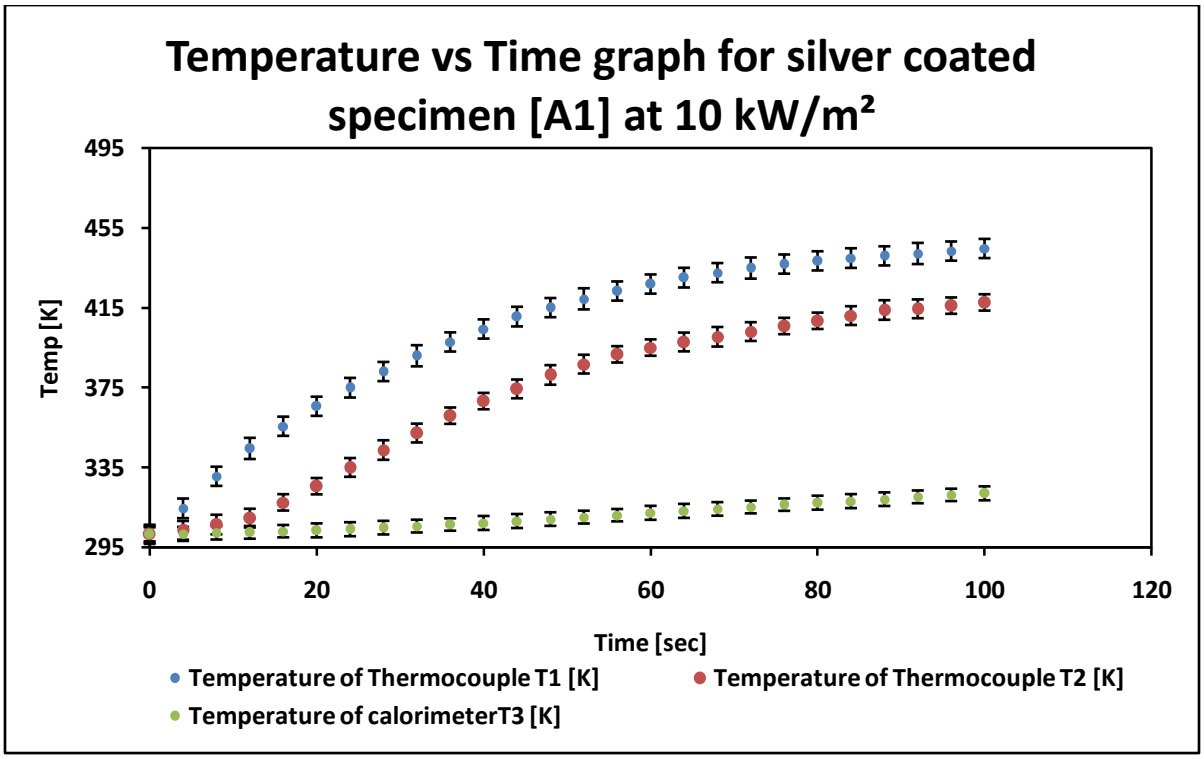

Figure 41: *Temperature of silver coated specimens with respect to time when specimens are exposed to 10 kW/m²*

7.2 Transmission of heat from heating source to firefighter clothing assembly

As described earlier, uncoated and silver coated fabric assemblies are subjected to a heat flux of 10 kW/m^2 with the help of heating source. This process of heat transfer in firefighter clothing assembly due to heat flux incident by heating rods can be represented with the help of an energy equation as mentioned by Su et al [126][127]:

$$\rho_{fb}\, Cp_{fb}.\frac{\partial T}{\partial t} = \frac{\partial}{\partial x}\left(\lambda_{fb}\frac{\partial T}{\partial x}\right) + \frac{\partial q_{rad\,-abs}}{\partial x} \qquad \text{[126][127]} \qquad (20)$$

Where, ρ_{fb}, Cp_{fb}, and λ_{fb} are density, specific heat capacity and thermal conductivity of firefighter fabric respectively. $\partial q_{rad\,-abs}$ absorbed portion of radiant heat flux from heating source to outer shell. Equation 20 can also be written as:

$$C_{pfb}\,(x).\rho_{fb}\,(x)\frac{\partial T\,(x,t)}{\partial t} = \nabla\left(\lambda_{fb}\,(x).\nabla T(x,t)\right) + \frac{\partial Q_{rad\,-abs}\,(x,t)}{\partial x} \quad [131][133][134][135] \qquad (21)$$

Where $T(x,t)$ is temperature field under investigation and t is total time during which we investigate the temperature field. This equation is second order transient parabolic differential equation. It was assumed that textile material was homogeneous and isotropic. Therefore, values of λ_{fb}, C_{pfb} and ρ_{fb} are assumed constant. The ∇ designate the Vector Hamilton operator in Cartesian coordinate system. $Q_{rad\,-abs}\,(x,t)$ is the part of radiation absorbed by outer shell from radiant heat source. It was assumed that textile material was homogeneous and isotropic. Therefore values of λ_{fb}, C_{pfb} and ρ_{fb} are assumed constant [131][133][134][135].

It is also possible to rewrite equation 21 in following way:

$$C_{pfb}\,(x).\rho_{fb}\,(x)\frac{\partial T\,(x,t)}{\partial t} = \lambda_{fb}.\Delta T(x,t) + \frac{\partial Q_{rad\,-abs}\,(x,t)}{\partial x} \quad [131][133][134][135] \qquad (22)$$

Where, the symbol Δ designates the Laplace operator. $\Delta T = \frac{\partial^2 T\,(x,t)}{\partial x_i^2}$.

The thermal energy from heating source to the surface of cloth is transported due to thermal radiation and convection of air. In this scenario, the mode of radiation is the dominant as compared to convection. The radiant heat transmission between the heating source and outer

shell is dependent on the differentiation of temperature and radiation view factor as shown in figure 42 [126][127].

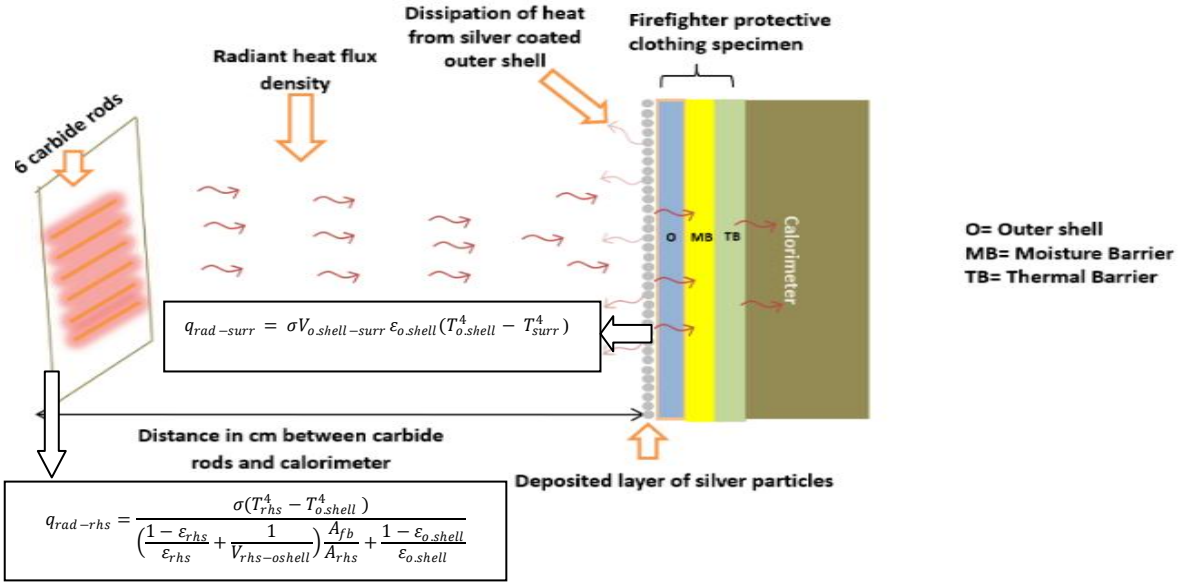

Figure 42: *Schematic diagram showing equations involved in transmission of heat from heat source towards outer shell*

7.3 Numerical solution

To solve equation 22, finite difference method was utilized. Implicit method was employed for discretization of second order parabolic differential equation. The values of temperature at discrete points (x_i and t_j) are indicated by T_i^j.

Due to scattering and absorption of radiation, Beer's law was utilized to explain extinction of incident thermal radiation (Q_{rad}) in multilayer fabric system [130][127]. Mostly Beer's law is used for liquid solutions, however it can also be utilized for porous medium like textiles.

$$\frac{\partial Q_{rad-abs}(x,t)}{\partial x} = [Q_{rad}](e^{-\gamma_{fb}\, i\Delta x})\gamma_{fb} \qquad [129]\ [127] \tag{23}$$

$$\frac{\partial Q_{rad-abs}(x,t)}{\partial x} = [q_{rad-rhs} - q_{rad-surr}](e^{-\gamma_{fb}\, i\Delta x})\gamma_{fb} \qquad [129]\ [127] \tag{24}$$

[127]

$$\frac{\partial Q_{rad-abs}(x,t)}{\partial x} =$$

$$\left[\frac{\sigma(T^4_{rhs} - T_i^{j\,4})}{\left(\frac{1-\varepsilon_{rhs}}{\varepsilon_{rhs}} + \frac{1}{V_{rhs-o.shell}}\right)\frac{A_{fb}}{A_{rhs}} + \frac{1-\varepsilon_{o.shell}}{\varepsilon_{o.shell}}} - \sigma V_{o.shell-surr} \cdot \varepsilon_{o.shell}\left(T_{i.}^{j\,4} - T^4_{surr}\right)\right](e^{-\gamma_{fb}\, i\Delta x})\gamma_{fb} \tag{25}$$

σ is Stefan boltzman (5.678×10^{-8}) W/m^2K^4

T_{rhs} is temperature of radiant heat source in K

T_{surr} is temperature of surrounding atmosphere in K

A_{fb} is area of firefighter fabric in m^2

A_{rhs} is the area of radiant heat source in m^2

ε_{rhs} is emissivity of radiant heat source

$\varepsilon_{o.shell}$ is emissivity of outer shell

$V_{rhs\text{-}o.shell}$ is view factor from radiant heat source towards outer shell [126][127]

$V_{o.shell\text{-}surr}$ view factor from outer shell towards surrounding atmosphere

$$V_{o.shell-rhs} \cdot A_{fb} = V_{rhs-o.shell} \cdot A_{rhs} \qquad [127] \qquad (26)$$

$$V_{o.shell-surr} + V_{o.shell-rhs} = 1 \qquad [127] \qquad (27)$$

View factor is fraction of radiation leaving one surface which is interpreted by another surface. It was assumed, that heating source and exterior shell are considered as disk to parallel coaxial disk of unequal radius [127] [129].

$$V_{rhs-o.shell} = \frac{1}{2}[S - \{s^2 - 4\left(\frac{r_{o.shell}}{r_{rhs}}\right)^2\}^{1/2}] \qquad [130] \qquad (28)$$

$$S = 1 + \frac{1+R_{o.shell}^2}{R_{rhs}^2} \qquad [130] \qquad (28a)$$

$$R_{rhs} = \frac{r_{rhs}}{L} \qquad [130] \qquad (28b)$$

$$R_{o.shell} = \frac{r_{o.shell}}{L} \qquad [130] \qquad (28c)$$

L is the distance between heating rods and multilayer clothing assembly in meters and $r_{o.shell}$ is the radius of outer shell and r_{rhs} is radius of heating source.

γ_{fb} is the extinction coefficient of outer shell which is illustrated by:

$$\gamma_{fb} = \frac{-\ln(\tau)}{h_{o.shell}} \quad [127] \tag{29}$$

Where τ is transmissivity of outer shell. h_{shell} is thickness of outer shell [131]. Some important values are mentioned in following table 20:

Table 20: *Values used in equation*

Symbols	**Values**
$\varepsilon_{o.shell}$ (uncoated)	0.86
$\varepsilon_{o.shell}$ (silver coated)	0.52
$\varepsilon_{rh.s}$	0.98 [132]
A_{fb}	0.002826 m^2
A_{rhs}	0.0397 m^2
$V_{rhs-o.shell}$	0.0065
$V_{o.shell-hs}$	0.091
$V_{o.shell-surr}$	0.909
τ (uncoated shell)	0.01
τ (silver shell)	0.007
C_p [uncoated fabric]	1241.5 j/kg.K
C_p [silver coated]	1221.5 j/Kg.K
ρ of fabric [Uncoated]	195.3 kg/m^3
ρ of fabric [silver coated]	198.1 Kg/m^3
λ of fabric [Uncoated]	0.036 W/[m.K]
λ of fabric [silver coated]	0.039 W/[m.K]

Equation 22 can also be written as:

$$\frac{\partial T(x,t)}{\partial t} = \frac{\lambda_{fb}}{C_{p.fb}(x).\rho_{fb}(x)} . \frac{\partial^2 T}{\partial x^2} + \frac{Q_{rad}\,((e^{-\gamma_{fb} i\Delta x}))\gamma_{fb}}{C_{p.fb}(x).\rho_{fb}(x)} \tag{30}$$

Partial derivatives in equation 30 were substituted by implicit finite divided scheme generating a discrete description related to position x_i and time t_j :

$$\frac{T_i^{j+1} - T_i^j}{\Delta t} = \frac{\lambda_{fb}}{C_{p.fb}.\rho_{fb}} . \left[\frac{T_{i+1}^{j+1} - 2T_i^{j+1} + T_{i-1}^{j+1}}{\Delta x^2}\right] + \frac{Q_{rad}\,((e^{-\gamma_{fb} i\Delta x}))\gamma_{fb}}{C_{p.fb}.\rho_{fb}} \tag{31}$$

$$\frac{T_i^{j+1} - T_i^j}{\Delta t} = \frac{\lambda_{fb}}{C_{p.fb}.\rho_{fb}} . \left[\frac{T_{i+1}^{j+1} - 2T_i^{j+1} + T_{i-1}^{j+1}}{\Delta x^2}\right] + \frac{Q_{rad}\,((e^{-\gamma_{fb} i\Delta x}))\gamma_{fb}}{C_{p.fb}.\rho_{fb}} \tag{31a}$$

$$T_i^{j+1} - T_i^j = \frac{\lambda_{fb}}{\Delta x^2 . C_{p.fb} . \rho_{fb}} . \Delta t \left[T_{i+1}^{j+1} - 2T_i^{j+1} + T_{i-1}^{j+1}\right] + \frac{Q_{rad}\left((e^{-\gamma_{fb} i\Delta x})\right)\gamma_{fb} . \Delta t}{C_{p.fb} . \rho_{fb}} \quad (31b)$$

$$T_i^j = -kT_{i-1}^{j+1} + (1+2k)T_i^{j+1} - kT_{i+1}^{j+1} - \frac{Q_{rad}\left((e^{-\gamma_{fb} i\Delta x})\right)\gamma_{fb} . \Delta t}{C_{p.fb} . \rho_{fb}} \quad (31c)$$

$$T_i^j + \frac{Q_{rad}\left((e^{-\gamma_{fb} i\Delta x})\right)\gamma_{fb} . \Delta t}{C_{p.fb} . \rho_{fb}} = -kT_{i-1}^{j+1} + (1+2k)T_i^{j+1} - kT_{i+1}^{j+1} \quad (31d)$$

For further solution, Thomas Algorithm method was employed to solve above mentioned equation. Where:

$$k = \frac{\lambda_{fb} . \Delta t}{\Delta x^2 . C_{p.fb} . \rho_{fb}} \quad (31e)$$

$$Interval\ of\ node\ \Delta x = \frac{Thickness\ of\ fabric}{Number\ of\ nodes}$$

The fabric assembly is divided into 5 nodes.

$$\text{Number of time steps} = \frac{Time_{final} - Time_{initial}}{\Delta t}$$

$$= \frac{100\,sec - 0sec}{1} = 100$$

Interval of time $\Delta t = 1$ sec

T_i^j corresponds to temperature at node i, that is

$x = i . \Delta x$ and $t = j . \Delta t$

7.3.1 Boundary conditions

Initial temperature was 301.45 K.

$$\lambda_{o.shell} . \frac{\partial T(x,t)}{\partial x} = -\alpha(T_{o.shell} - T_{surr}) + q_{rad-abs} \quad (32)$$

Where, α represent coefficient of heat transfer. T_{surr} is temperature of surrounding atmosphere. $q_{rad\ -abs}$ is absorbed part of radiation absorbed by outer shell [126] [127].

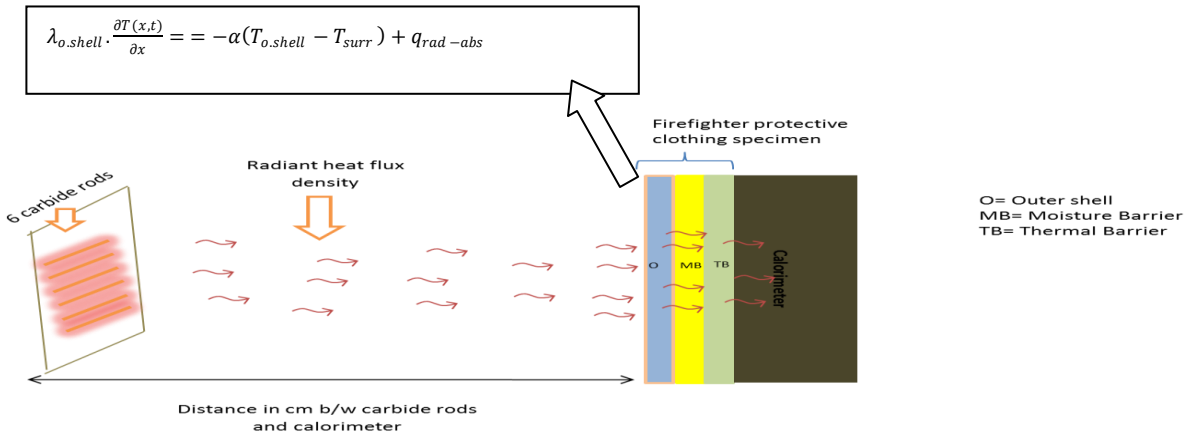

Figure 43: *Schematic diagram showing boundary condition of outer shell*

$$\lambda_{T.B} \cdot \frac{\partial T(x,t)}{\partial x} = Q_{calorimeter} - \lambda_{air} \cdot \frac{\partial T}{\partial x} \qquad [126]\ [127] \tag{33}$$

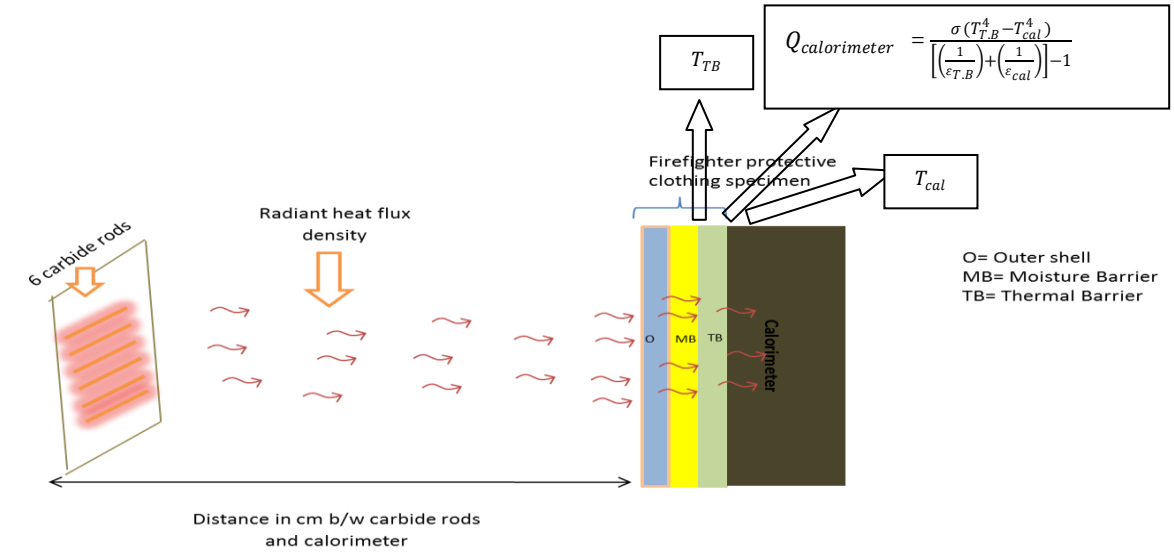

Figure 44: *Schematic diagram showing equation for boundary condition of thermal barrier*

$$Q_{calorimeter} = \frac{\sigma(T_{T.B}^4 - T_{cal}^4)}{\left[\left(\frac{1}{\varepsilon_{T.B}}\right) + \left(\frac{1}{\varepsilon_{cal}}\right)\right] - 1} \qquad [126] \tag{34}$$

$\varepsilon_{T.B}$ is emissivity of thermal barrier and ε_{cal} is emissivity of calorimeter. $T_{T.B}$ is temperature of thermal barrier in Kelvin and T_{cal} is temperature of calorimeter in Kelvin [126].

The distribution of temperature at different nodes in different interval of time for uncoated and silver coated specimen was depicted in figure 45 and figure 46 respectively.

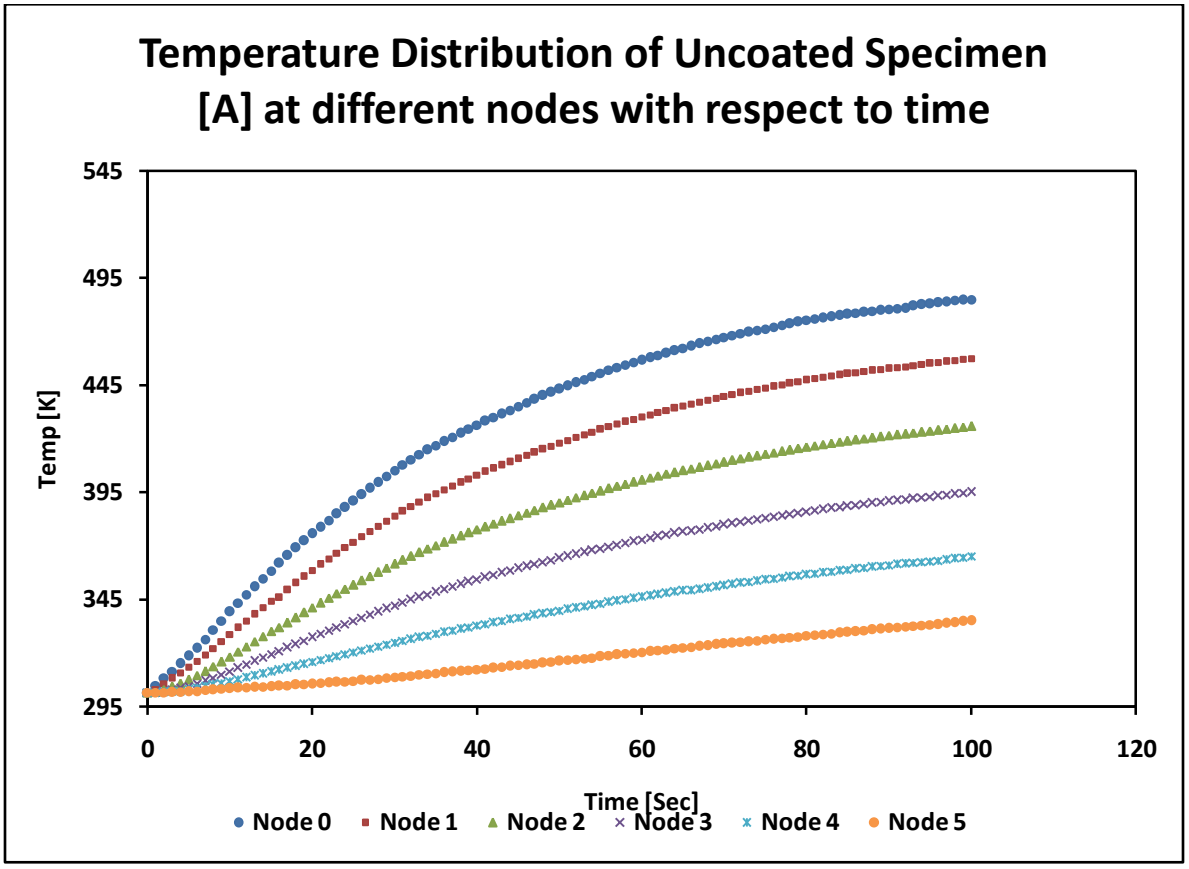

Figure 45: *Temperature distribution in uncoated specimen with respect to time*

It can be witnessed from figure 45 and figure 46, that there was sequential increment in rise of temperature for different curves with increase in time. However, this increment was not in linear form. It was also noticed that as the number of nodes increases, there was decline in values of temperature for same time period. This indicates decline in temperature values with increase in thickness of firefighter clothing assembly for both uncoated specimen *A* and silver coated specimen *A1*.

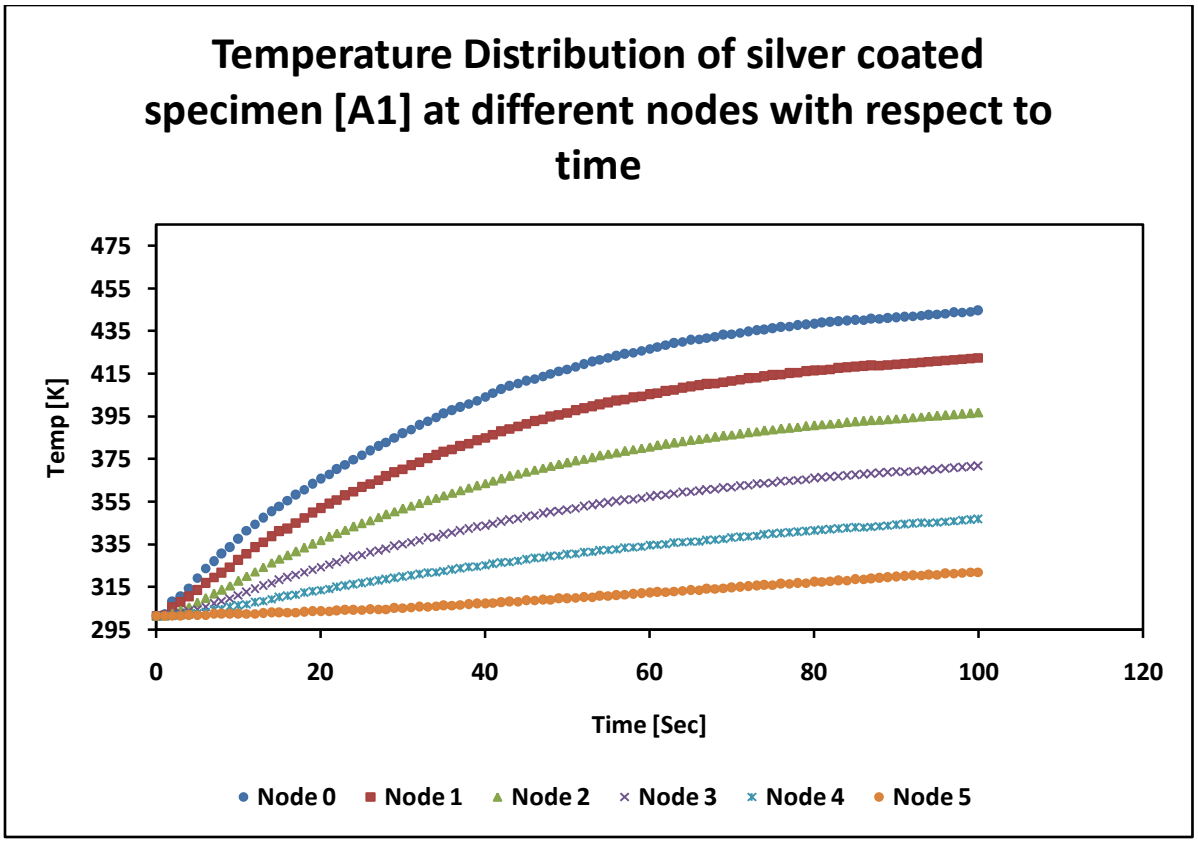

Figure 46: *Temperature distribution in silver coated specimen with respect to time*

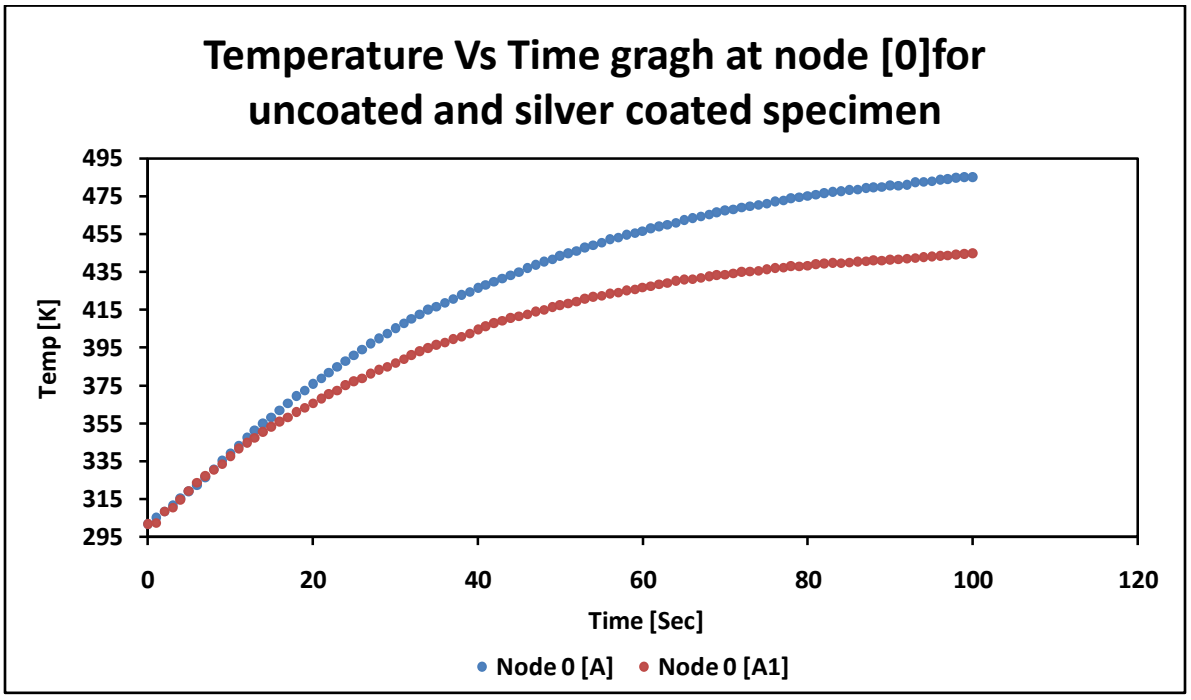

Figure 47: *Comparison of temperature distribution of uncoated and silver coated specimen at node [0]*

It can be noticed from figure 47 that till first sixteen seconds the curve of uncoated specimen *A* and silver coated specimen *A1* overlapped with each other. Afterwards, a gap appears between curve of silver coated and uncoated specimen. This gap went on increasing with the increase in time.

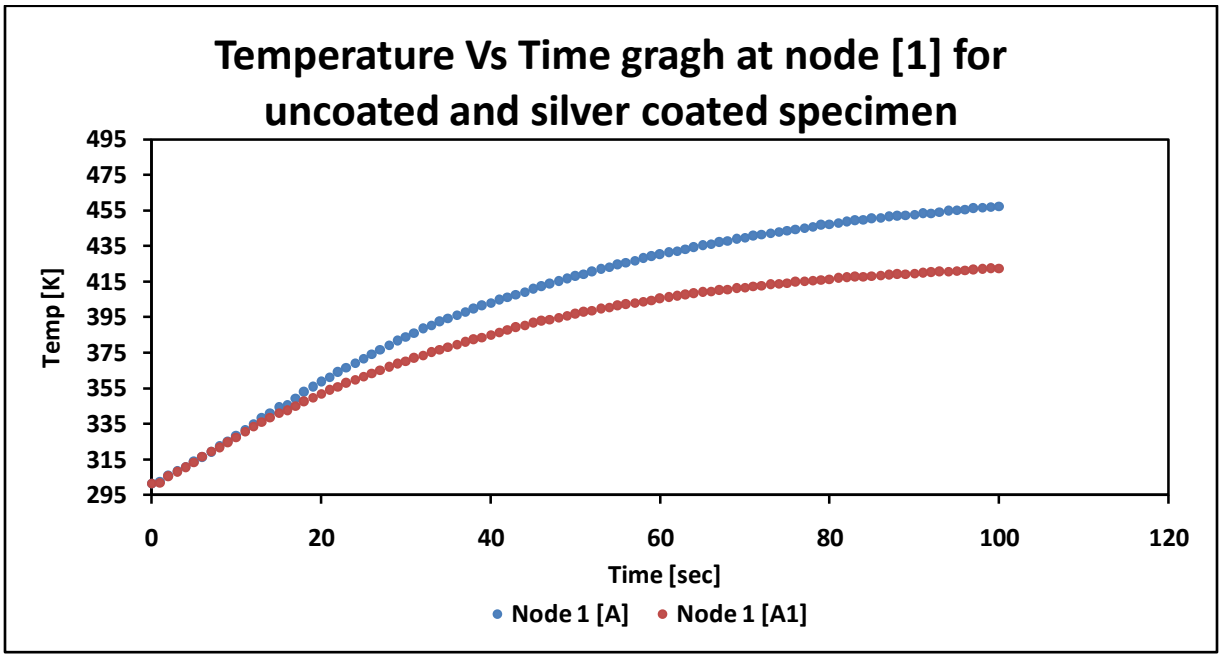

Figure 48: *Comparison of temperature distribution of uncoated and silver coated specimen at node [1]*

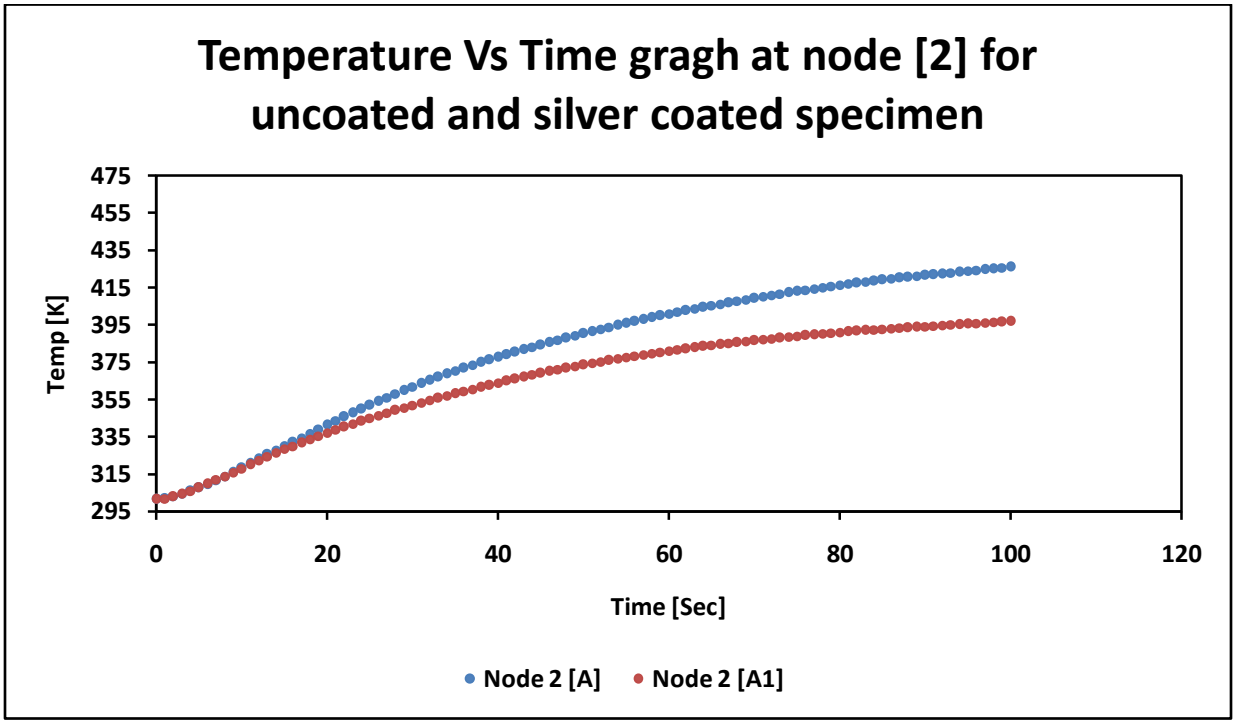

Figure 49: *Comparison of temperature distribution of uncoated and silver coated specimen at node [2]*

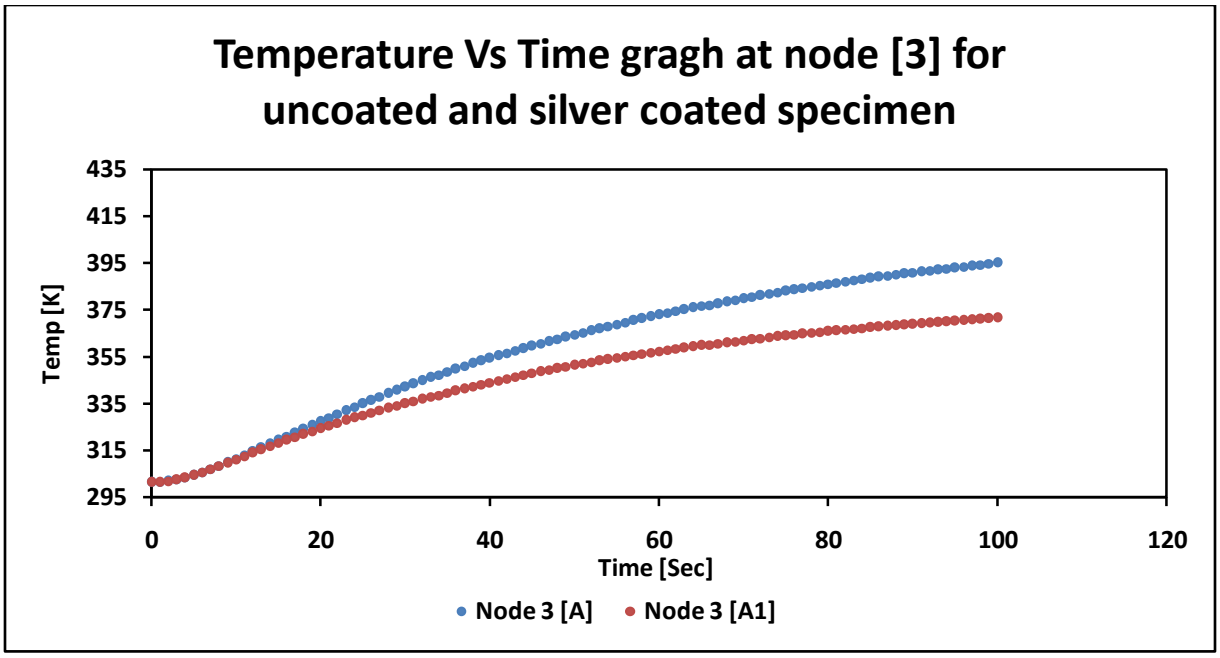

Figure 50: *Comparison of temperature distribution of uncoated and silver coated specimen at node [3]*

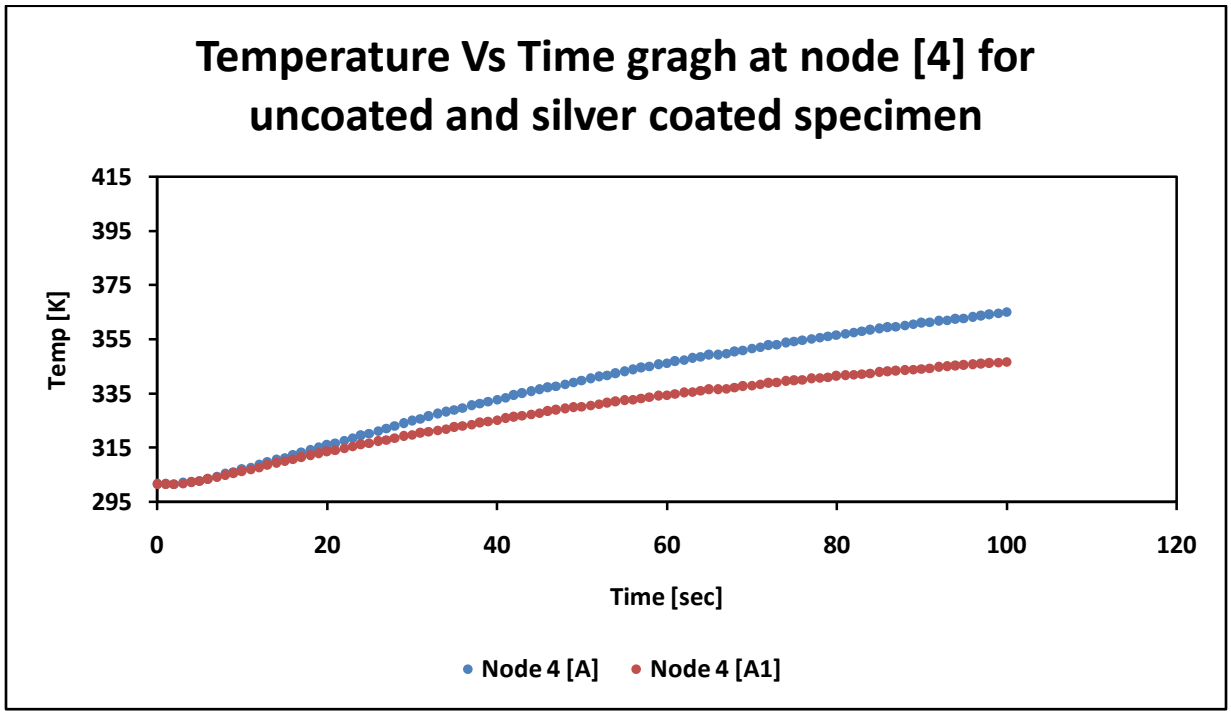

Figure 51: *Comparison of temperature distribution of uncoated and silver coated specimen at node [4]*

It can be witnessed from figure 48 to figure 51 that till first 15 seconds; both curves of uncoated and silver coated specimen were superimposing each other. Later on the curve of uncoated specimen started to get steeper as compared to curves silver coated specimen. It was also observed that as the number of nodes increases, the curve of both uncoated and silver coated

specimen became flatter as compared to previous nodes. The slackness in the curve indicates that rate of rise of temperature takes place slowly. As a consequence better will be thermal protective performance because less amount of heat is transmitted towards fabric assembly.

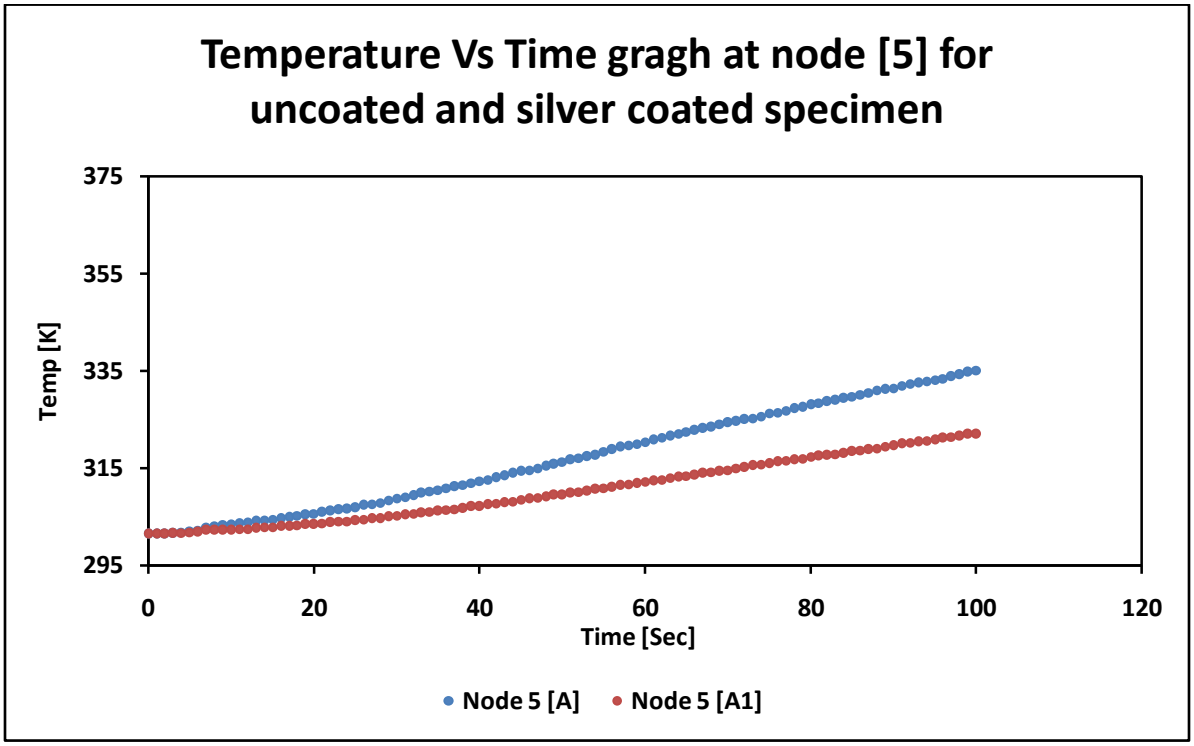

Figure 52: *Comparison of temperature distribution of uncoated and silver coated specimen at node [5]*

It was evident from figure 52, the pattern of curve for uncoated and silver coated specimen was almost same after initial 5 seconds. Later on, the curve of uncoated specimen starts to raise by creating gap between the curves of uncoated *A* and silver coated specimen *A1*. The wideness of this gap increases between two curves increases till end of 100 seconds. This indicates better thermal protective performance of silver coated specimen *A1*.

It can be inferred that numerical model solution predicts temperature distribution at different nodes for uncoated specimen *A* and silver coated specimen *A1* at different interval of time. This model also shows the silver coated specimen *A1* incurs less steep curve of temperature values as compared to uncoated specimen *A* at different nodes. This flatness of curve was also witnessed in case of silver coated specimen *A1* for experimental work. With the help of numerical model it was possible to estimate temperature distribution at different places along thickness of fabric which was not possible in experimental work.

CHAPTER 8: CONCLUSIONS

1. It can be inferred that thermal protective performance is one of the most important feature of firefighter protective clothing. Thermal protective performance determines capability of the firefighter protective clothing to protect the body of firefighter against second degree burns. The greater the thermal protective performance, the better will be thermal protective ability of firefighter clothing. Initially four different combinations of firefighter clothing were made. These combinations were *specimen 1*, *specimen 2*, *specimen 3* and *specimen 4*. Each combination arrangement consists of outer shell, moisture barrier and thermal barrier. When thermal insulation properties were evaluated. It was noted, that *specimen 4* which has slighter higher thickness as compared to other specimens and greater percentage of Nomex fibers in outer shell shows higher thermal insulation values as compared to other specimens. On the other hand specimen 1 has lower thickness as compared to all other specimens and has lowest thermal insulations values in comparison with other specimens. The outer shell of *specimen 4* has lowest value of air permeability as compared to other specimen. When these specimens were evaluated with contact heat plate test as per ISO 12127 standard, threshold time for rise of 10 ^{o}C for *specimen 4* was 111 seconds which was greater as compared to other specimens. When these specimens were evaluated on radiant heat transmission machine as per ISO 6942 standard, it was noted that *specimen 4* has better thermal protective performance as compared to other specimen on exposure to 10 kW/m^2 and 20 kW/m^2. *Specimen 4* has lowest value of transmitted heat flux density and greater value of radiant heat transmission index *RHTI 24*. Lesser the value of transmitted heat flux density, better will be thermal protective performance as low value of heat is transmitted towards the body of fire fighters. Greater the value of radiant heat transmission index *RHTI 24*, better will be thermal protective performance as time for rise of 24 ^{o}C is increased and more time can be utilized by firefighters in carrying out their operational activities without acquiring second degree burns. It was witnessed by flatter curves of *specimen 4* as rate for rise of temperature is slow as compared to other curves of specimen. At exposure to 10 kW/m^2, *RHTI 24* value of *specimen 4* was greater than *specimen 1* by **35.25 percent**.

When specimens were exposed to 20 kW/m^2, *specimen 4* has enhanced value of *RHTI 24* as compared to specimen 1 by **38 percent**.

2. In this research some of the alternate methodologies have been employed to increase thermal protective performance. One approach was to employ aerogel layer as a substitute to thermal barrier. Four specimen assemblies were made. *Specimen A* and *specimen B* used thermal barrier. *Specimen C* and *specimen D* employs aerogel blanket as substitute to thermal barrier. When aerogel blanket was used as an alternate layer to thermal barrier:

   i. The specimens having aerogel blankets have greater thermal resistance value as compared to specimen in which thermal barrier was used. This might be due to nano-porous structure of aerogel due to which gaseous molecules become immobile and this might block conductive heat transmission. Convective heat transfer is also obstructed due to no circulation of air. Furthermore, thermal conductivity of aerogel [0.015 W/m.K] which was also less than still air [0.026 W/m.K].

   ii. Specimens having aerogel blanket as substitute to thermal barrier have higher water vapor resistance values as compared to other specimens. This high water vapour resistance values might be due to hydrophobic character and closed porous configuration of aerogel structure.

   iii. When specimens were exposed to different levels of radiant heat flux density levels [kW/m^2] in radiant heat transmission machine. Those specimens in which aerogel blanket was used have lower values of transmitted heat flux densities Q_c [kW/m^2] and high values of *RHTI 24*. The high value of *RHTI 24* indicates that time for rise of 24 ºC was more in case of specimen using aerogel as an alternate layer due to which transmission of heat is delayed. This might be due to fact that aerogel layer is able to absorb infra red radiation. When specimens were subjected to 10 kW/m^2, *specimen C* has improved *RHTI 24* values as compared to *specimen A* by **61.7 percent**. Whereas, *specimen D* has better *RHTI 24* values by **51.5 percent** as compared to *specimen B*. When specimens were exposed to 20 kW/m^2, RHTI 24 value in *specimen C* was enhanced by **24 percent** as compared to *specimen A*. Similarly, *Specimen D* has better value of *RHTI 24* as compared to *specimen B* by **36.5 percent.** When subjected to 30 kW/m^2, *RHTI 24* value of

specimen C was enhanced by **51 percent** in comparison with *specimen A* and there was **56.74 percent** improvement in *RHTI 24* value of *specimen D* as compared to *specimen B*. When specimens were facing 40 kW/m^2, *specimen C* has increased value of *RHTI 24* by **82.4 percent** as compared to *specimen A*. However, *specimen D* has improved value of *RHTI 24* by **80.6 percent** in comparison with *specimen B*.

3. Another way to improve thermal protective performance was to coat exterior side of outer shell by silver particles through magnetron sputtering (new approach) at 1 μm, 2 μm and 3 μm thickness level. Previously this method of coating was used to coat metallic particles on thin films. As a result, four different combinations of specimens are formed. *specimen A* (uncoated), *specimen A1* (1 μm coating), *specimen A2* (2 μm coating) and *specimen A3* (3 μm coating).

   i. It was also witnessed that when silver coated and uncoated specimens were exposed to various levels of radiant heat flux density, silver coated specimen have low values of transmitted heat flux density Q_c and high values of *RHTI 24*. This indicates improvement in thermal protective performance. As the thickness level of silver metallic particles increases there was further reduction in transmitted heat flux density values and increase in *RHTI 24* values. On exposure to 10 kW/m^2, *specimen A1* has improved thermal protective performance in terms of *RHTI 24* by **43 percent** as compared to *specimen A*. When specimens are exposed to 20 kW/m^2, *specimen A1* has improved *RHTI 24* values by **30.35 percent** as compared to *specimen A*. When specimens are subjected to 30 kW/m^2, *RHTI 24* value of *specimen A1* enhanced by **17 percent** in comparison with uncoated *specimen A*. On facing radiant heat flux density of 40 kW/m^2, *specimen A1* has increased value of *RHTI 24* as compared to *specimen A* by **28 percent**. There was minor difference between values of water vapour resistance for silver coated and un-coated specimens indicating that breathability of silver coated specimen was not compromised. There was also no significant differentiation in values of air permeability indicating that porous configuration of silver coated specimen was not completely blocked. A slight increase in bending moment values of silver coated specimen was witnessed.

   ii. The emissivity value of silver coated specimen was 0.52 which was very low as compared to emissivity value of uncoated specimen 0.86. The lower value of emissivity indicates better reflectivity which indicates that incident radiant flux density is dissipated

towards the surrounding atmosphere and transmitting less heat towards calorimeter. The reflectivity value of 1 μm silver coated specimen was 0.46 which was greater than reflectivity value of uncoated specimen having value of 0.09.

iii. The durability of 1 μm silver coated specimen was investigated after 5 washing cycles as per standard NFPA 1851 and there was minor decline in values of transmitted heat flux density Qc [kW/m^2] after 5 washing cycles when exposed to 40 kW/m^2. This indicates stability and durability of silver particles coating on surface of outer shell.

4. Lastly the Numerical model and its solution were established using the appropriate equations for transmission of heat. The distribution of temperature through multilayer sandwich structure was determined with the help of Numerical model and its solution. Previously no attempt was made to predict the distribution of temperature for fighter clothing coated with low emissivity silver coated particles. The distribution of temperature through multilayer firefighter clothing assembly was deeply studied in this technique. The results can be useful for the researcher and the industrial partner to predict the thermal protection of firefighter clothing with low emissivity coating.

Future Work

1. For future studies, different coating techniques can be employed to impregnate metallic coating on outer shell via different metallic particles of aluminium, copper and titanium.
2. Evaluation of moisture management (mass transfer properties) between different layers of firefighter can provide lot of help in future research.
3. Numerical solution with the help of computer simulation using python/MATLAB software.

REFERENCES

[1] C. Keiser and R. M. Rossi, "Temperature analysis for the prediction of steam formation and transfer in multilayer thermal protective clothing at low level thermal radiation," *Text. Res. J.*, vol. 78, no. 11, pp. 1025–1035, 2008.

[2] P. Bajaj and A. K. Sengupta, "Protective clothing," *Text. Prog.*, vol. 22, no. 2–4, pp. 1–110, Jun. 1992.

[3] J. R. Lawson, "Firefighters' Protective Clothing and Thermal Environments of Structural Firefighting," *Engineering*, vol. 1273, pp. 335–352, Jan. 1997.

[4] R. Nayak, S. Houshyar, and R. Padhye, "Recent trends and future scope in the protection and comfort of fire-fighters' personal protective clothing," *Fire Sci. Rev.*, vol. 3, no. 1, p. 4, 2014.

[5] L. Jin, K. Hong, and K. Yoon, "Effect of Aerogel on Thermal Protective Performance of Fire-Fighter Clothing," *J. Fiber Bioeng. Informatics*, vol. 6, pp. 315–324, 2013.

[6] G. Song, S. Paskaluk, R. Sati, E. M. Crown, J. Doug Dale, and M. Ackerman, "Thermal protective performance of protective clothing used for low radiant heat protection," *Text. Res. J.*, vol. 81, no. 3, pp. 311–323, 2010.

[7] H. Ma''Kinen, "Firefighter Protective Clothing," in *Textile for Protection*, Ist., R. A. Scott, Ed. Woodhead Publishing, 2005, pp. 622–647.

[8] G. Song, P. Chitrphiromsri, and D. Ding, "Numerical Simulations of Heat and Moisture Transport in Thermal Protective Clothing Under Flash Fire Conditions," *Int. J. Occup. Saf. Ergon.*, vol. 14, no. 1, pp. 89–106, 2008.

[9] F. Ming, W. Wenguo, and H. Yuan, "Thermal Insulations of multilayer clothing systems measured by a bench scale test in low level heat exposures," *Int. J. Cloth. Sci. Technol.*, vol. 26, no. 5, pp. 412–423, 2013.

[10] T. A. Negawao, "Analyzing and Modelling of Comfort and Protection properties of

firefighters protective clothing," Istanbul Technical University, 2015.

[11] I. Holmer, "Protective Clothing in Hot Environments," *Ind. Health*, vol. 44, no. 3, pp. 404–413, 2006.

[12] NFPA, "Protective clothing for structural firefighting," Quincy MA, 1997.

[13] D. C. Adolphe, L. Schacher, and J. -Y. Drean, "Comparison between thermal insulation and thermal properties of classical and microfibers polyester fabrics," *Int. J. Cloth. Sci. Technol.*, vol. 12, no. 2, pp. 84–95, 2000.

[14] E. Onofrei, S. Petrusic, G. Bedek, D. Dupont, D. Soulat, and T.-C. Codau, "Study of heat transfer through multilayer protective clothing at low-level thermal radiation," *J. Ind. Text.*, vol. 45, no. 2, pp. 222–238, 2014.

[15] J. Huang, "Thermal parameters for assessing thermal properties of clothing," *J. Therm. Biol.*, vol. 31, no. 6, pp. 461–466, 2006.

[16] J. Roguski, K. Stegienko, D. Kubis, and M. Błogowski, "Comparison of requirements and directions of development of methods for testing protective clothing for firefighting," *Fibers Text. East. Eur.*, vol. 24, no. 5, pp. 132–136, 2016.

[17] ISO 6942, "Protective clothing -- Protection against heat and fire -- Method of test: Evaluation of materials and material assemblies when exposed to a source of radiant heat," 2002.

[18] J. Geršak, H. Meinander, and D. Celcar, "Heat and moisture transmission properties of clothing systems evaluated by using a sweating thermal manikin under different environmental conditions," *Int. J. Cloth. Sci. Technol.*, vol. 20, no. 4, pp. 240–252, Jun. 2008.

[19] M. T. Northwest, "Sweating Guarded Hotplate," *Meas. Technol. Northwest*, pp. 1–2, 2012.

[20] K. Min, Y. Son, C. Kim, Y. Lee, and K. Hong, "Heat and moisture transfer from skin to environment through fabrics: A mathematical model," *Int. J. Heat Mass Transf.*, vol. 50,

no. 25–26, pp. 5292–5304, 2007.

[21] M. Venkataraman, R. Mishra, T. M. Kotresh, T. Sakoi, and J. Militky, “Effect of compressibility on heat transport phenomena in aerogel-treated nonwoven fabrics,” *J. Text. Inst.*, vol. 107, no. 9, pp. 1150–1158, 2016.

[22] S. B. Stabkovic, D. Popvic, and G. B. Poparic, “Thermal properties of textile fabrics made of natural and regenerated cellulose fibers,” *Polym. Test.*, vol. 27, pp. 41–48, 2008.

[23] L. Jin *et al.*, “New approaches to evaluate performance of firefighter protective clothing.,” *Fire Technol.*, vol. 54, pp. 1283–1307, 2018.

[24] M. Fu, W. Weng, and H. Yuan, “Effects of multiple air gaps on the thermal performance of firefighter protective clothing under low-level heat exposure,” *Text. Res. J.*, vol. 84, no. 9, pp. 968–978, Dec. 2013.

[25] A. Shaid, L. Wang, and R. Padhye, “The thermal protection and comfort properties of aerogel and PCM-coated fabric for firefighter garment,” *J. Ind. Text.*, vol. 45, no. 4, pp. 611–625, 2015.

[26] A. H. M. Ali and R. Mohmmed, “A review of the firefighting fabrics for flashover temperature,” *Int. J. Eng. Sci. Res. Technol.*, vol. 4, no. 3, pp. 247–257, 2015.

[27] B. E. Yoldas, M. J. Annen, and J. Bostaph, “Chemical Engineering of Aerogel Morphology Formed under Nonsupercritical Conditions for Thermal Insulation,” *Chem. Mater.*, vol. 12, no. 8, pp. 2475–2484, 2000.

[28] L. W. Hrubesh, “Aerogel applications,” *J. Non. Cryst. Solids*, vol. 225, no. 1–3, pp. 335–342, 1998.

[29] Anon, “Aspen Aerogels Safety data sheet,” 2008. .

[30] A. H. A. Ali and R. Mohmmed, “A Review Of the firefighting fabrics for flashover temperature,” *Int. J. Eng. Sci. Res. Technol.*, vol. 4, no. 3, pp. 247–257, 2015.

[31] W. M. Raslan, “Ultraviolet Protection, Flame Retardancy and Antibacterial Properties of Treated Polyester Fabric Using Plasma-Nano Technology,” *Mater. Sci. Appl.*, vol. 02, pp.

1432–1442, 2011.

[32] Azom, “Silver (Ag), Properties and Applications,” *Azo matreials*, 2013. [Online]. Available: https://www.azom.com/article.aspx?ArticleID=9282. [Accessed: 24-Feb-2018].

[33] I. Holmer, “How is perofrmance in heat affected by clothing,” *Text. Bioeng. informatics Symp. proceddings*, vol. 1, pp. 700–705, 2008.

[34] G. Havenith, I. Holmér, and K. Parsons, “Personal factors in thermal comfort assessment: Clothing properties and metabolic heat production,” *Energy Build.*, vol. 34, no. 6, pp. 581–591, 2002.

[35] A. K. Haghi, *Heat and mass transfer in textiles,*. WSEAS Press, 2011.

[36] J. T. Williams, *Textiles for cold weather apparel*. Woodhead Publishing, 2009.

[37] R. T. Ogulata, “The effect of thermal insulation of clothing on human thermal comfort,” *Fibers Text. East. Eur.*, vol. 15, no. 2(61), pp. 67–72, 2007.

[38] J. Blankenbaker, “Ventilating systems for hot industries.,” *Heating/Piping/Air Cond.*, p. 54, 1982.

[39] G. Song, *Improving comfort in clothing.* UK: Woodhead Publishing, 2011.

[40] A. Das and R. Alagirusamy, *Science in comfort*. Woodhead Publishing, India, 2010.

[41] J. L. Threlkeld, *Thermal Environmental Engineering*, 2nd Ed. New Jersey: Prentice Hall, Inc, 1970.

[42] S. Chakraborty, A. A. Pisal, V. K. Kothari, and A. Venkateswara Rao, “Synthesis and Characterization of Fiber Reinforced Silica Aerogel Blankets for Thermal Protection,” *Adv. Mater. Sci. Eng.*, pp. 1–8, 2016.

[43] R. P. Patel, N. S. Purohit, and A. M. Suthar, “An overview of silica aerogels,” *Int. J. ChemTech Res.*, vol. 1, no. 4, pp. 1052–1057, 2009.

[44] A. C. Pierre and M. Pajonk, “Chemistry of aerogels and their applications,” *Chem. Rev.*, vol. 102, pp. 4243–4265, 2002.

[45] A. Soleimani Dorcheh and M. H. Abbasi, “Review: Silica aerogel; synthesis, properties and characterization,” *J. Mater. Process. Tech.*, vol. 199, no. 1–3, pp. 10–26, 2008.

[46] N. Hüsing and U. Schubert, “Aerogels—Airy Materials: Chemistry, Structure, and Properties,” *Angew. Chemie Int. Ed.*, vol. 37, no. 1–2, pp. 22–45, 1998.

[47] A. C. Pierre and A. Rigacci, “SiO2 Aerogels,” in *Aerogels Handbook*, M. A. Aegerter and N. Leventis, Eds. Springer, 2011, pp. 20–25.

[48] N. Bheekhun, A. R. Abu Talib, and M. R. Hassan, “Review Article Aerogels in sapce An overview,” *Adv. Mater. Sci. Eng.*, pp. 1–18, 2013.

[49] S. Kistler, “Coherent Expanded aerogel,” *J. Phys. Chem.*, vol. 36, pp. 52–64, 1932.

[50] S. R. Hostler, A. R. Abramson, M. D. Gawryla, S. A. Bandi, and D. A. Schiraldi, “Thermal conductivity of a clay-based aerogel,” *Int. J. Heat Mass Transf.*, vol. 52, no. 3–4, pp. 665–669, 2009.

[51] B. Jelle, R. Baetens, and A. Gustavsen, “Aerogel Insulation for Building Applications: A state of the art review,” *Energy Build.*, vol. 43, no. 4, pp. 761–769, 2011.

[52] J. Fricke, “Aerogels,” *Proc. First Int. Symp.*, pp. 1–173, 1985.

[53] D. Lee, P. C. Stevens, S. Q. Zeng, and A. J. Hunt, “Thermal characterization of carbon-opacified silica aerogels,” *J. Non. Cryst. Solids*, vol. 186, pp. 285–290, 1995.

[54] J. Fricke *et al.*, “Thermal Properties of silica aerogels,” *Rev. Phys. Appl.*, vol. 50, pp. 87–97, 1989.

[55] B. Xu, J. Y. Cai, N. Finn, and Z. Cai, “An improved method for preparing monolithic aerogels based on methyltrimethoxysilane at ambient pressure Part I: Process development and macrostructures of the aerogels,” *Microporous Mesoporous Mater.*, vol. 148, pp. 145–151, 2012.

[56] S. H. and L. Svensson, “Production of Silica Aerogel,” *Phys. Scr.*, vol. 23, no. 4B, p. 697, 1981.

[57] A. Venkateswara Rao, S. D. Bhagat, H. Hirashima, and G. M. Pajonk, “Synthesis of flexible silica aerogels using methyltrimethoxysilane (MTMS) precursor,” *J. Colloid Interface Sci.*, vol. 300, no. 1, pp. 279–285, 2006.

[58] A. Shaid, M. Furgusson, and L. Wang, “Thermophysiological Comfort Analysis of Aerogel Nanoparticle Incorporated Fabric for Fire Fighter’s Protective Clothing,” *Chem. Mater. Eng.*, vol. 2, no. 2, pp. 37–43, 2014.

[59] G. Restuccia, A. Freni, S. Vasta, and Y. Aristov, “Selective water sorbent for solid sorption chiller: Experimental results and modelling,” *Int. J. Refrig.*, vol. 27, no. 3, pp. 284–293, 2004.

[60] N. Kim, K. Kim, D. Payne, and R. Upadhye, “Fabrication of hollow silica aerogel spheres by a dropletgeneration method and sol-gel processing,” *J VacSciTechnolA*, vol. 7, pp. 1181–1184, 1988.

[61] M. Koebel, A. Rigacci, and P. Achard, “Aerogels for superinsulation: A synoptic View,” in *Aerogel Handbook*, M. . Agerter, L. N, and K. M, Eds. New York: Springer, 2011, pp. 625–623.

[62] C. G. Bankvall, “Natural Convective heat tarnsfer in insulated stuctures,” Lund University, Lund, 1972.

[63] L. Jin, K.-A. Hong, H. D. Namb, and K. J. Yoon, “Effect of Thermal Barrier on Thermal Protective Performance of Firefighter Garments,” *J. Fiber Bioeng. Informatics*, vol. 4, pp. 245–252, 2011.

[64] J. Rosenfeld, “How are burns categorized.” [Online]. Available: https://www.rosenfeldinjurylawyers.com/how-burns-categorized.html. [Accessed: 19-Jan-2019].

[65] R. Nute, “Principles of thermally caused injuries,” *Prod. Saftey Eng. Newsl.*, vol. 3, pp. 1–29, 2007.

[66] D. Holmes, “Waterproof breathable fabrics’,” in *Handbook of Technical Textiles*, H. A. R and Anand S C, Eds. Woodhead Publishing, 2000, pp. 281–315.

[67] F. W. Behmann, “Protection against flames and radiant heat,” in *Handbook on clothing*, Biomedical effects of Military clothing and study group 7, 2007.

[68] J. R. Lawson, “Fire Facts. Heat Flux, Temperature, & Thermal Response,” *NIST Spec. Publ.*, 2009.

[69] “Nomex and Kevlar Firefighter Apparel,” 2019. [Online]. Available: http://www.dupont.com/products-and-services/personal-protective-equipment/thermal-protective/brands/nomex/products/nomex-kevlar-firefighter-protection.html.

[70] P. Bajaj, “Heat and Flame Protection,” in *Handbook of Technical Textiles*, Horracks A., A. R. Horracks and Anand S C, Eds. Woodhead Publishing, 2000, pp. 223–263.

[71] R. El Aidani, Pa. I. Dolez, and T. Vu-Khanh, “Effect of Thermal Aging on the Mechanical and Barrier Properties of an e-PTFE/ Nomex Moisture membrane used in Firefighters’ Protective suits,” *J. Appl. Polym. Sci.*, vol. 121, pp. 3101–3110, 2011.

[72] H. M, L. Strauss, and W. Nocker, “Firefighter garment with non textile insulation,” in *Proceddings of Nokobetef 6 and first european conference on protective clothing*, 2000.

[73] NFPA, “Standard on protective ensembles for structural firefighting and proximity firefighting,” 2013.

[74] R. Tutterow, “Understanding the Thermal Protective Performance of your PPE: Firefighter safety and health,” 2012. [Online]. Available: https://www.firerescuemagazine.com/articles/print/volume-7/issue-6/firefighter-safety-and-health/understanding-the-thermal-protective-performance-of-your-ppe.html.

[75] ISO 15025, “International Standard Protective clothing — Protection against flame — Method of test for flame,” 2016.

[76] E. 12127-1, “Clothing for protection against heat and flame- Determination of contact heat transmission through protective clothing,” 2007.

[77] EN ISO 9151, “Protective clothing against heat and flame - Determination of heat transmission on exposure to flame,” 2016.

[78] N. Oğlakcioğlu and A. Marmarali, “Thermal comfort properties of some knitted structures,” *Fibers Text. East. Eur.*, vol. 15, no. 5, pp. 94–96, 2007.

[79] Z. S. Abdel-Rehim, M. M. Saad, M. El-Shakankery, and I. Hanafy, “Textile fabrics as thermal insulators,” *Autex Res. J.*, vol. 6, no. 3, pp. 148–161, 2006.

[80] E. Clulow, “Comfort indoors,” *Text. Horizons*, pp. 20–22, 1984.

[81] Ashrae, “Thermal environmental conditions for human occupancy,” Atlanta, 1992.

[82] E. E. Clulow and W. H. Rees, “The transmission of heat through textile fabrics. PART III. A New Thermal-Transmission apparatus,” *J. Text. Inst.*, vol. 59, no. 6, pp. 285–294, 1968.

[83] A. P. Gagge, A. C. Burton, and H. C. Bazett, “A Practical system of units for the description of the heat exchange of man with his environment,” *Science (80-.).*, vol. 94, pp. 428–430, 1941.

[84] M. J. Pac, M. Bueno, and M. Renner, “Warm cool feeling relative to tribological properties of fabrics,” *Text. Res. J.*, vol. 71, no. 9, pp. 806–812, 2001.

[85] T. Tzanov, R. Betcheva, and I. Hardalov, “Thermophysiological comfort silicone softeners- treated woven textile materials,” *Int. J. Cloth. Sci. Technol.*, vol. 11, no. 4, pp. 189–197, 1999.

[86] A. Mitra, A. Majumdar, P. Majumdar, and D. Bannerjee, *Prediciting thermal resistance of cotton fabrics by artificial neural network model*, vol. 50. 2013.

[87] L. Hes, “Thermal Properties of Nonwoven,” in *Proceedings of Congress Index 87 Genf*, 1987.

[88] L. Hes, “Non-destructive determination of comfort parameters during marketing of functional garments and clothing,” *IJFTR*, vol. 33, pp. 239–245, Sep. 2008.

[89] A. E. Mangat, L. Hes, V. Bajzik, and A. Mazari, “Thermal absorptivity model of knitted rib fabric and its experimental verification,” *Autex Res. J.*, vol. 18, no. 1, pp. 20–27, 2018.

[90] L. Hes and I. Dolezal, “New method and Equipment by measuring thermal properties of

textiles," *J. Text. Mach. Soc. Japan*, vol. 71, pp. 806–812, 1989.

[91] A. Woodcock, "Moisture transfer in textile systems', Part 1," *Text. Res. J.*, vol. 32, pp. 628–633, 1962.

[92] C. BenzartiK., "Understanding the durability of advanced fiber-reinforced polymer (FRP) composites for structural applications," in *Advanced Fiber-Reinforced Polymer (FRP) Composites for Structural Applications*, J. Bai, Ed. Woodhead Publishing, 2013.

[93] G. Marianne, *Brydson's Plastics Materials*. Elsevier, 2016.

[94] ASTM International, "ASTM E1933-97: Standard test methods for measuring and compensating for emissivity using infrared imaging radiometers," *ASTM Int.*, no. Standard E 1933–99a, pp. 5–7, 2006.

[95] Anon, "The Facts Behind the Performance of Nomex® when Exposed to Intense Heat," 2019. [Online]. Available: https://www.dupont.co.uk/knowledge/time-of-essence.html. [Accessed: 15-Feb-2020].

[96] R. A. Scott, *Textiles for Protection*. Cambridge: Woodhead Publishing, 2005.

[97] Anon, "Aramid Fibers." [Online]. Available: https://www.chem.uwec.edu/chem405_s01/malenirf/project.html. [Accessed: 18-Jun-2018].

[98] "Polyamide-imdie PAI." [Online]. Available: https://www.swicofil.com/commerce/products/polyamide-imide/294/properties. [Accessed: 21-Aug-2018].

[99] A. Burrow, T., & Lenzing, "Flame Resistant Man made Fibers," in *Hand Book of Fire Resistant Textile*, F. S. Kilinc, Ed. Oxforf: Woodhead Publishing, 2013, pp. 221–243.

[100] C. Keiser, "Steam burns moisture management in firefighter protective clothing," Swiss Federal Institute of Technology, ETH Zurich, 2007.

[101] A. Handermann, *Oxidized Polyacrylonitrile Fiber Properties, Products and Applications*, vol. 27. Zoltek Corporation, 2017.

[102] Anon, “Proban.” [Online]. Available: http://www.formula1-dictionary.net/proban.html. [Accessed: 20-Dec-2018].

[103] Belltron, “Aramid HPM, LLC High Perfromance Materials.” [Online]. Available: http://www.aramid.com/belltron/.

[104] Anon, “Belltron.” [Online]. Available: https://www.swicofil.com/commerce/products/carbon/228/belltron. [Accessed: 04-May-2020].

[105] SDL Atlas, “Sweating guarded hot plate,” 2019. [Online]. Available: https://admin.sdlatlas.com/public/content/resources/SDL_SGT_BROCHURE%5BCURRENT%5D WEB 102515.pdf. [Accessed: 15-Jan-2020].

[106] A. V. Oliveira, A. Gasper, and D. Quintela, “Measurement of clothing insulation with a thermal manikin operating under the thermal comfort regulation mode: comparative analysis of the calculation methods.,” *Eur. J. Appl. Physiol.*, vol. 104, no. 4, p. 679–688, 2008.

[107] Anon, “VWR Professional Hot Plates.” [Online]. Available: https://us.vwr.com/store/product/4639460/vwr-professional-hot-plates. [Accessed: 20-Jan-2019].

[108] Meb G W and P. GmbH P. ., “Combustion behavior Test equipment,” Berlin, 2002.

[109] SDL Atlas, “Air Permeability tester.” [Online]. Available: https://admin.sdlatlas.com/public/content/product_brochures/eng_M021A_Air Permeability (1).pdf. [Accessed: 18-Jan-2019].

[110] L. Hes, “The use of comfort parameters in marketing of functional garments and clothing. Research paper presented at the 2nd International Conference on Intelligent Textiles and Mass Customization. Casablanca.,” in *Research Paper presented at 2nd International Conference on Intelligent Textiles and Mass Customization*, 2010.

[111] L. Hes, “Optimisation of shirt fabrics’ composition from the point of view of their appearance and thermal comfort,” *Int. J. Cloth. Sci. Technol.*, vol. 11, no. 2/3, pp. 105–

119, May 1999.

[112] M. Lau, “Graphene-Based Materials For Supercapacitor Electrodes,” PhD Thesis, National University of Singapore, 2013.

[113] CSN 800858, “zkouseni tuhosti A Pruznosti Plosnych Textili.” [Online]. Available: http://www.technicke-normy-csn.cz/800858-csn-80-0858_4_5765.html.

[114] ISO 5470-2, “Rubber or plastic coated fabrics Determination of abrasion resistance, Part2, Martindale Abrader.,” 2003. [Online]. Available: https://www.sis.se/api/document/preview/903767/. [Accessed: 14-Oct-2019].

[115] Pike Technologies, “Integrating spheres- Introduction and theory,” 2018. [Online]. Available: https://docs.google.com/viewerng/viewer?url=http://69.175.81.122/~piketech/wp-content/uploads/2019/06/PIKE_Integrating_Spheres_Theory-Applications.pdf&hl=en. [Accessed: 14-Aug-2019].

[116] Anon, “Magnetron Sputtering: Overview.” [Online]. Available: https://angstromengineering.com/tech/magnetron-sputtering/. [Accessed: 01-Feb-2020].

[117] Anon, “Magnetron Sputtering Solutions,” 2020. [Online]. Available: https://www.dentonvacuum.com/products-technologies/magnetron-sputtering/.

[118] H. Matt, “what is magnetron sputtering,” 2014. [Online]. Available: http://www.semicore.com/what-is-sputtering. [Accessed: 24-Feb-2018].

[119] L. Surdu *et al.*, “Comfort properties of multilayer textile materials for clothing,” *Ind. textilă*, vol. 64, pp. 75–79, 2013.

[120] L. Hes and C. Loghin, “Heat, moisture and air transfer properties of selected woven fabrics in wet state,” *J. Bioeng. informatics*, vol. 2, no. 3, pp. 141–149, 2009.

[121] R. L. Barker and R. C. Heniford, “Factors affecting the thermal insulation and abrasion resistance of heat resistant hydro-entangled nonwoven batting materials for use in firefighter turnout suit thermal liner systems,” *J. Eng. Fiber. Fabr.*, vol. 6, no. 1, pp. 1–10,

2011.

[122] M. Bogusławska-Baczek and L. Hes, “Effective water vapour permeability of wet wool fabric and blended fabrics,” *Fibers Text. East. Eur.*, vol. 97, no. 1, pp. 67–71, 2013.

[123] H. Zhang, G. Song, H. Su, H. Ren, and J. Cao, “An exploration of enhancing thermal protective clothing performance by incorporating aerogel and phase change materials,” *Fire Mater.*, vol. 41, no. 8, pp. 953–963, 2017.

[124] M. J. Xiong X., Yang T., Mishra R., “Transport Properties of Aerogel-based Nanofibrous Nonwoven Fabrics,” *Fibers Polym.*, vol. 17, no. 10, pp. 1709–1714, 2016.

[125] Anon, “Fluke process instruments,” 2020. [Online]. Available: https://www.flukeprocessinstruments.com/en-us/service-and-support/knowledge-center/infrared-technology/what-is-emissivity. [Accessed: 29-Jan-2020].

[126] Y. Su, J. He, and J. Li, “Modelling transmitted and stored energy in multilayer protective clothing under low level radiant exposure’’,” *Appl. Therm. Eng.*, vol. 93, pp. 1295–1303, 2016.

[127] Y. Su, J. He, and J. Li, “Numerical simulation of heat transfer in protective clothing with various heat exposures distances,” *J. Text. Inst.*, vol. 108, no. 2, pp. 1412-1420., 2016.

[128] D. A. Torvi and J. D. Dale, “Heat transfer in thin fibrous materials under high heat flux conditions,” Edmonton University of Alberta.

[129] M. F Modest, *Radiative heat transfer*. New York,: N Y : McGraw-Hill, 1993.

[130] I. Martinez, “Radiative view factors,” 1995. [Online]. Available: http://webserver.dmt.upm.es/~isidoro/tc3/Radiation View factors.pdf. [Accessed: 25-Sep-2019].

[131] Y. A. Cengel, A. J. Ghajar, and H. Ma, *Heat and mass transfer fundamentals and applications*, 4th editio. New York: McGraw-Hill, 2011.

[132] ASTM F2731, “Test method for measuring the transmitted and stored energy of firefighter protective clothing systems,” 2011.

[133] M. Feistauer and K. Najzar, "Finite Element Approximation of a Problem with a Nonlinear Boundary Condition", *Numer. Math*., vol. 78, pp. 403-425, 1998

[134] J. Mlýnek and R. Knobloch, "Model of Shell Metal Mould Heating in the Automotive Industry", *J. Appl. Math.*, vol .63 , pp. 111-124, 2018.

[135] M. Křížek and L. Liu, "Finite Element Analysisof a Radiation Heat Transfer Problem", *J. Comput. Math.*, vol. 16 , No. 4, pp. 327-336, 1998.

List of papers published by the author

Publications in journals

[1a] **Naeem J**, Mazari A, Havelka A. REVIEW: RADIATION HEAT TRANSFER THROUGH FIRE FIGHTER PROTECTIVE CLOTHING, Fibers and Textiles in Eastern Europe, 25(4), 2017, page: 65-74, ISSN # 12303666.

[2a] **Naeem J**, Mazari A, Akcagun E, Kus, Z: REVIEW: SIO_2 AEROGELS AND ITS APPLICATION IN FIREFIGHTER PROTECTIVE CLOTHING, Journal of Industria Textilia, 69 (1), 2018, page 50-54, ISSN # 12225347

[3a] **Naeem J,** Mazari A, Akcagun E, Kus Z, Havelka A; ANALYSIS OF THERMAL PROPERTIES, WATER VAPOR RESISTANCE AND RADIANT HEAT TRANSMISSION THROUGH DIFFERENT COMBINATIONS OF FIREFIGHTER PROTECTIVE CLOTHING, Accepted, Journal of Industria Textilia, vol 69(6), 2018, page: 458-465. ISSN # 12225347

[4a] **Naeem J,** Mazari FB, Mazari Areport: INSTRUMENTS USED FOR TESTING MOISTURE PERMEABILITY, Vlakna a Textil, 23 (1), 2016, page 42-48, ISSN # 13350617

[5a] Mazari F B, Chotebor M, **Naeem J,** Mazari A, Havelka A; PERFORATED POLYURETHANE FOAM ON MOISTURE PERMEABILITY OF CAR SEAT COMFORT, Fibers and Textiles in Eastern Europe, 24 (6), 2016, pages 165-169, ISSN # 12303666

[6a] **Naeem J,** Mazari A: COMPARATIVE STUDY OF RADIANT HEAT FLUX DENSITY TRANSMISSION THROUGH FIREFIGHTER PROTECTIVE CLOTHING, Vlakna Textile,2 pages:79-86 ISSN # 13350617

[7a] **Naeem J,** Mazari A, Volskey L: EFFECT OF NANO SILVER COATING ON THERMAL PROTECTIVE PERFORMANCE OF FIREFIGHTER PROTECTIVE CLOTHING, Journal of Textile Institute, vol 10(6), 2019, page: 847-858. ISSN # 0040-5000

[8a] **Naeem J**, Mazari A, Kus Z: COMPARISON OF THERMAL PROTECTIVE PERFORMANCE OF FIREFIGHTER PROTECTIVE CLOTHING AT DIFFERENT LEVEL OF RADIANT HEAT FLUX DENSITY, Journal of Tekstilec, vol 61(3), 2018 pages: 179-191. ISSN # 2350-3696.

Conferences and Workshops

1. **Naeem J**, Mazari A, Volskey L, ENHANCEMENT OF THERMAL PROTECTIVE PERFORMANCE OF FIREFIGHTER PROTECTIVE CLOTHING, Autex Conference 2018, ISBN 978-961-6900-17-1.
2. **Naeem J,** Mazari A, Krejcik M, Impact of Metallic Coating on Thermal Protective Behavior of Multilayer Protective Clothing, NART Conference, 2019**.**
3. **Naeem J** : INVESTIGATION OF THERMAL RESISTANCE AND WATER VAPOR RESISTANCE OF MULTILAYER PROTECTIVE CLOTHING BY USING AEROGEL BLANKET, Billa Voda Workshop, 2016, ISBN # 978-80-7494-293-8
4. **Naeem J**, Mazari A, Krejcik, M, INFLUENCE OF METALLIC COATING ON THERMAL PROTECTIVE PERFORMANCE OF FIREFIGHTER PROTECTIVE CLOTHING, PhD Work shop, Technical University of Liberec, 2019.